FlexiGrid

Project Acronym:	FlexiGrid
Project Full Name:	Enabling flexibility for future distribution grid – FlexiGrid
Grant Agreement:	No 864048
Project Duration:	3,5 years (starting 1 November 2019)

Deliverable 3.4

Task 3.4 – Report on quantification of flexibility

Work Package:	WP3
Task:	T3.4
Lead Beneficiary:	LIST, TU/e, TUS, EMAX
Due Date:	30/04/2021
Submission Date:	03/05/2021
Deliverable Status:	final
Deliverable Style:	Report
Dissemination Level:	Public
File Name:	Tasks3.4_Quantify_flex-v2_00.docx

This project has received funding from the European Union's Horizon 2020 research and innovation program under grant agreement No 864048

Authors

Surname	First Name	Beneficiary	e-mail address
Nguyen	Phuong	TU Eindhoven	p.nguyen.hong@tue.nl
Tran	Minh-Quan	TU Eindhoven	m.q.tran@tue.nl
Mohandes	Baraa	LIST	baraa.mohandes@list.lu
Koster	Daniel	LIST	daniel.koster@list.lu
Vu	Van Thong	EMAX	thong.vuvan@emaxgroup.eu
Apap	Gustave	EMAX	gustave.apap@emaxgroup.eu
Mladenov	Prof. Valeri	TU Sofia	valerim@tu-sofia.bg
Chobanov	Assoc. Prof Vesselin	TU Sofia	vesselin_chobanov@tu-sofia.bg
Antoniadou-Plytaria	Kyriaki	Chalmers Univ.	kyriaki.antoniadou@chalmers.se

Reviewers

Surname	First Name	Beneficiary	e-mail address
Tobiasson	Wenche	RISE	wenche.tobiasson@ri.se
Rey	Tristan	HES-SO	tristan.rey@hevs.ch
Bobochikov	Teodor	ENTRA Energy	teodor.bobochikov@entra.energy

Version History

Version	Date	Modifications made by
V1.0	30/04/2021	Final version
V2.0	26/11/2021	Final, revised version

List of abbreviations

Abbreviation	Definition
ADEME	*(French Environment and Energy Management Agency)*
AE	Auto-Encoder
ANN	Artificial Neural Networks
ASHP	Air Source Heat Pump
BESS	Battery Energy Storage System
CPS	Cyber-Physical Systems
CNN	Convolutional Neural Network
DA	Day-ahead
DER	Distributed energy resources
DR	Demand Response
DSM	Demand Side Management
DSO	Distribution system operator
DW	Dish washer
EV	Electric vehicle
FED-EM	Fossil-free Energy district- Energy market
FlexiGrid	Enabling flexibility for future distribution grid – FlexiGrid
GHG	Greenhouse gases
GSHP	Ground Source Heat Pump
HVAC	Heating, Ventilation, Air conditioning and Cooling
IEA	International Energy Agency
LEM	Local energy market
LFM	Local flexibility market
LV	Low Voltage
NREL	National Renewable Energy Laboratory (US)
MAE	Mean Absolute Error
MG	Microgrid
MSE	Mean Square Error
OEM	Original Equipment Manufacturer
P2P	Peer-to-peer
PCR	Primary Control Reserve
RES	Renewable energy sources
RH	Rolling Horizon
SoE	State-of-Energy
TSO	Transmission system operator
V2G	Vehicle-to-Grid
CPS	Cyber-Physical Systems
vRE	Variable Renewable Energy
WM	Washing machine
WSHP	Water Source Heat Pump

Table of Contents

List of figures

List of tables

Executive Summary

The ability of the electric power system to adjust its operating point by modulating its inputs and outputs is known as Power System Flexibility. A power system with a low flexibility characteristic is deemed insecure, and is unable to cope with very fast or unforeseen disruptions. In classical power systems, navigating the system safely through unpredictable events was a challenge limited to accommodating load variations, and rare equipment failures, and thus, conventional generation units were sufficient to provide the classical power system with the flexibility needed. In contrast, operators today are faced with larger uncertainty, caused by renewable energy sources (RES). The existing flexibility in classical power systems falls seriously short of accommodating the variability of RES. In fact, the lack of power system flexibility remains the main obstacle in the face of higher penetration of RES in the power grid. To achieve high penetration of RES in the power system, flexibility is needed on versatile levels (transmission & distribution grids), by different stakeholders (DSOs, TSOs, energy providers, balance responsible parties and aggregators), serving various needs (such as balancing, mitigation of congestions, voltage regulations). This report adopts this approach, utilizing all sources of flexibility to operate the system securely, and optimally, but focusing on the distribution level.

Chapter 2 introduces the various distributed energy resources (DER), which have the potential to provide different types of flexibility services, e.g. by shifting loads, curtailment or buffering of energy. These privately owned assets, such as electric vehicles, heat pumps, decentralised storage or smart appliances, come with constrains: their availability is limited, they have restricted control options and the flexibility service may not compromise the comfort of the user to an unacceptable extend. Furthermore, the interrelation with incentives, tariff schemes and demand response programs has further influence on the available amount of flexibility – which is illustrated in this chapter by examples from different studies and demo projects.

Chapter 3 takes a closer look at flexibility at the distribution system level, and particularly, flexibility from the demand side incentivized by dynamic electricity prices. Characteristics of loads and constrains concerning flexibility provision are highlighted. The parameters to quantify load flexibility are explained. Consequently, loads are classified to 5 classes based on their aptitude/potential to provide flexibility. This general framework is materialized in an optimisation formulation and integrated in a set of procedures and algorithms for the acquisition of flexibility from loads at the distribution system level. The response of loads (hence their flexibility) to a dynamic price signal and resulting grid operations risks, are explored in this numerical study.

The numerical results obtained in Chapter 3 pertain to a physical and a mathematical optimisation model run on level of the individual households, respectively on device level. If availability of flexibility shall be quantified from perspective of a central agent, as a DSO or aggregator for instance, evaluation time is critical during real-life applications. A data-driven model is trained in Chapter 3, to replicate the results of the optimisation model in shorter time, and with less computational effort than mathematical optimisation. The deep-learning based model encodes the data from a human-readable format to a hidden space, where it can be solved, and then decodes the data back to a human-readable format. The model demonstrates good performance at predicting the time-shift in discrete load events. However, the model is less accurate at predicting the magnitude of load in response to a dynamic price profile.

Finally, the model in Chapter 4 assumes that the operator sets a price profile, and the operator observes the system's response. The operator cannot set directly the desired amount of flexibility. Chapter 4 solves a stochastic optimisation model where the flexibility requirement (limiting the peak load of a micro grid) is set explicitly in a stochastic optimisation problem for a set of generated random forecast scenarios (incorporating load forecasts as well as renewable generation forecasts and their uncertainties). The amount and the time of provided flexibility are recorded for each forecast scenario, separately. These results are analysed statistically to evaluate the certainty of securing the required amount of flexibility.

1 Introduction

This report constitutes the deliverable of Task 3.4 – Quantification of availability and certainty for various flexibility resources – within WP3 of FlexiGrid. As discussed in the deliverable of Task 3.3 – Process design for flexibility procurement and dispatch, the available amount of flexibility at a given time strongly depends on locational and temporal constraints. From the demand side, these include the behaviour of the end-users, occupancy, automated set points of the appliances and willingness of participating in the flexibility services. On the other hand, grid-oriented flexibility services require flexibility at a particular network area for a certain duration in a day. The distribution system operator (DSO) can request these services either with implicit or explicit flexibility implementation [1]. In any case, these services strongly depend on the availability of the flexibility resources which are planned to offer the service. Depending on the nature of each flexibility source, e.g. heat pumps vs. electric vehicles, the availability of a flexibility source might vary e.g. with their interdependencies with geographical conditions, timing, and social behaviours. Significant discrepancies might occur without a thorough assessment on the availability and certainty of each flexibility sources. These may lead to conflicts of interest among the actors involved in flexibility procurement, valuation and exploitation.

1.1 The objective and scope

This task was designed to formulate a methodology to quantify available flexibility from the demand side. An inventory of flexible devices, e.g. heat pumps, electric vehicles, or stationary storage technologies, and demand response programs will be incorporated in order to assess the availability of flexibility and associated limiting factors of various flexibility resources.

In this report, the characteristics of each flexibility source and their dependencies on various aspects (geographical conditions, timing, behavioural factors etc.) will be specified. A deterministic approach in modelling flexibility from distributed energy resources will be presented, based on a study using dynamic electricity prices to incentivise flexibility. Moreover, the results of a developed data-driven model for various flexibility resources (heat pumps, electric vehicles, different household appliances etc.), applied to the same example, will be presented and assessed.

Finally, the certainty of flexibility provision under the uncertainty of load forecasts, as well as renewable generation forecasts, will be determined. This use case is based on the behaviour of micro grids, consisting of loads, battery storage systems and photovoltaic generation capacities, delivering a capacity limitation flexibility service to the grid operator. The certainty of flex provision, its capacity and schedule is determined by means of a stochastic programming model.

1.2 Deliverable structure

The following Chapter 2 presents an overview about the available flexibility sources with their potential and limiting factors in offering flexibility services. Chapter 3 presents a set of deterministic models for various types of flexibility, e.g. time-shifting, buffering, curtailing. This includes a market-based demand response mechanism to assess the impact of demand-side flexibility in relieving congestion by adjusting electricity prices. In Chapter 4, different data-driven models, which might be used to capture flexibility

behaviours of the demand-side, have been discussed. Chapter 5 provides an insight on potential uncertainty of exploiting demand-side flexibility, in form of a capacity limitation flexibility service, via a stochastic assessment process.

2 Flexibility resource inventory

The aim of this chapter is to list the main flexibility options in order to ensure a stable and secure delivery of power to all end-users and to enable the utilisation of distributed energy resources to provide flexibility to DSOs mainly. An analysis of opportunities and limitations of every option will be made.

Traditionally, flexibility needs arise from changing consumption pattern, forecast errors or power plant outages. But the increase of variable renewable generation sources (predominantly wind and solar) is changing the way the balance of the power system needs to be assured. Compared to conventional electricity sources, wind and solar-based renewables do not provide a stable, arbitrarily controllable power production, rather they are intermittent and stochastic. Since the power output depends on the meteorological conditions, it cannot be modulated by the producers, at least not increased and not easily decreased without loss or storage capacity. As a result, the produced electrical power is fed into the grid whenever available and can only be forecasted with a certain accuracy [2]. This stochastic nature of variable Renewable Energy (vRE) leads to challenges regarding balancing the system, which in turn, leads to the increasing needs for flexibility and other methods to resolve these rising concerns.

The challenge has further, different aspects and is particularly acute at the distribution level. The previously mentioned development of decentralised energy resources, as well as the electrification of transport and heating, put increased pressure on the medium and low voltage networks. Besides the described increasing balancing issues (mainly on higher voltage levels), decentralised fluctuating generation and massively changing consumption patterns (due to the penetration of heat pumps and EVs in particular), might result in voltage band violations and local congestions, e.g. transformer overloads. DSOs need to change from a rather passive role in grid operation, characterised by a security driven planning approach, to a more active grid management paradigm, observing the operational state of the grid and controlling actively the operational parameter. In this framework, flexibility from the demand side (DSM) both from power to heat (heat pumps, electric boiler etc.), electric vehicles, battery storage and other devices, will be increasingly necessary.

With heating representing almost one third (27%) and transport one fifth (19.4 %) of Europe's final energy consumption, the procurement of flexibility from heat pumps and electric vehicles will be critical at the distribution level. Stationary battery storage also holds great potential to help balance the grid at the low and medium voltage and actively remove congestions and voltage band violations. Stationary battery storage and electric vehicles, could both (theoretically) provide buffer storage flexibility, but their availability as well as the economic incentive to provide power flexibility, will be very different. Other technologies, such as air conditioning, refrigerators, white ware etc., even with low flexibility potential for the single appliance, can be managed smartly to increase flexibility options in the grid, and will be relevant considering the massive amount of these appliances operating in the LV grids.

2.1 Power-to-heat

There are different ways to convert electricity into heat, respectively running thermal processes by means of electricity, which could in return be utilised to provide flexibility. The following chapter will focus on small scale thermal systems in the low voltage grids. Power-to-heat options could be centralised and decentralised, as depicted in Figure 2-1 : In a centralised system, electricity is mainly converted into heat

and injected to a district heating system, using industrial-scale heat pumps or electric boilers. In the second case, the decentral option, power-to-heat is used right at, or very close to the location of heat demand, by means of heat pumps, electric boilers or other types of electric heating systems.

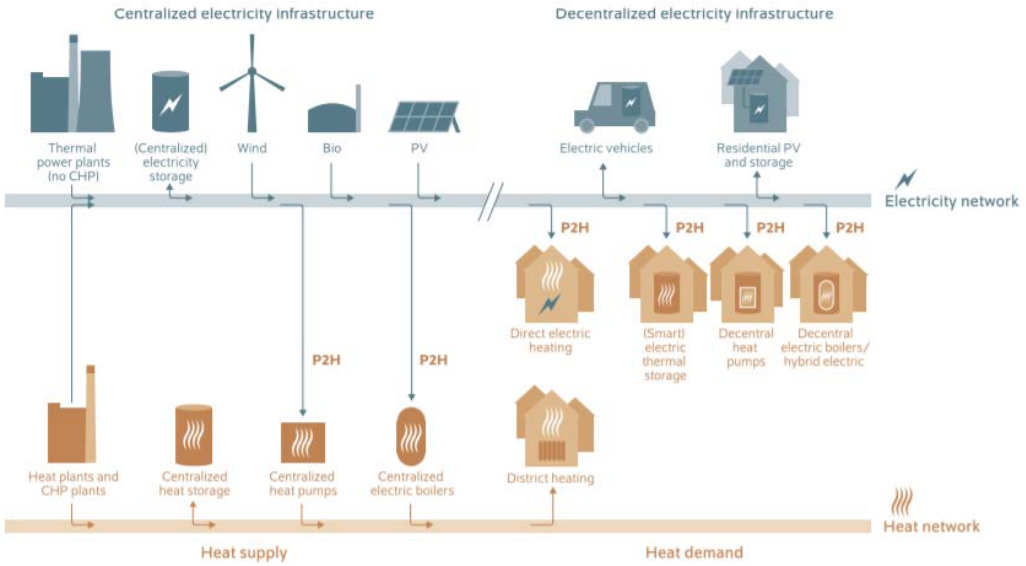

Figure 2-1: Interconnections of power-to-heat options with electricity and district heating networks [2].

Buildings or domestic hot water storage tanks have relatively high thermal inertia, which is very suitable to "store" energy in form of heat, since the electric load can relatively easily be shifted towards a more suitable point in time.

In the sub-chapters below, we will give further insights in the use of heat pumps, electric boilers/heaters and HVAC systems (heating, ventilation, air-conditioning and cooling), to convert power to thermal energy and their usability as flexibility asset.

2.1.1 Heat pumps

a) Characteristics of load curves:

There are three main types of the heat pumps, namely air source heat pump (ASHP), ground source heat pump (GSHP), and water source heat pump (WSHP). The absorbed heat is transferred to the heat sink, for example radiators, floor heating, or domestic hot water storage.

The load curve of heat pumps show a certain daily characteristic and differs according to seasons (respectively outdoor temperatures). Load patterns are at roughly the same shape, independent of the technologies, since it depends on the heat demand which is directly influenced by the meteorological conditions. Furthermore, the domestic hot water demand influences the shape. Generally, according to the seasonal fluctuation of the heating demand, the consumption of a heat pump is obviously much higher during the winter season due to low temperatures.

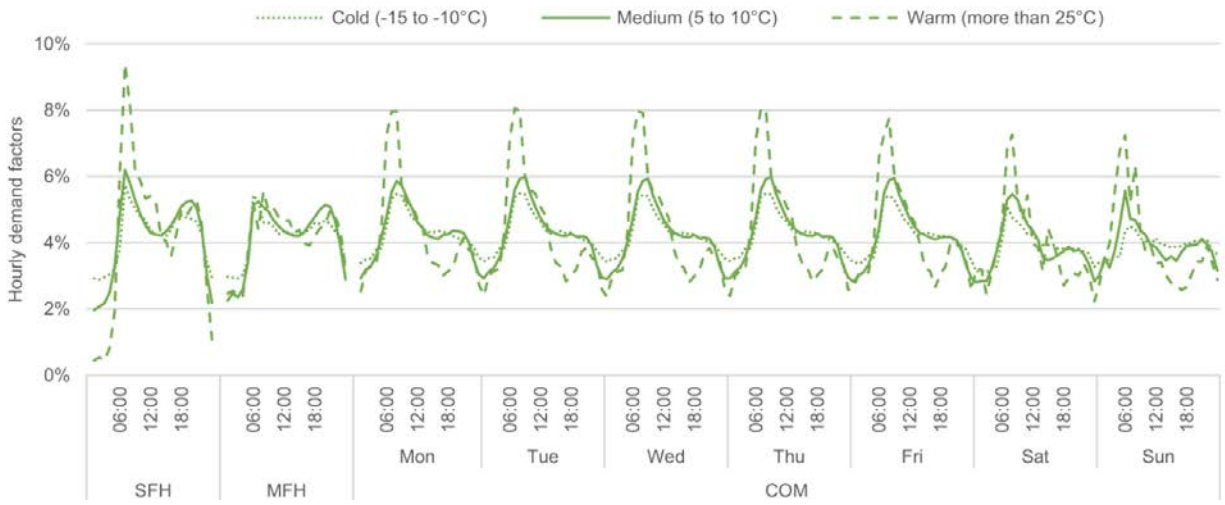

Figure 2-2: Hourly demand factors at different temperature ranges. Exemplary functions for single-family houses (SFH), multi-family houses (MFH), and commercial buildings (COM)[3].

Heat demand and resulting pump load curves also depend on the type of household or building considered. The most relevant types to be considered here are single-family houses, multi-family houses and commercial buildings. As illustrated by Figure 2-2, heat demand is higher in the morning and has a second peak towards the evening in single-family houses and multi-family houses. Commercial buildings show a similar peak during the morning, at slightly later times, but flatten towards noon and drop after the business hours. The graph shows the hourly demand factors, which indicate how the daily heat demand distributes over the day (the sum of demand factors of a full day sum up to 100%). Hence, it shows how the "profile" varies over the season, but does not give insight how the total heat demand increases with lower temperatures.

Besides the heating demand, depending on outdoor temperature, building type and energy efficiency of the building, heat pumps differ in the energy efficiency which furthermore influences the load profile. The different types of heat pumps can have large differences in their efficiency, which depends on the temperature level of the heat source (as well as the heat sink). Hence, air source heat pumps are less efficient at colder temperature compared to ground sourced heat pumps or water based systems. Similarly, heat pump systems using floor heating operate more efficiently than those using radiators as heat sink, since the latter require higher temperatures.

b) Potential flexibility provision type

Flexibility from heating (and cooling) can be used in several ways in a power system. Moving loads from electricity net load peaks to net valleys can smooth variations. When the heating devices have suitable controllability, they can also be valuable sources of reserves that mitigate forecast errors and faults.

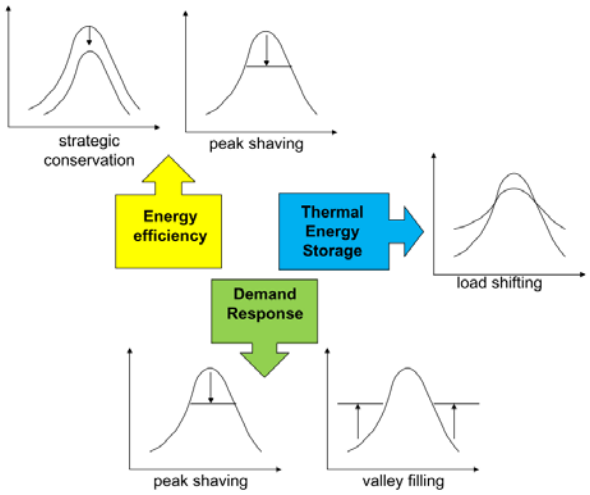

Figure 2-3: Different DSM strategies implemented for heat pumps[4].

[4] Arteconi et.al. discuss the options to implement DSM strategies by means of heat pumps, and identified three technologies (see Figure 2-3) providing different flexibility:

- **a)** Energy efficiency – a variable capacity heat pump, as opposed to an "ON/OFF"-controlled heat pump, would enable to generally decrease the load profile or allow peak shaving.
- **b)** A heat pump system in combination with thermal storage enables load shifting (time shifting).
- **c)** Demand response (DR), e.g. dynamic pricing, could automatically influence the internal temperature setpoints and provide peak shaving or valley filling.

The value of such flexibility e.g. for balancing purposes might depend on factors such as geography. The appearance of strong wind generation in winter correlates with the heating period in central and northern European countries, which makes heat pumps and wind power a great match in this geographical area. Whether a flexible dispatch in combination with real-time pricing is economically profitable for the consumer, however, depends on the electricity pricing regime.

According to a study published by Tennet in 2020[1] for the Netherlands, smart use of flexible heat pumps could provide between 0.5 and 1 GW of power flexibility and relieve the network during hours of high solar and wind generation. This would lead to a significant reduction in curtailment and reduce the demand during peak hours. The flexibility from heat pumps would also contribute to CO_2 reduction by reducing the need for gas-fired plants, which would have increased consumer's energy bills.

Another study led by KU Leuven for Belgium show that 1 million electric heating systems have the potential to offset up to 1,4 TWh of curtailment (1 MWh of curtailment reduction per electric device)[2] [5].

The Cost reduction is significant, as highlighted in the picture below, with up to 35 million € saved for 1 million systems installed, in the case of 33% non-flexible nuclear power plant fleet capacity as today, at

[1] https://www.pv-magazine.com/2021/01/29/flexible-heat-pumps-ideal-for-power-grids-congested-by-solar-and-wind/
[2] In the case of a plant fleet of 1/3 nuclear power, as today, with low flexibility and 3-times the current renewable capacity

total operation costs of 457 million € - for the scenario of a triple of current renewable capacity installed (R3).

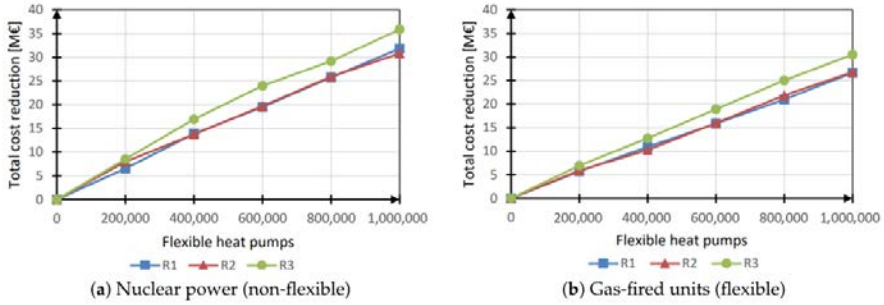

Figure 2-4: Total cost reductions of operational costs (flexible heat pumps) [5].

c) Restrictions

A communication interface on modern heat pumps, eventually in combination with a thermal storage capacity to avoid comfort restrictions during off-times, would enable the (constrained) flexibility usage, without harming the comfort of the building occupants. Some utilities already offer specific heat pump tariffs, which allow the utility to switch off the heat pump during peak times, e.g. for 1 hour per day (for instance in Germany). Several producers of heat pumps include a communication interface, which allows to remotely disconnect the device for a certain idle period, typically limited to 1 or 2 hours. Some producers also market their products a "smart-grid ready" offering further remote-control option, such as triggering a start remotely or the reduction of the current load.

The electrification of heat is, however, highly dependent on an energy-efficient building stock. Heat pumps are most efficient when they supply heat at low temperatures. Their efficiency decreases if applied in buildings that are not well insulated. This has been identified as one of the key risks for the deployment of heat pumps and flexible services to the grid. It highlights how important it is to couple power, heat and building sectors in order to reach a zero-carbon economy by 2050.

2.1.2 Electric heater/boiler

Electric heater or electric boiler can also provide some flexibility, even if they are less energy efficient compared to heat pumps. On the other hand, if deployed in a large scale, their power demand can have large impact on power systems daily and seasonal (peak) load variations. For example, in France, the majority of residential heating is based on electric heating and causes considerable temperature sensitivity in the power demand (2300 MW/°C)[3]. It is a major driver for extreme peak loads and risk for the security of supply.

However, a controllable electric heating (as well as cooling) can draw on the potential flexibility of heating (thermal inertia) to facilitate renewables integration and manage peak loads. The use of Information and Communications Technologies (ICT) in electric heaters could therefore provide the option to shift demand loads according to power system conditions, while also meeting the building occupant's comfort requirements. Direct transformation of electric energy to heat would include electric heating systems

[3] RTE, Bilan electrique 2019, RTE, Direction innovation et donnees, Janvier 2020, Paris.

(fans, radiators, electric floor heating, infrared heating), electric boilers to provide domestic hot water demand (with or without buffer storage) and electric heaters included in heat pumps. These additional heaters are normally used once the outdoor temperature reaches very cold values, or to provide the higher temperatures for the domestic hot water demand (see Figure 2-5 below). The potential for time shifting flexibility services for electric heating systems are then rather similar to heat pumps.

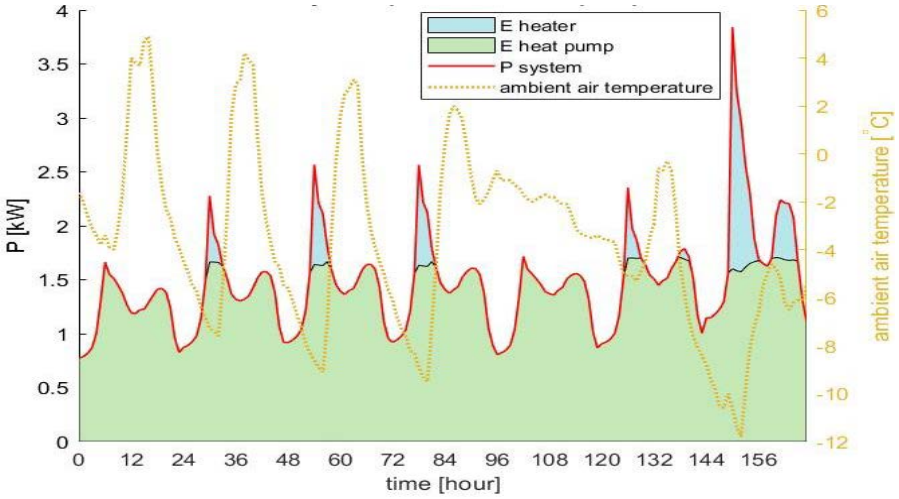

Figure 2-5: Weekly load profile of the heat pumps [6].

The flexibility provision by electric boilers, providing domestic hot water demand, requires a hot water storage – flow type heaters are unsuitable. Their potential to deliver flexibility services for balancing in the Belgian power system has been assessed in [5] using two scenarios, a) the current plant fleet containing 1/3 of non-flexible nuclear plants and b) switch those towards gas-fired units: As depicted in Figure 2-1, the high curtailment needs, occurring in scenario a) under the assumption for a tripled renewable capacity (R3) can be substantially reduced by deploying flexible water heaters (from 10% to 6% for 1 million devices on the grid).

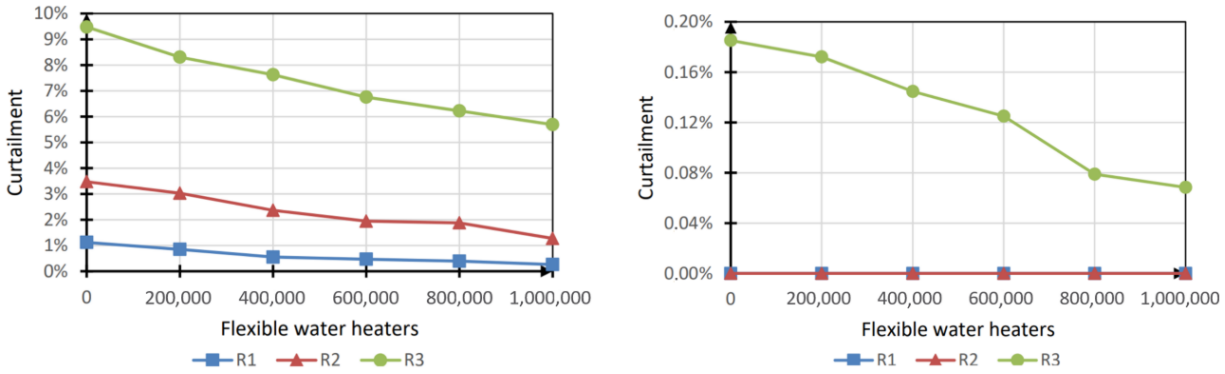

Figure 2-6: effect of reducing curtailment by flexibility provision from flexible water heaters

2.1.3 HVAC – Heating, Ventilation, Airconditioning and Cooling

In Europe, the general cooling demand is considerably smaller than heating, but it is growing fast with increasing building cooling demand and due to the strong urban development in warmer climates and new uses in services and industries, such as cooling of large data centres. HVAC systems, as used in residential and commercial buildings, describe normally air handling units, used to (eventually) heat, cool and de/humidify an air stream supplying the building. Ventilation, conditioning and cooling is mainly provided on systems based on electricity. For HVAC to provide energy flexibility to a building requires its systems must be designed, controlled and operated appropriately for the intended purpose. If managed flexible, the HVAC systems will contribute to the building's ability to manage its energy demand and still provide flexibility to the power system. But as different as HVAC systems can be, their use (mainly in commercial buildings) is also versatile, the climate conditions add to this uncertainty and it is difficult to draw general conclusions on the characteristics of their load curves and flexibility potential.

2.2 Electric vehicles (smart charging / vehicle-to-grid)

At a continental or country level, the impact of EV charging on the power demand at the expected growth rates of electromobility, will be significant. In its latest global electric vehicles Outlook, IEA forecasts the share of EVs on the total electricity consumption in 2030 growing to as high as 4% in Europe.

But the impact of EV charging on the power grid will be especially significant in the distribution networks, specifically at the LV network level as EV demand sharply increases the household peak demand in residential areas. According to a study led by McKinsey [8], the increase in peak demand could reach 30% in specific areas, such as suburban districts, once a 25% penetration share of EV of the total car fleet is reached (see Figure 2-7).

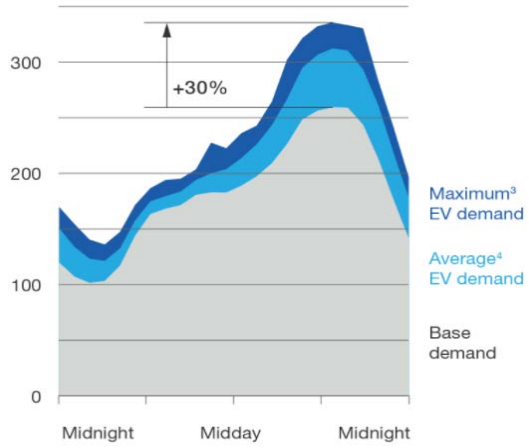

Figure 2-7: The increase in peak demand due to EV penetration of 25% [7].

Current network tariff systems for household connections are not designed to regulate or hamper such increase in peak power demand. There is currently almost no incentive for EV drivers to charge during off peak periods. However, from a pure balancing perspective, off peak times would be suitable to charge electric vehicles, since there is generally sufficient power available and often excess of variable renewable generation.

a) Characteristics of load curves:

Electric Vehicles (EVs) typical charging pattern is daily, showing differences by weekdays and charging locations. People use their vehicles on a daily basis, and charge it either at home, at work or at public charging points. According to users' needs and habits, charging patterns can be different. These load patterns, for different localisations (at home, at work, public charging points or other) can be seen in Figure 2-8. The chart shows, that the load pattern for EV charging at home, has its minimum around 6:00 and rises continuously over the day until it reaches its peak between 18:00 and 22:00. After the evening peak, which is the most problematic for the distribution grid management as well as the system wide balancing, the demand drops until the minimum is reached again. The demand profile for charging at work is different, peaking between 9:00 and 12:00 and dropping again continuously until the minimum is reached between 24:00 and 6:00. For public charging, the curve is similar to the work profile during the early morning, but flattens after 9:00 and does not reach such a high peak, while it drops rather slowly towards the evenings.

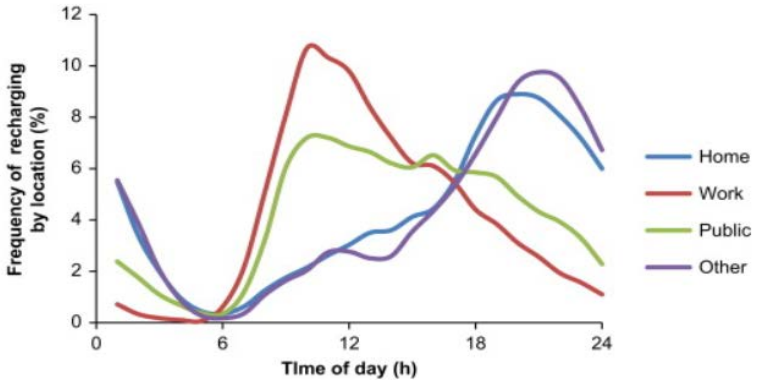

Figure 2-8: charging profiles by location [8].

A recent report from the US (figure below) published the modelled, aggregated load curves of 100,000 EVs (generated by a model from NREL, called EVI-Pro) for a typical work day and weekend. Furthermore, two scenarios have been studied: an "uncontrolled charging", where EVs charge immediately, at full power, when plugged in and stop only when the car is fully charged, and a "maximally delayed charging" where EVs only charge during the last possible period that guarantees the EV to be fully charged before the foreseen departure time. The two graphs at the top of Figure 2-9 show that the uncontrolled charging on weekdays results in a peak demand of 150 MW between 18:00 and 22:00 at the evening, while during weekend the peak spreads out a bit further with 100 MW between 16:00 and 22:00. In case of a maximum delayed charging, the peaks for both days are shifted towards the mornings and got more concentrated: reaching 200 MW at weekdays around 7:00 and almost 150 MW on weekends between 7:00 and 9:00. Both resulting peaks (in the mornings if "uncontrolled" and during the evenings "max. delay") are unfavourable, since they correspond to the peak times in the electricity grid in middle European and Northern countries.

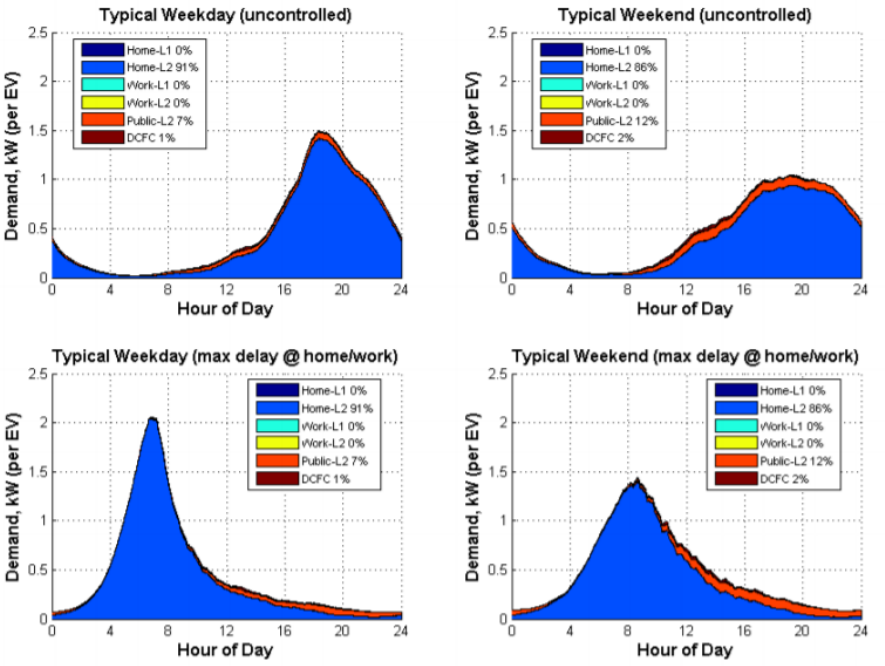

Figure 2-9: Aggregate demand profiles for 100,000 EVs under weekday and weekend uncontrolled and maximum delay charging conditions [9].

b) Potential flexibility provision type - time shifting (V1G) & buffering (V2G)

Smart charging means adapting the charging cycle of EVs to both, the conditions of the power system and the needs of vehicle users. Such mechanisms range from simply switching on and off the charging, to unidirectional control of vehicles charging (V1G), that allows for increasing or decreasing the rate of charging, to the technically challenging bidirectional vehicle-to-grid (V2G), which allows the EV to provide services to the grid in the discharge mode.

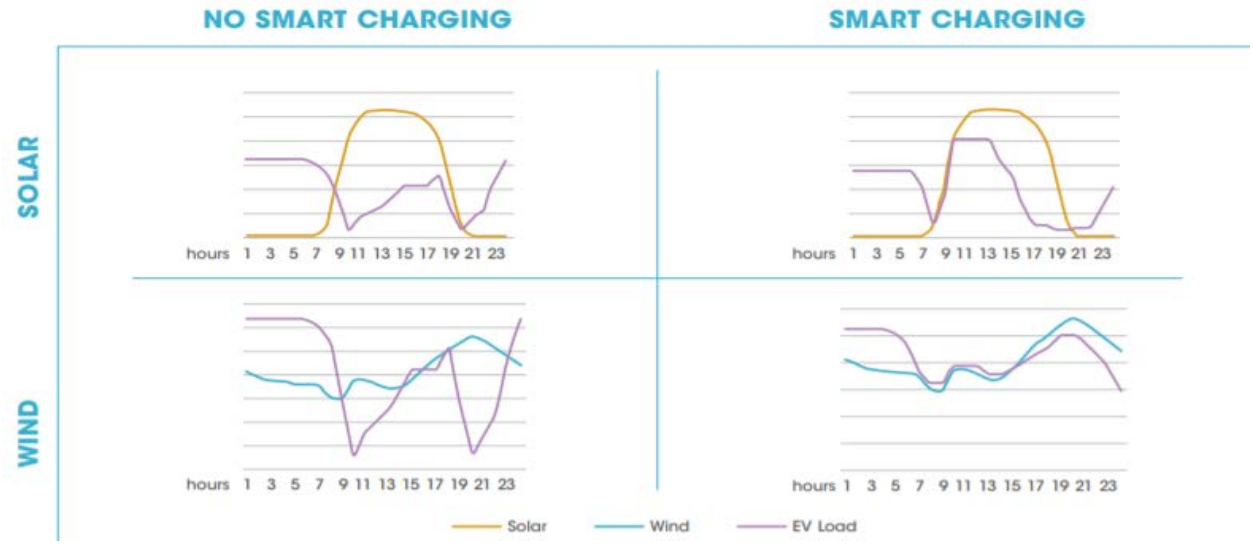

Figure 2-10: Effect of smart charging adapting to a renewable production curve [10].

In a report published by IRENA (International Renewable Energy agency), the (system-wide) impacts of smart charging on the integration of renewables have been presented. The graphics above (Figure 2-10) show on the right hand side the EV charging load (purple) vs. the production curve of solar PV (top) and below against a wind power dominated power supply. The authors argued, that the correlations with the wind power supply curves are much higher than for the solar PV case, which underlines the need for smart charging in a solar-dominated energy mix [10].

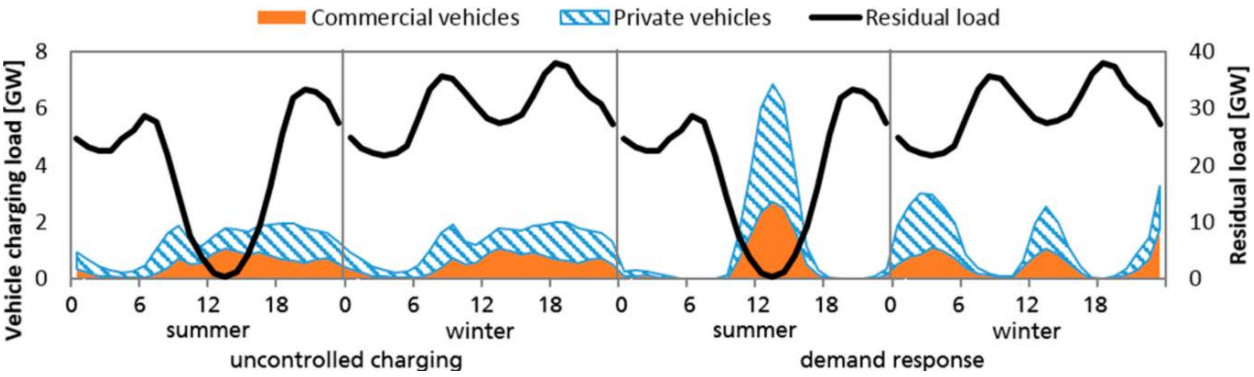

Figure 2-11: Average vehicle charging and residual load in 2030 with charging options at home, at work and in public [11].

Demand response (DR) schemes could largely influence the charging schedules of EVs. Gnann et.al. discussed the availability of EVs, meaning whenever they are connected to the grid, and would be available to provide flexibility, and found that, as soon as people have the ability to charge at work, EV availability is largely increased. This give the opportunity to orient the charging schedule on the residual load in the grid (which is the remaining load after the feed-in of decentralised renewable energy resources). Figure 2-11 shows the demand profile for EVs (commercial and privately used) during summer and winter season (according to their scenarios). Aligning the charging behaviour of EVs by demand response programmes to the renewable dominated residual load, if charged at home, at work and in public, would shift the charging towards noon during summer (high PV feed-in). During winter, the PV feed-in is far less shaping the residual load, which results in charging peaks during night and in a limited amount at noon.

Time-of-use tariffs are considered as one of the possible ways to limit electric vehicles impact on the grid. Some studies have estimated that these measures could limit the impact of EV charging on peak loads by 50% (as indicated in Figure 2-12). Time-of-use rates could not only create an incentive to reduce EV charging at peak system demand, they could further be used to reduce the risk of local congestions and voltage band violations in LV grids. Their use could thereby dilute the need for upgrades to flexible generation, transmission and distribution assets. It could also increase the economic interest of Vehicles-to-Grid (V2G). Indeed, EV can not only alleviate the problem caused by their combined charging at peak time via smart charging, but they can also actively provide energy to the grid at suitable times via V2G.

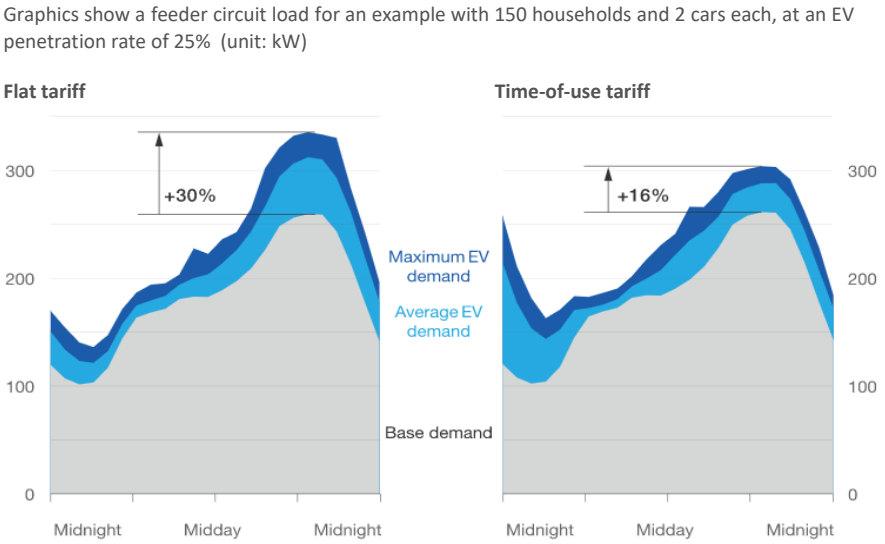

Figure 2-12: Load shape for a typical feeder with 150 houses at 8 MWh per year [7].

Vehicle-to-grid (V2G)

Vehicle-to-grid refers to the possibility of electric vehicles to offer some flexibility service to the grid by reinjecting (for instance during peak times) electricity they have charged before (during off-peak periods). Technically, the owner's vehicle becomes a self-contained resource that can manage the power flow (charge and discharge) according to the needs of the distribution network operators (DSO). Optimally, EVs would charge during the night or during the afternoon when there is excess of vRE and discharge during peak hours, especially in the morning and the evening – considering the supply balance only. Figure 2-13 illustrates this principle.

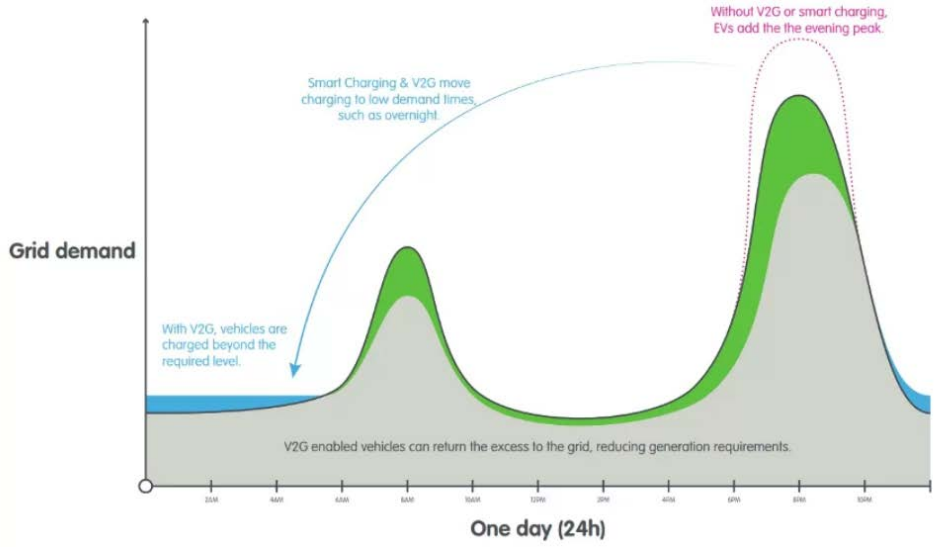

Figure 2-13: Demand scenario with and without V2G technology [12].

According to IEA, even accounting for all the different limitations, around 5% of total global EV battery capacity could be available for V2G at suitable times. Despite being a very small share of the total EV battery capacity by 2030, the total technically available potential for V2G deployment exceeds the additional generation capacity required to meet peak demand in almost all major EV markets, including

European Union, and would be available to compensate lower renewable production when necessary (see Figure 2-14).

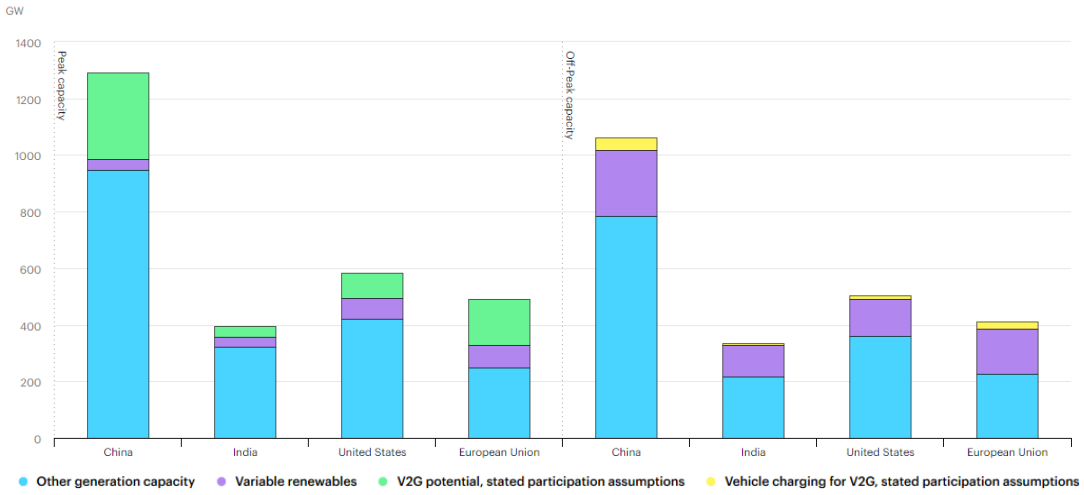

Figure 2-14: Vehicle-to-grid potential and variable renewable capacity relative to total capacity generation requirements in the Sustainable Development Scenario, 2030 [13].

Smart charging and vehicle-to-grid can significantly reduce peak load, limit curtailment and decrease CO_2 emissions. According to a study published by IRENA [14] on a solar-dominated energy mix, especially in case of V2G deployment, average short-run marginal cost can be reduced up to 13% compared to business as usual (Figure 2-15). Such actions can help displace more expensive and often more carbon intense generation assets, as well as lowering electricity prices by easing the integration of zero marginal cost technologies.

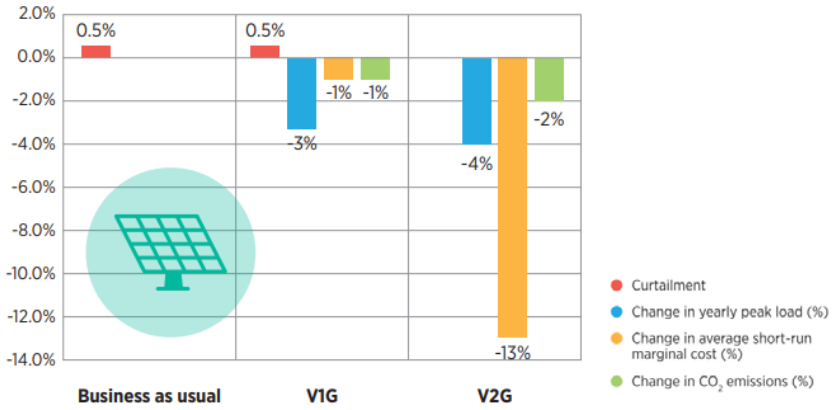

Figure 2-15: Short-term impact of EV charging [10].

Nevertheless, unlocking the full flexibility potential of electric vehicles through dynamic controlled charging (V1G) and vehicle-to-grid services (V2G) will require the adaptation of regulatory and market frameworks. Various challenges remain to optimize synergies with variable renewable generation. But electric vehicles smart charging, as well as V2G technologies, remain a promising way to balance renewables, limit grid reinforcements and manage congestion at the distribution level in a smart and digital way.

c) Restrictions

Smart charging and V2G applications depend on the availability and willingness of electric vehicles users. Some basic concerns include range anxiety and compromising comfort and potential battery degradation. EV owners might also be confused regarding different concepts (smart charging and V2G).

Regarding availability, this depends on the time the EVs remain plugged in at charging stations while not driving. Hence, Gnann et.al. modelled the share of plug-in EVs (for a Tuesday in this example) following three Scenario: S1 - private cars charge at home / commercial at work; S2 – additional to S1, private cars charge at work; S3 – additional to S2, EVs can be publicly charged. The resulting availability can be seen in Figure 2-16.

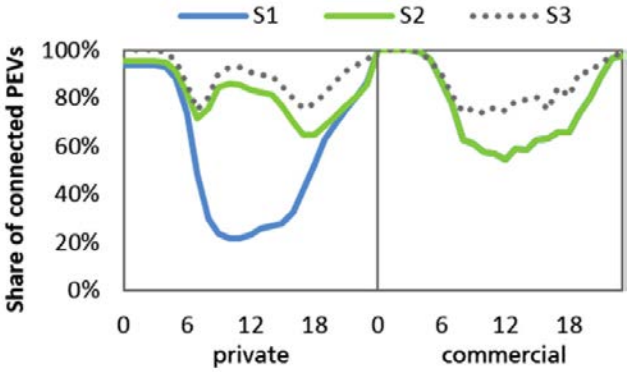

Figure 2-16: average shares of connected EVs for private and commercial use

To increase the acceptance of such new charging concepts, longer autonomy, fast charging as well as deployment of public charging infrastructures have to be progressed. In addition, intelligent exchange of information, standardised communication protocols through smart meters and other intelligent infrastructure will be needed. Aggregators acting as middlemen between EV users, utilities and network operators will also be an essential part of this nascent ecosystem. Developing the right market design, business models and economic incentives will be critical to empower citizens and allow them to fully benefit from new technologies. An exemplary contractual relationship scheme is depicted in Figure 2-17. In this framework, the development of national/European standardised procedures to share and access the data from individual consumers will increasingly be needed.

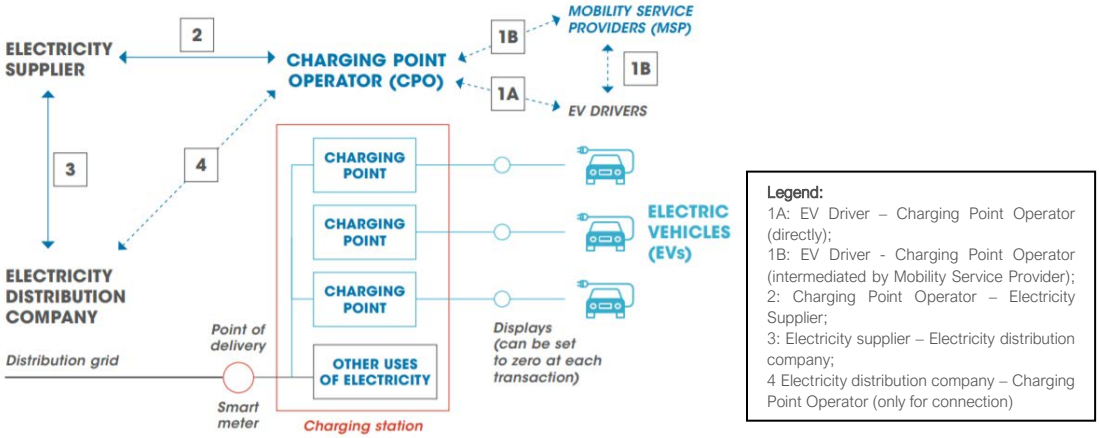

Figure 2-17: Contractual relationship between actors involved in electric mobility [15].

2.3 Photovoltaics and decentralised storage

Electricity storage combined with solar PV brings several benefits to residential customers. The installation of a solar battery provides a mean to extend the use of solar energy beyond the times of solar generation (e.g. making PV electricity available during night times). Increasing the share of self-consumption will be the main driver for small-scale energy storage in Europe, since the consumption of own PV generated energy is financially more appealing compared to grid feed-in (in many EU countries). While typical on-site solar systems can achieve a physical self-consumption rate of around 20 to 35%, smart solar and storage prosumers can even reach a 60 to 90% ratio. The aggregation of prosumers' loads and battery flexibility can provide services to the grid, however, the potential for flexibility will be intrinsically limited since storing and discharging electricity to the grid will (likely) be economically less interesting than self-consumption.

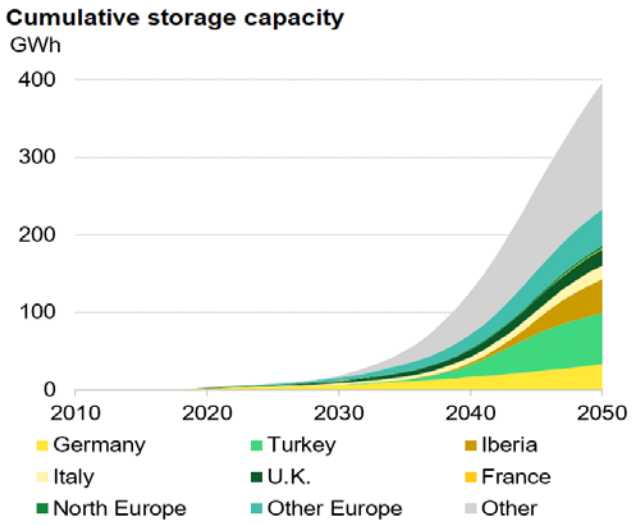

Figure 2-18: cumulative storage capacity [16].

The small-scale residential energy storage capacity will be part of the generally expected growth of storage capacities worldwide, driven by the rising needs for flexibility, indicated in Figure 2-18. Flexible energy storage, from a grid perspective, is useful when there are periods with surplus energy production, or periods with high demand and low supply. One of the potential methods for storing electrical power at LV are the above mentioned flexible storage batteries. Depending on the chemical concept, their capacity and efficiency differ. Currently lithium-ion batteries have the largest storage capacities, of the established battery types, and have up to 90% efficiency. However, compared to large scale storage concepts on grid level, their capacity is limited. They can be implemented mainly in households to balance when there is high electricity demand, or in micro grids, due to their high cost.

According to SolarPower Europe's new European Market Outlook For Residential Battery Storage report [17], currently only 7% of installed solar panels are coupled with battery storage. Maximum battery energy storage system (BESS) capacity remains concentrated in Germany, with close to 500 MWh installed. Followed by Italy, the United Kingdom, Austria and Switzerland. Altogether, the five countries represent over 90% of the European market. The forecasted decrease in battery prices combined with the continuous rise in electricity prices should lead to a large integration of residential batteries in European power mix.

a) Characteristics of load curves:

Photovoltaic battery storage can be operated in different ways, affecting the resulting load curve of the PV system. Figure 2-19 indicates 4 potential modes of operation:

1) The direct charging option, which might result in the steep rise of the PV feed-in once the storage is fully charged, being rather counterproductive.
2) The delayed charging, lowering the peak production around noon but grid operators still would need to reserve the full grid capacity, since the reduction would not be effective once the storage is fully charged (no additional grid capacity liberated).
3) Peak shaving, which would have the same effect that curtailment, if the max. active power is limited to a fixed certain share, which would liberate grid capacities. But opposed to a curtailment, where the capped power would result in a loss of energy yield, the storage could take up the capped energy production, to be used at a later stage.
4) The forecast-based charging, smartly limiting the peak power and optimising the self-consumption.

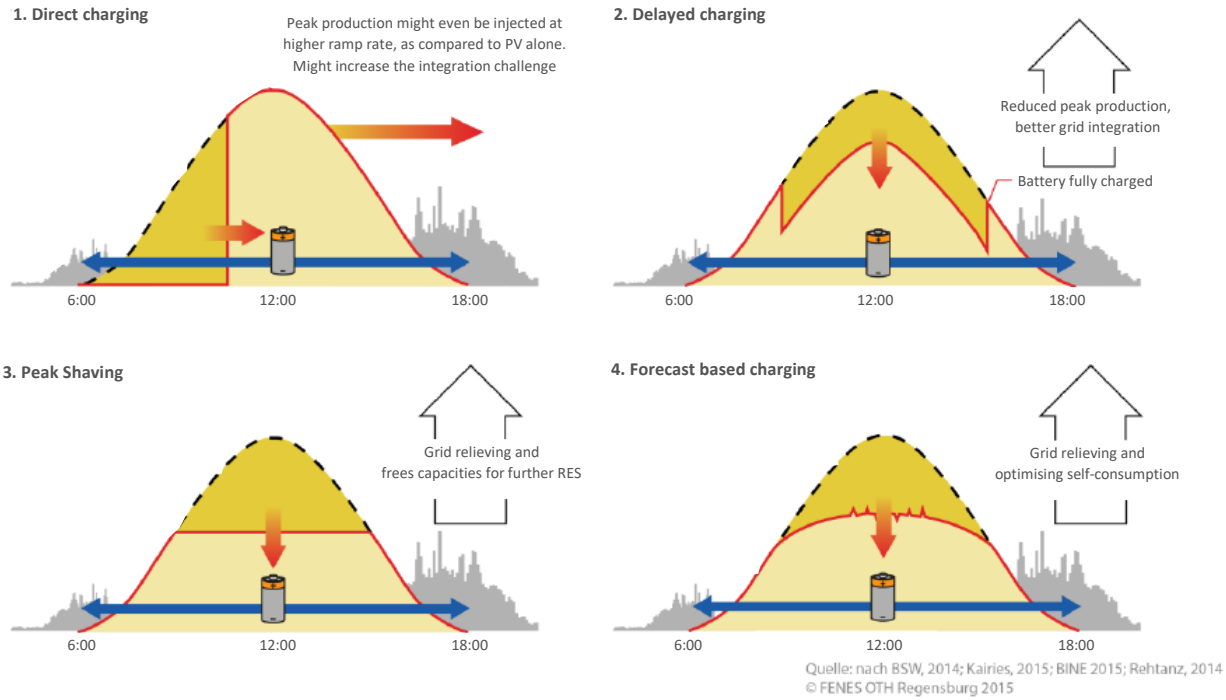

Figure 2-19: different way of operation for decentralize PV connected battery storage systems [18]

b) Potential flexibility provision type - buffering

Battery energy storage systems can be used for multiple applications in the power system, such as storing excess renewable generated energy for later consumption, wholesale market arbitrage or providing ancillary services to the grid operators. Providing reserves for frequency control, i.e. supporting the stability of the grid frequency, is one of the applications that has the highest value for a battery storage system. In Europe, Germany is currently the most developed market, in terms of residential battery installations.

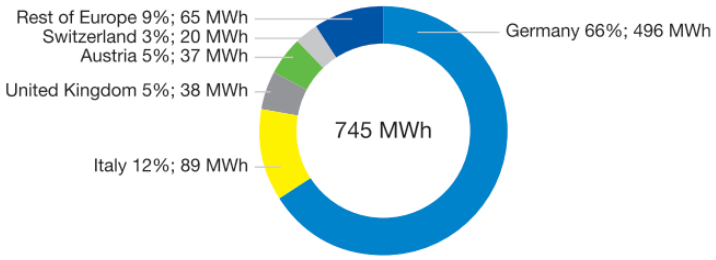

Figure 2-20: Battery energy storage markets (new installations 2019) – Europe's Top 5 [17]

In Germany, battery manufacturer Sonnen has been granted pre pre-qualification to enter Germany's Primary Control Reserve (PCR) market by grid operator TenneT, for its battery energy storage units installed across the country. If every solar home in Germany, around 1.5 million, was equipped with a Sonnen-Batterie, the power capacity would add up to 4.5 GW, with an energy capacity of 15GWh. Such a virtual power plant (VPP), would be equivalent to four large thermal power plants or the equivalent to the entire capacity currently being used for PCR across the European continent.

In the UK, new services such as dynamic containment frequency response service was launched last year. Due to challenging prequalification requirements, the service is currently undersubscribed allowing 280 MW of batteries to bid on this market each day. Battery domination is likely to persist, in these fast frequency response (FFR) services, due to very fast reaction time in milliseconds. Dynamic containment prices settled around an unofficial floor price of 17 pounds/MW/h. Market participants will seek alternative opportunities if prices are lower and National Grid (TSO) rarely accepts higher bids [16].

c) Restrictions

Restrictions on operational level, which should be considered when estimating availability of flexibility for PV-battery storage, or when planning its use, are:

i. storage charging state, when battery is fully charged or empty it could only deliver flexibility in one direction;
ii. conflict of interest between storage owner (optimising self-consumption) vs. flexibility aggregator
iii. limitations in dis-/charging cycles per time period – to maintain battery health

From an economic perspective, according to some studies, the return on investment in battery energy storage systems is often hard to reach in ten years, the typical battery warrant from OEMs. Also, technical preconditions for flexibility provision, as the roll out of smart meters, are lagging behind in several countries [17].

Furthermore, although there are positive examples, as the ones mentioned above, in many European countries, the regulatory and market conditions are not yet established to provide flexibility from BESS, and it lacks tangible business cases. Another problem is the potential saturation of frequency services with large battery and DSM deployment. The example of Germany, where the prices have dropped in parallel with growing residential battery installations, highlights this phenomenon (Figure 2-21).

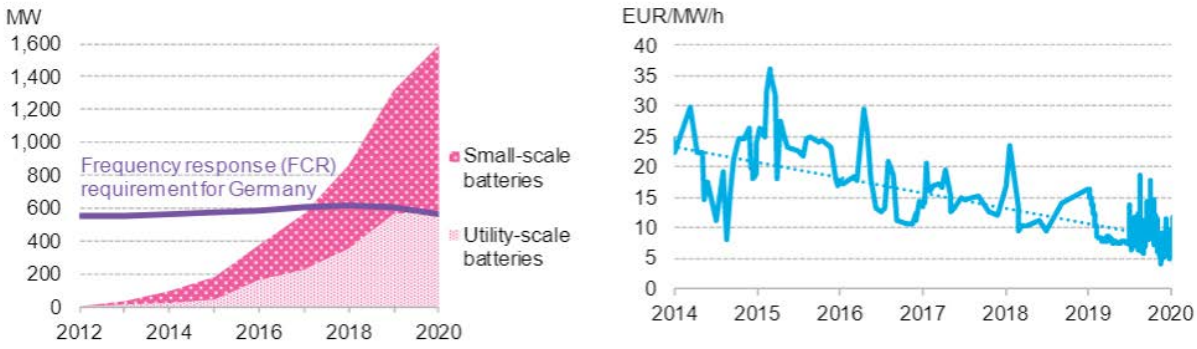

Figure 2-21: German cumulative battery build and frequency control reserve, left (requirement), right (prices) [16] .

Even in Australia's State Victoria, taking into account public incentives at retail prices that are significantly higher than in Europe, the economic operation of battery storage remains difficult, as depicted in Figure 2-22.

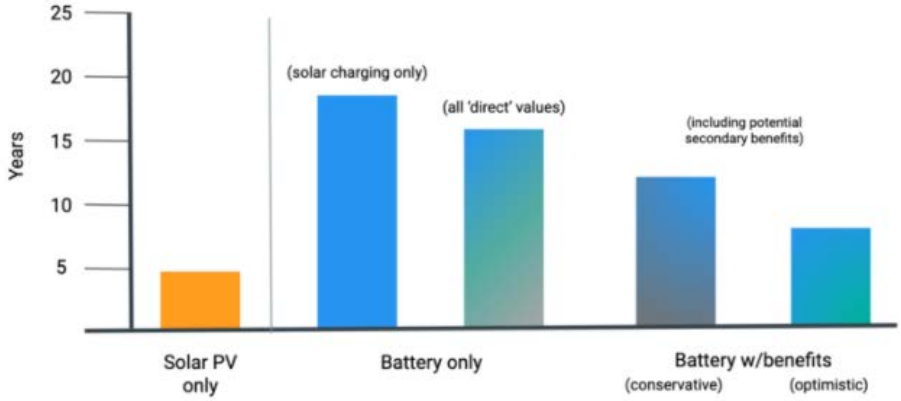

Figure 2-22: Estimates of battery storage system payback periods in Victoria under the state's battery incentive program and different value stream scenarios [19].

2.4 Other flexibility sources

2.4.1 Refrigerator

a) Characteristics of load curves:

Domestic fridge power consumption is typically between 100 and 250 watts. Over a full day operation, a fridge is likely to use between 1 to 2 kilowatt-hours (kWh). The demand is typically influenced by its storage volume, location, season, usage frequency, temperature set point, age and condition.

Contrary to other appliances, such as heat pumps or electric vehicles, refrigerators consume electricity throughout the entire day. They must be considered as appliances working 24 hours a day. In fact, the only time the compressor rests is when the inside temperature is lower or equal to the set temperature of the refrigerator.

Also, refrigerators are non-adjustable loads. They are interruptible, either switched on (with fixed power) or off. The duration of each "ON" and "OFF" cycle depends on user preference settings and temperature conditions. A typical load profile of a refrigerator is illustrated below.

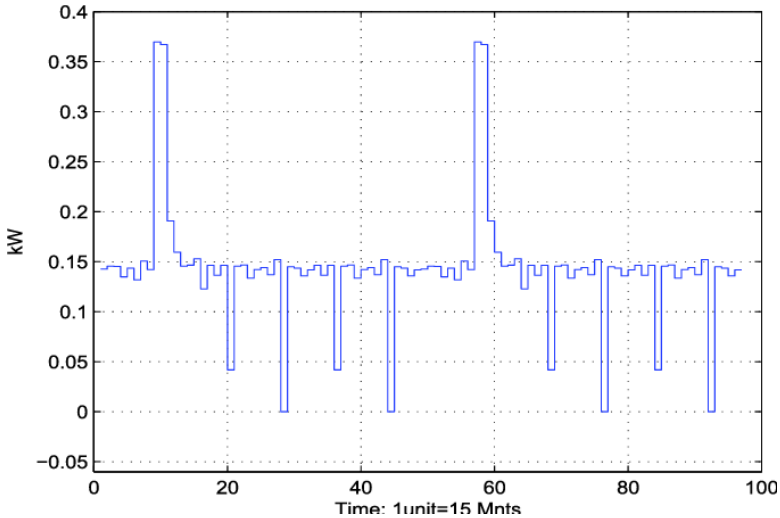

Figure 2-23: Load profile of refrigerator [20].

Their typical load pattern is made of regular spikes (up to 0.37 kW here) and load stop (0 kw) when the desired temperature is reached.

An average load pattern for refrigerators, independently of meteorological condition (Figure 2-24), has been realised by ADEME (French Environment and Energy Management Agency). It shows the lack of flexibility from a typical refrigerator/deep freezer. This is why refrigerators can be classified as continuous non-shift-able loads [20].

Nevertheless, some manufacturer produce refrigerators intended to be able to provide flexibility, such as LG[4] in 2011, with their so called "smart grid ready" product line. These devices could, for instance, adapt temperature set points in a narrow range, in order to shift load of the next compressor start to a later point in time – based on time-of-use tariff or external signals.

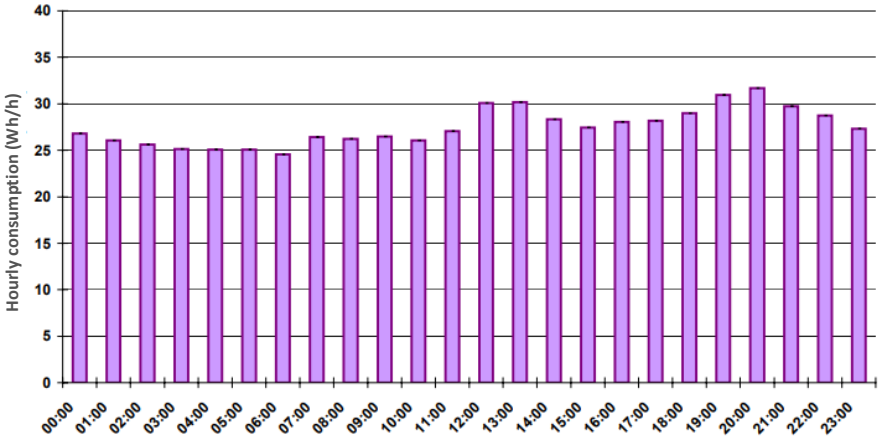

Figure 2-24: hourly averaged load curve of refrigerators [21].

[4] http://www.lgnewsroom.com/2011/04/lg-officially-launches-first-in-range-of-smart-grid-ready-smart-appliances/

b) Potential flexibility provision type - time shifting:

Some studies have tried to simulate the flexibility potential of refrigerators combined with a thermal storage system and a supply-following controller responding to fluctuating renewable generation. In a simulation, led by Taneja et. al [22], a typical home refrigerators was augmented with a network of thermocouples and power sensors to monitor its environmental and electrical operation.

In the simulation, the refrigerator is able to use its communicative capability to react to grid constraints and consume more electricity in time of low demand and excess of variable renewable energy sources, consuming less in period of peak consumption.

The results, illustrated in Figure 2-25, assume that with only 10% penetration of this kind of thermal storage, the load peak can be reduced by nearly 1 GW, representing around 10% of typical peak load from traditional generators in California.

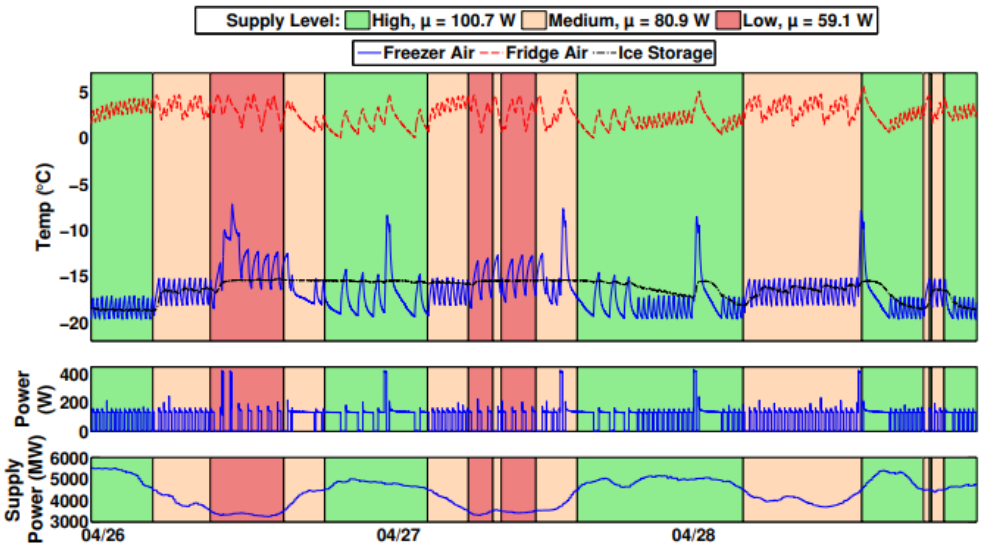

Figure 2-25: Operation of a thermal storage refrigerator as supply-following load. The refrigerator is works in three modes – High, Medium, and Low – based on the availability of renewable power by a real-time signal from the grid operator [22].

2.4.2 Washing machine

a) Characteristics of the load curve:

The typical load curve of a washing machine cycle will depend on several factors such as the program, the washing load and the energy class. The program often determines the selected temperature, the water demand and the spinning need.

Washing machines have a base load during the execution of a cycle, which can vary between 100 W and 120 W, depending on the washing machine type and brand. A washing machine cycle has four different states: switched off, base load, heating and spinning. The states are based on the operating principle. Spinning mode is hard to distinguish from base load in fifteen-minute data: the drum motor only spins for some minutes at full speed or spins lower than rated power.

Figure 2-26 below represents a modelled, aggregated load curve comprising 1000 washing machines, using a mean hourly load curve. We can see here a peak in the morning consumption towards 10:00 and a continuous decrease during the day.

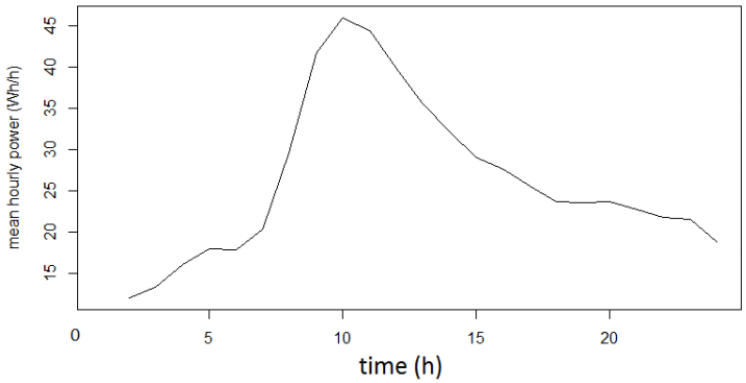

Figure 2-26: Example of a mean hourly load curve obtained by simulations of 1000 laundries for one year [23].

An average load pattern for washing machines, has also been realised by ADEME (French Environment and Energy Management Agency). It shows that the load curve is low during nights (22:00 – 06:00) and up from 07:00 steeply rises towards its peak around 08:00 to 09:00. During the day, the load profile progressively decreases, with a minor temporary rise between 19:00 and 20:00 (see figure below).

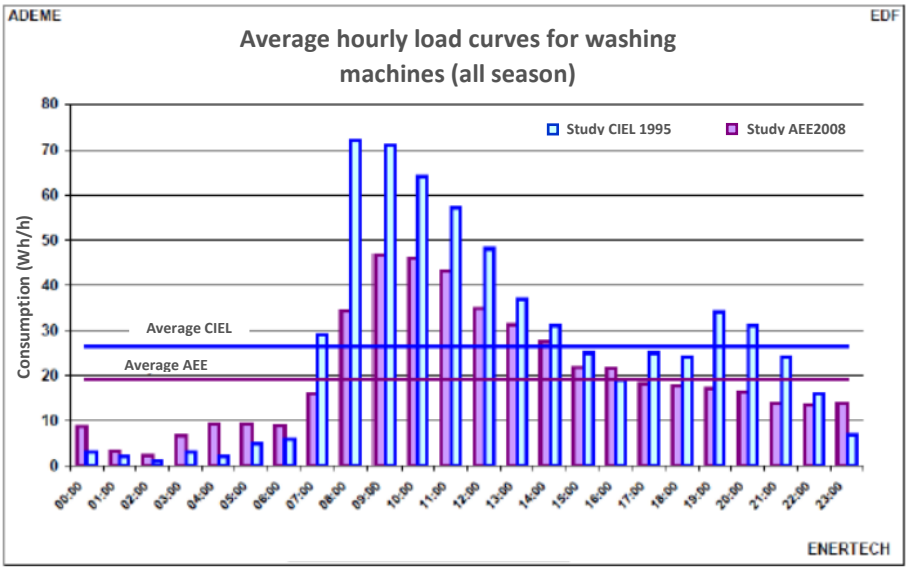

Figure 2-27: average load profiles for washing machines.

b) Potential flexibility provision type - time shifting:

Some analysis to evaluate their flexibility potential has been made by comparing the load patterns of customers with single retail tariff prices and the ones of customers with peak and off-peak tariffs. This results in higher demand during the night, when the prices are lower. But one can notice that the peak demand is very similar and also arises in the morning between 9:00 and 10:00 (see figure below).

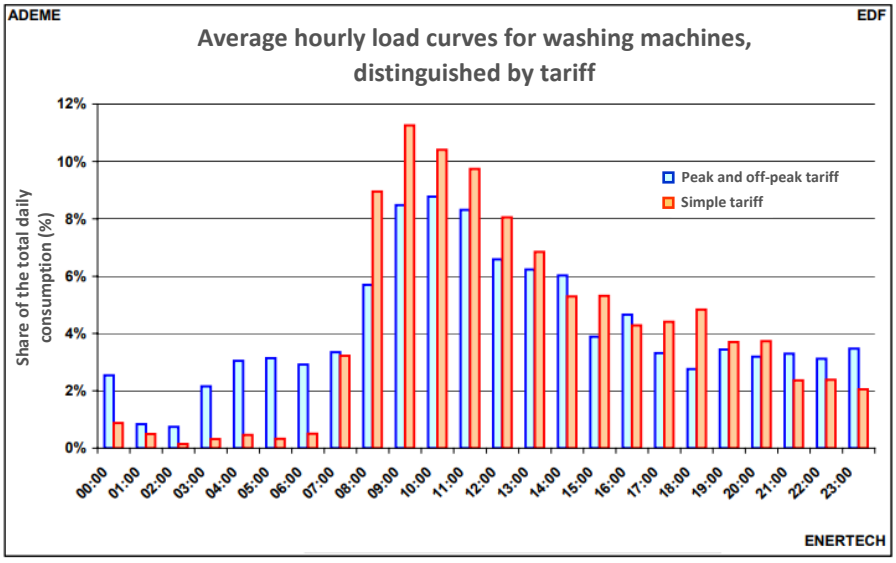

Figure 2-28: average load profiles for washing machines, single tariff vs. "peak / off peak" tariff.

The load consumption of washing machines could eventually be shifted but is not interruptible (at least not without compromising energy efficiency, washing performance and comfort). The progress in home automation can help end-users manage this kind of devices smartly. The consumers could then plan the start of their washing machine based on DA prices or real time messages from third-party service providers, triggering the washing process within a customer defined time window.

2.4.3 Dish washer

a) Characteristics of the load curve:

The determining factors for the load pattern of a dishwasher cycle are the washing programme and the energy class of the device. The programme can require extra water and has a temperature setting for washing and hot rinsing.

Dishwasher cycles can be broken down in four different states: wash, rinse, dry and off. The states are translated into the detectable states heating, base load and off. Heating covers washing and hot rinsing, while base load is mainly intended for cold rinsing. It takes the device in average approximately 105 minutes to complete all the cycles. During the operation of a dish washer, load may generally vary from maximum 1.2 kW to minimum 0.6 kW.

Boßmann et.al. published analysis data from 5000 households in Ireland, measured over almost 1,5 years [24]. The aggregated load profile for these households, isolating the data of the dishwasher operation only and normalised per household, shows a small peak in the morning during weekdays (Figure 2-29). A second peak appears in the beginning of the evening, independently of the day of week or week-end. The load pattern is then quite similar for weeks-ends even if a higher volume is evident on Sundays. There is no real seasonal effect regarding dishwasher load pattern, which is similar in winter and summer time.

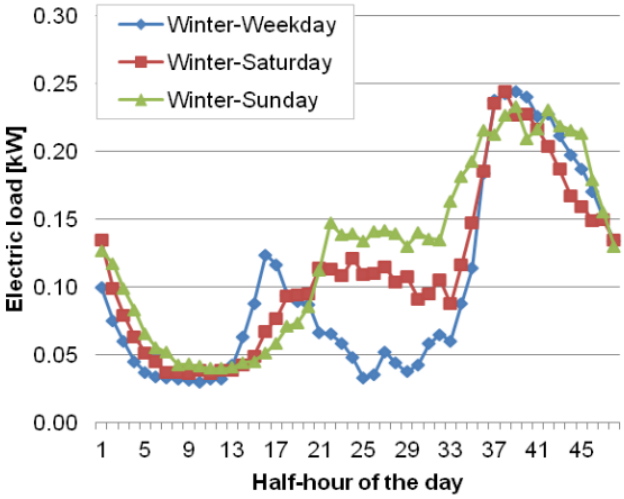

Figure 2-29: household load profile for their dishwasher operation [24].

b) Potential flexibility provision type - time shifting:

A study led by KU Leuven in Belgium [25] tried to model the flexibility potential from dishwashers in the country, besides others. According to them, the potential time shift for this kind of device is between 3 and 8 hours a day.

Although the availability of these appliances is low, in practice this could be compensated by large numbers of controllable appliances, leading to an aggregated potential for flexibility. Figure 2-30 shows the results of this analysis for time shifting (or rather blocking) the start of dishwashers for either 0.5 hour, 1 hour, 1,5 hours or 2 hours. The graphic shows the delay in the effective impact of setting the blocking signal for the different scenarios and the effect of a steep rise, once the blocking period is over. The absolute values account for all the devices in Belgium, available for participation at this point in time.

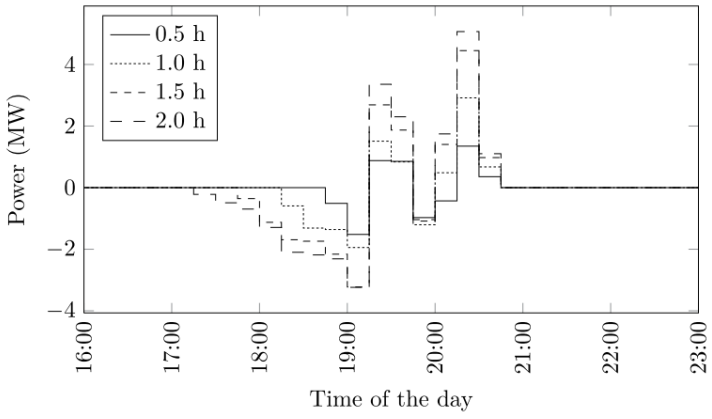

Figure 2-30: Load profiles for time shifting flexibility from dishwashers (in Belgium) [25].

The conclusion from these studies is, that using this device in a flexible way has a low impact on total electricity demand. Nevertheless, an aggregated flexible load could be useful in the case of congested distribution grid with low flexibility available.

2.4.4 Tumble dryer

a) Characteristics of load curves:

Tumble dryers are more and more common in European households. In Europe, 4.9 million tumble dryers were sold for domestic use in 2005. More than 40 million tumble dryers are estimated to be in use in European households nowadays. It has been estimated for the US, where 79% of households owned a laundry dryer, that drying alone accounts for approximately 7% of US electricity consumption.

The energy efficiency labelling system has shown to be effective in the development of more efficient products. A few years ago, most dryers were marked with a C label. Today, there are conventional tumble dryers marked with a B label, and some heat pump equipped dryers are even marked with an A label. According to the European Union, switching to one of the most efficient tumble dryers can reduce energy costs up to 50%. With more efficient tumble dryers, Europe will be able to save up to 3.3 TWh of electricity, equivalent to the annual final energy consumption of Malta.

The main energy consumption elements of a tumble dryer are the resistive heating element and the electric motor that spins the drum. Air is heated by the resistive element with a rated power between 1.8 and 2.5 kW. The energy consumption of the average load profile is considered to be around 2.46 kWh per cycle. An approximate cycle of a tumble dryer is illustrated with six power phases. The duration of each power phase is assumed to be 15 min.

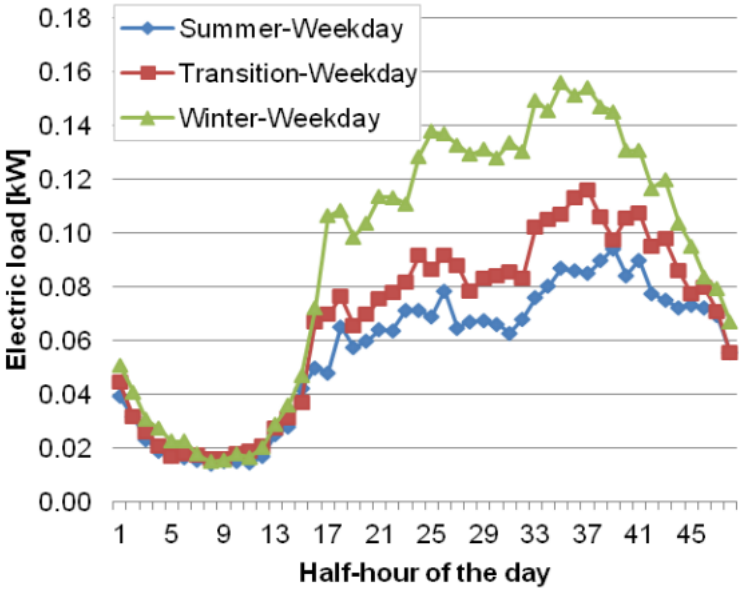

Figure 2-31: aggregated load profile for a dryer [24] .

The aggregated load curve for tumble dryers, based on the analysis of smart meter data of 5000 households in Ireland for the period of 1,5 years, normalised to the households, is illustrated in Figure 2-31. The curve shows the steep rise of the demand after 6:30 approximately, followed by a moderate rise from 8:30 to 18:00, and dropping again towards the night. The winter week-day depicts a much higher load for tumble dryers, as compared to the summer period. Since this is aggregated data for 5000 households broken down to the single home level, this can be explained by the fact that more people are drying their laundry outside during the summer.

b) Potential flexibility provision type - time shifting:

One of the potential features of smart appliances that could facilitate load shifting is the used of communication modules. In this configuration, equipped households could respond to external signals based on prices, grid constraints or renewable production to provide different services to the grid.
Labeeuw et.al. studied the effects of a delayed start, triggered by a remote signal, on the accumulated load of tumble dryers in Belgium (see Figure 2-32), delayed by 0.5 hours, 1 hour, 1.5 hours or 2 hours. In this example, it took longer until the full effect of all the available dryers for this time range was obtained since tumble dryers have rather long cycles and running dryers were not interrupted,. After the "recovery peak", when the dryers are collectively allowed to start, it also took longer until "catch up" effect was run out.

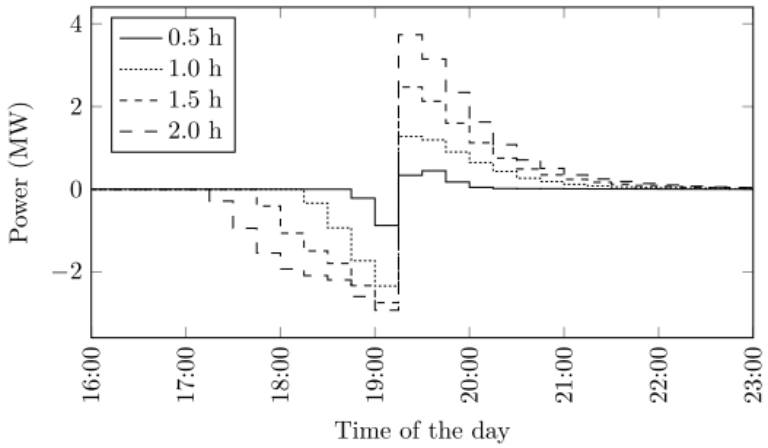

Figure 2-32: Impact of time shifting flexibility provided by tumble dryers [25]

A study published in 2014 in *Applied Energy* [26] studied the flexibility potential of tumble dryers (in addition to washing machines and dishwashers) and considered these devices as very suitable for DR, since the user acceptance for flexibility services by these appliances is high due to the effects on comfort are low and the ownership rate of households (in the UK) high. The load management features of this study are smart start and cycle interruption. The smart start feature allows the appliance cycle to be shifted for example from evening to night, avoiding peak electricity rates, as illustrated in the figure below.

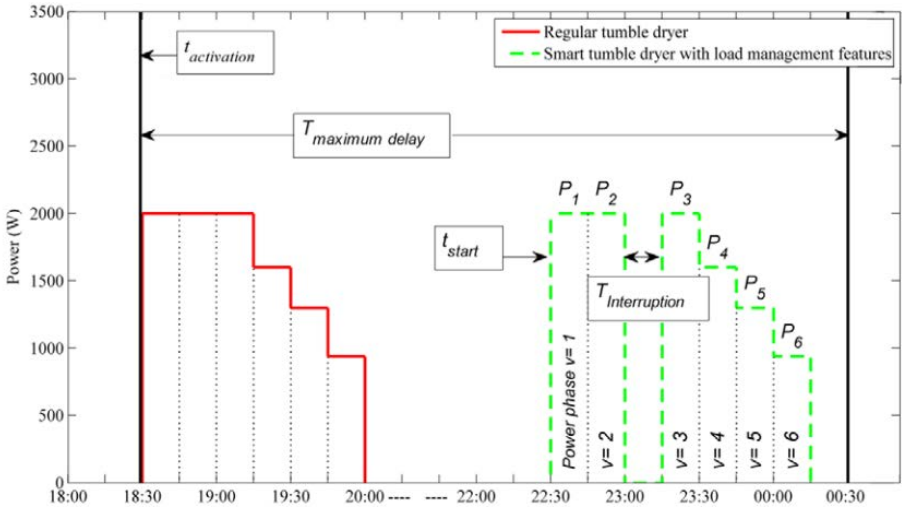

Figure 2-33: Tumble dryer load profile and flexibility provision via smart appliance features [26].

The results from this study indicated that the response of the considered appliances (washing machine, dishwasher and tumble dryer) is well suited to be integrated in the balancing services. The shifting and interruption of appliance operation, according to user preferences, resulted in a fast decrease in consumption at the system level.

Indeed, using only 20% of smart white ware appliance in the UK (washing machines, dish washers and tumble dryers) could provide as much as 1.5 GW of reserve power in the UK, or up to 54% of the operating reserve requirements of the UK power system, depending on the time of day.

3 Deterministic Flex Source Models

3.1 Flexibility metrics and parameter

The widespread uses of various demand-side flexibility resources will create challenges and opportunities for the distribution system operators (DSOs) to improve their task of power supply. Along with enabling digital technologies, pro-(con)sumers can adjust their energy profiles, motivated by incentives or price signals. In turn, this will make the demand response (DR) and demand side management (DSM) methodologies some of the reliable solutions to problems caused by renewable and distributed energy sources. Modelling techniques to capture such flexibility resources are important for planning, scheduling, and real-time operation. According to [27], there are three essential directions in order to be successful in developing these methodologies, including:

1) Tractable models for individual device/consumer level, where the model is able to capture the most important characteristic of power consumption, but the model is still tractable for design and analysis.
2) Aggregated models to show the aggregate behaviours of large number of consumers.
3) Data-driven models based on identification and validation with actual data.

In order to develop these models in a comprehensive manner, it is important to investigate different aspects of flexibility metrics and parameters associated with each of the flexible resources, such as fridges, freezers, washing machines, electric vehicles, heat pumps. Therefore, it is important to take these characteristics of flexibility, i.e. weather, time and geographical dependencies, into account to enable the development of demand-side flexibility for network and system services.

3.1.1 Metrics for flexibility

Harvesting (demand-side) flexibility implies tackling uncertainty which is usually simplified due to its mathematical complexity, such as by defining it in the form of a confidence interval [28], [29]. Flexibility metrics are therefore included in the market clearing formulations to incorporate the cost of remunerating its providers.

Flexibility metrics were traditionally presented in form of *magnitude*, *response*, and *frequency* [30]. Magnitude metrics will capture the maximum positive or negative change, in a defined direction, provided by the sources or loads. Ramp response characteristics can be used to capture the dynamics of flexibility resources, measuring maximum magnitude change over various time scales. According to NERC [30], frequency metrics measure the frequency of ramp events for various sizes. Flexibility measurement based on econometrics was also achieved/demonstrated in [31], where the flexibility calculation is determined by unit capacity, minimum generation levels, start-up time, time horizon and production level, calculating both flexibility from offline and online units. There has been research concerning procurement and utilisation of flexibility in the power system in general, and the distribution system in particular. The flexibility requirements for proper wind and solar power integration in Europe are assessed in [32]. From this research, the *ramp envelopes*, the *net load ramps*, and *ramp magnitude* are found, and the resulting scenarios facilitate quantifying flexibility requirements. It has been shown that, when the share of wind and solar energy surpass 30% of the load consumption, the flexibility requirements increase abruptly.

To extend the concept of operational flexibility into demand flexibility, [33] addressed a possible metric framework, integrating the characteristic of comfort management and building operation in possible flexibility services. In this research, a flexibility action, i.e., flexible power P_f in $[kW]$, can be described as: a) an increase in the power demand (up regulation); and b) a decrease in the power demand (down regulation) with the following main (electricity) metrics:

I. Ramping rate (ρ) $[kW/min.]$, i.e. how fast the flexibility asset can react;
II. Power capacity (π) $[kW]$, i.e. how much power can be delivered as flexibility power;
III. Energy capacity (ε) $[kWh]$, i.e. how much energy can be delivered during the flexibility action.

In this particular research of exploiting flexibility from building thermal mass, two other metrics were considered, including the comfort capacity (σ^+) $[min]$ and the comfort recovery (σ^-) $[min]$ which reflect the building physical characteristics, e.g. construction type, area, or location. Depending on the nature of a flexibility source, this set of metrics should be adapted.

3.1.2 Flexibility Parameters

Flexibility resources can be classified based on their capability of adjusting their energy profiles. According to [34], [35], typical classes of flexible units are :

- Uncontrollable;
- Curtailable;
- Time shiftable;
- Buffer time shiftable;
- Buffer;
- Buffer-converter.

By consolidating the profiles of these units, either price-based or incentive-base demand response (DR) programs can be deployed to procure the necessary flexibility. This, however, needs a consistent set of generic, formal device data models and associated parameters [35]. These parameters need to be generic and abstract to cover the most important characteristics of each flexibility class. Some main attributes of the parameters used in [34], [35] are presented in Table 3-1.

Table 3-1: Main parameters used for each flexibility unit class.

Class	Main parameters			Examples
	Availability	Power	Capacity	
Uncontrollable	[Starttime, Endtime]	[Static]	Constant	Television, lighting
Curtailable	[Starttime, Endtime]	[Min - Static]	Variable	Solar PV
TimeShiftable	[Starttime, Startbefore, Endtime]	[Static]	Constant	Washing machine, dishwasher
BufferTimeshiftable	[Starttime, Startbefore, Endtime]	[Min – Static – Max]	Variable	EV (smart) charging, freezer
Buffer	[Starttime, Validtime, Endtime]	[Min – Static – Max]	Variable	Battery storage
Buffer-Converter	[Starttime, Validtime, Endtime]	[Min – Static – Max]	Variable	Heat pump, water-tank storage

Depending on the chosen method to exploit demand-side flexibility, the flexibility parameters can be used in various forms, which have some advantages as well as disadvantages. In case of day-ahead (time-of-use) price scheme, all flexibility unit profiles can be stacked on top of each other with full knowledge of associated parameters to ensure the synchronization with automated demand response [34]. The drawback is a lack of controllability at the customer premise, especially when the flexibility is higher than needed. On the contrary, real-time prices can be used to stimulate user responses, depending on priority and availability of user's devices [36]. This however lacks transparency on how to determine an appropriate price to end-users and its alignment with other market prices. Furthermore, there is no feedback of the actual response, which can only be learned in the upcoming steps. In between these two typical schemes, incentive based methods are considered to accommodate both, the functionality perspective of involved stakeholders, e.g. DSO, and flexibility/comfortability of the user. The underlying concept is to translate incentives on the device level into a (day-ahead) scheduling problem to be solved by tailor-made optimisation algorithms with low computation power [35].

Due to limited flexibility resource from the demand side, the above so-called (market-based) indirect control methods might resolve network problems, such as congestion, only partially. A combination with direct control methods is therefore important to secure the required flexibility for congestion management [37], with high certainty and reliability. The following sections will explain, in more detail, the aspects of flexibility modelling of this solution.

3.2 Model Formulation

3.2.1 Nomenclature

π_t	Price
$P^0_{t,a}$	Original (benchmark) load of appliance *a* at time *t*
T	Set of all time steps in a day
A^{bf}	Set of buffer appliances
x_a	Maximum buffer time for appliance *a*
S_{tf}	Transformer loading at time t
S_{rated}	Transformer's rated power
π_{adj}	Price adjustment
τ	Time shift of appliance
$\tau_{\mathrm{a,min}}/\tau_{\mathrm{a,max}}$	Minimum and maximum allowable time shift for appliance a
A^{ts}	Set of all time shift appliances

3.2.2 Foreword

This chapter focuses on the tractable models for individual device/consumer level as mentioned in section 3.1. Flexibility, in the case described in this chapter, is enabled via market-controlled demand response, where the households respond to dynamic prices sent by the aggregator, by adjusting their initial load profile [37]. The same principle can be applied to different DR schemes by replacing the dynamic prices with appropriate incentives.

To enable load modelling, the load curves of the home appliances can be generated with a bottom-up Markov Chain Monte Carlo approach as discussed in [12]. The preferential household load curve can be determined comprising of different devices. The devices are modelled differently for each type of

flexibility classes as mentioned in Table 3-1. The EV, heat pump and freezer are categorized in the Buffer (including Buffertime, shiftable, and Buffer-Converter) classes. The Dishwasher and washing machine belong to the Time-shiftable class, while solar PV is considered as the Curtailable class. The Uncontrollable class, i.e. base load, does not respond to dynamic prices.

The following sub-sections explain how the household load is subjected to the dynamic price from the aggregator as well as how the appliances in the household react to a dynamic price.

3.2.3 Flexible Load Response Based on Dynamic Prices

From [37], the detailed models of Buffer, timeshiftable, and curtailable flexibility classes are formulated as follows:

1) Buffer Response Modelling

$$\min_{P_{t,a}} \sum_{t}^{N_T} \pi_t \times P_{t,a}\,, \qquad \forall a \in A^{bf} \tag{3-1}$$

subject to,

$$\sum_{t=k}^{k+x_a} P_{t,a} = \sum_{t=k}^{k+x_a} P^0_{t,a}\,, \qquad \forall a \in A^{bf}, k \in T \tag{3-2}$$

$$P_{t,a} = P^0_{t,a}, \qquad t \notin [k, k+x_a], \forall a \in A^{bf} \tag{3-3}$$

$$\min_{t\in T}\{P^0_{t,a}\} \le P_{t,a} \le \max_{t\in T}\{P^0_{t,a}\}, \qquad \forall a \in A^{bf}, k \in T \tag{3-4}$$

The objective of optimization in Equation (3-1) is to minimize the cost of electricity, which consists of the electricity price π_t times the power consumption at the same hour $P_{t,a}$. The decision variable of optimization is the consumption level $P_{t,a}$ at each hour. Constraint in (3-2) forces the total energy consumption over the period: $k \le t \le k + x_a$ to stay the same, thus, allowing energy to be only redistributed within this period. Therefore, the parameter x_a defines the width of the time window in which energy consumption can be redistributed. The value of x_a is different for each appliance. Constraint (3-3) prevents any change in power consumption outside the period $k \le t \le k + x_a$. Constraint (3-4) forces the adjusted energy consumption to remain within reasonable limits, such as the limits of the benchmark load throughout the whole day.

2) Timeshiftable Response Modelling

$$\min_{\tau} \sum_{t=1}^{N_T} \pi_t \times P_{t+\tau,a}\,, \qquad \forall a \in A^{ts} \tag{3-5}$$

subject to:

$$\sum_{t=1}^{N_T} P^0_{t,a} = \sum_{t=1}^{N_T} P_{t+\tau,a}\,, \qquad \forall a \in A^{ts} \tag{3-6}$$

$$\tau_{min,a} < \tau < \tau_{max,a} \quad \forall_a \in A^{ts} \tag{3-7}$$

The objective of optimization in Equation (3-5) is to minimize the cost of electricity. In contrast with the previous device type, the decision variable now is the time-shift τ. This refers to the amount of time the device is delayed, or advanced. Equation (3-6) ensures that the total energy consumption after shifting stays the same as before shifting. Equation (3-7) constrains the time-shift within two $\tau_{a,min}$ and $\tau_{a,max}$. These limits are defined by the nature of the appliance a and consumer preferences. It is worth mentioning that shifting a load beyond the 24th hour of the day $t + \tau \geq 24$ pushes this load automatically to the first few hours of the next day.

3) Curtailable Appliances Response Modelling

$$\min_{P_{t,PV}} \sum_{t=1}^{N_T} \pi_t \times P_{t,PV} \tag{3-8}$$

subject to,

$$0 < P_{t,PV} < P_{t,PV}^0 \quad \forall t \in T \tag{3-9}$$

The objective of optimization in Equation (3-8) is to maximize the revenue from selling the PV's energy yield. Since P_{PV} is defined as negative consumption, the revenue maximization is expressed as cost minimization. Constraint (3-9) bounds the PV's generated active power during time t to the benchmark value for the same hour, which corresponds to the maximum power point tracking.

3.2.4 Market Based Price Adjustment

Based on the model described above for the optimisation of the load profile, in order to adapt to the flexible price, the device agents on level of each household participating in the DR scheme, will minimize their energy costs. During this optimisation based on electricity prices, carried out by several consumers in the LV grid taking similar decisions, a congestion problem might happen due to high flexible load during a time where electricity prices are low –. as a result, transformers may become overloaded. In such cases, the household load profiles will be re-adjusted. With an iterative process, the aggregator sends a new control signal, and the device agent will react by optimizing each device using (3-1) - (3-9). The adjusted price signal $p_{t,new}$ is obtained as follows:

$$\pi_{t,new} = \frac{1}{5} \sum_{tf=t-2}^{t+2} \begin{cases} \pi_t + \pi_{adj} & : \ S_{tf} \geq S_{rated} \\ \pi_t & : \ \text{otherwise} \end{cases} \tag{3-10}$$

where, p_{adj} is the incremental price adjustment, S_{tf} is the transformer loading at time t and S_{rated} is the rated power. After every price adjustment, the system apparent power is recalculated using the optimized load profile with the adjusted price $p_{t,new}$. The aggregator will run 20 iterations with the same optimisation routine, and if the load is still higher than the transformer rating, there will be no new control signal, the load will not be subject to change and other methods need to be investigated/explored.

3.3 Numerical Simulation

The study is performed on a modified IEEE European LV test feeder with 55 houses connected in single phase, with base load and flexible load variations. A 250 kVA rated transformer is used to supply the LV

network. There is also an additional LV feeder with an aggregated peak load of 150 kW assumed. The single line diagram of the IEEE European LV test feeder is shown in Figure 3-1. The simulation is repeated in 15 minutes time steps, giving rise to 96 time steps per day [37]. The simulation in this study is done using MATLAB file exchange [38] and the MATLAB Global Optimisation Toolbox [39].

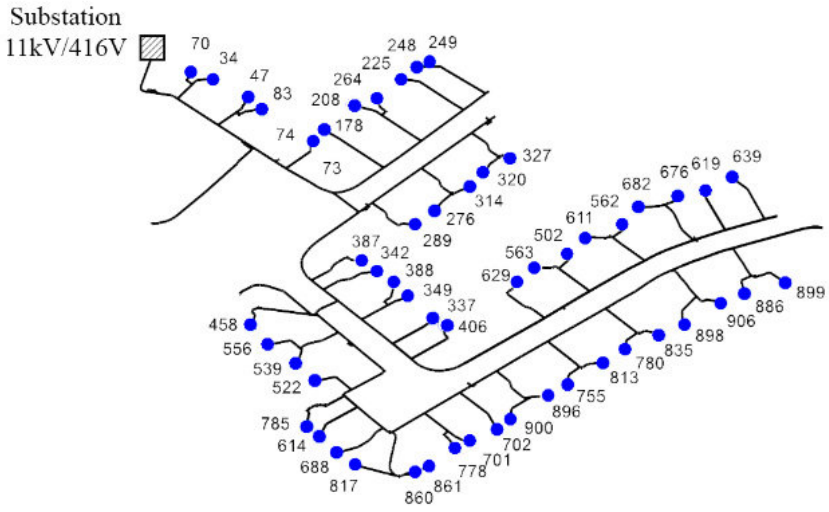

Figure 3-1: Topology of IEEE European LV network.

3.3.1 Effects of Dynamic Price

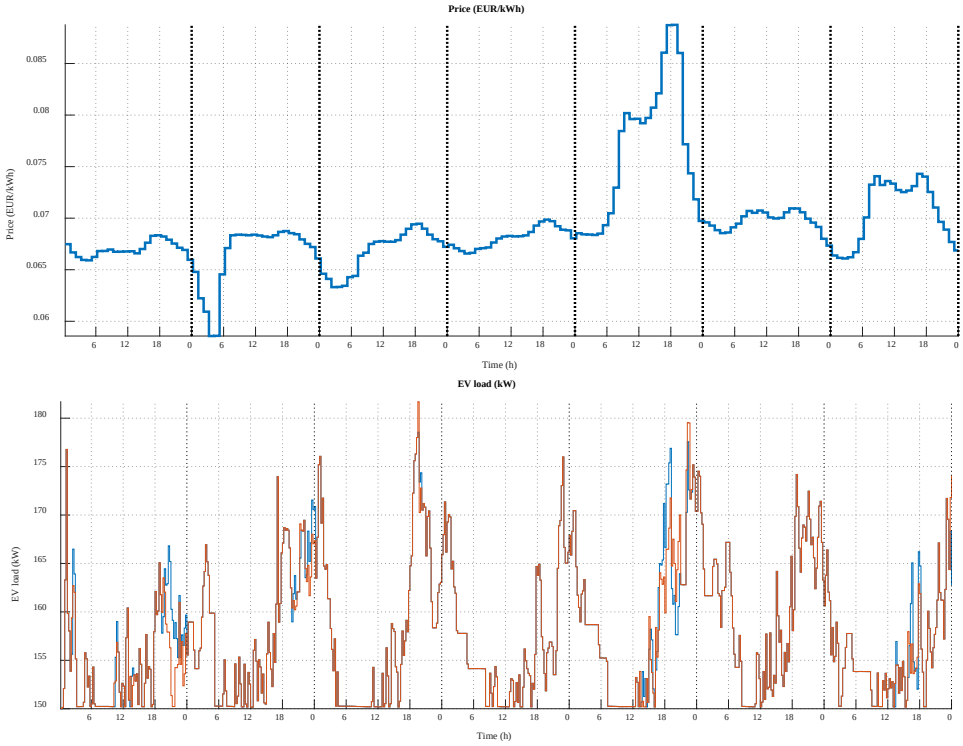

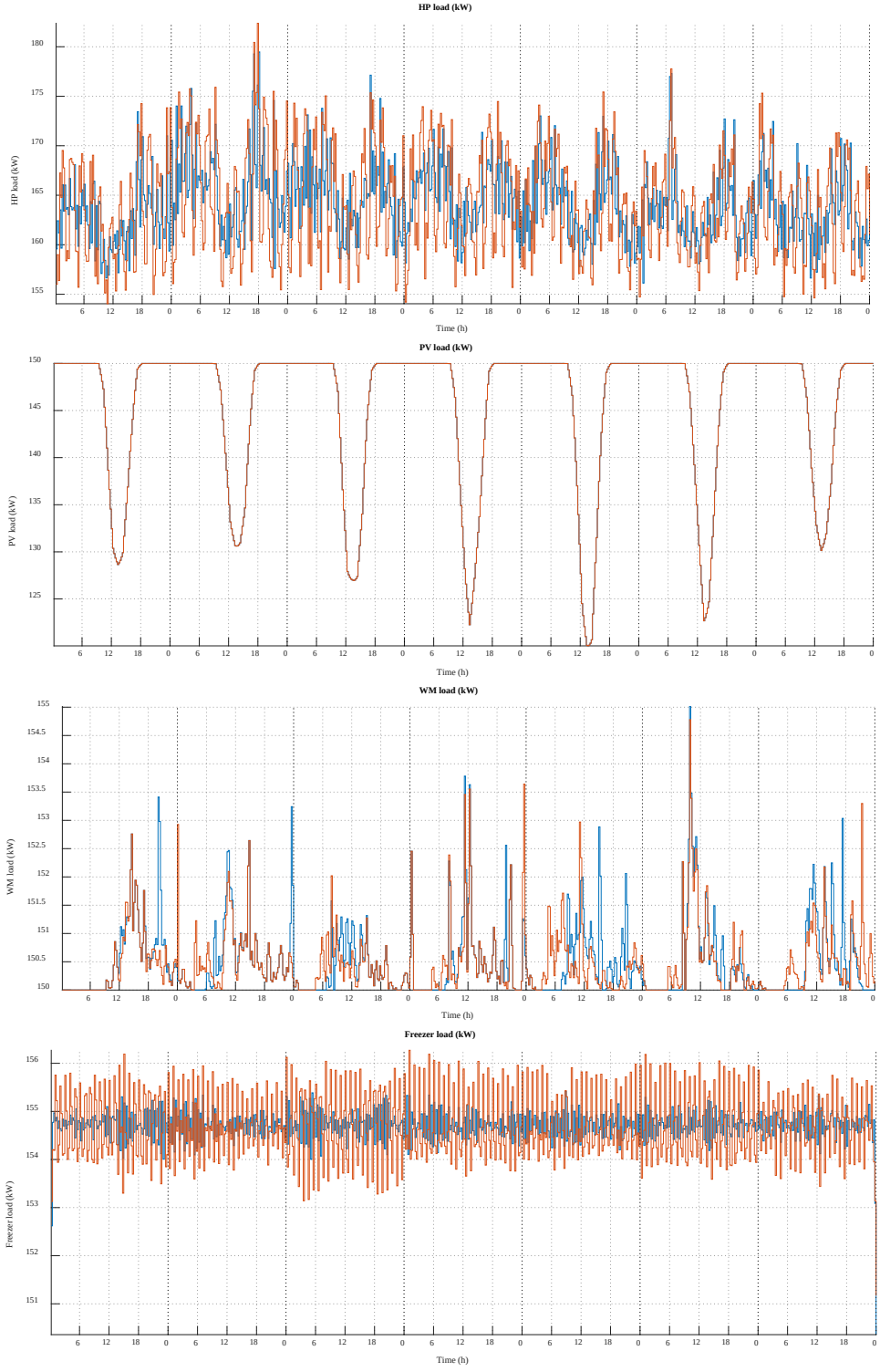
HP load (kW)
HP load (kW)
Time (h)
PV load (kW)
PV load (kW)
Time (h)
WM load (kW)
WM load (kW)
Time (h)
Freezer load (kW)
Freezer load (kW)
Time (h)

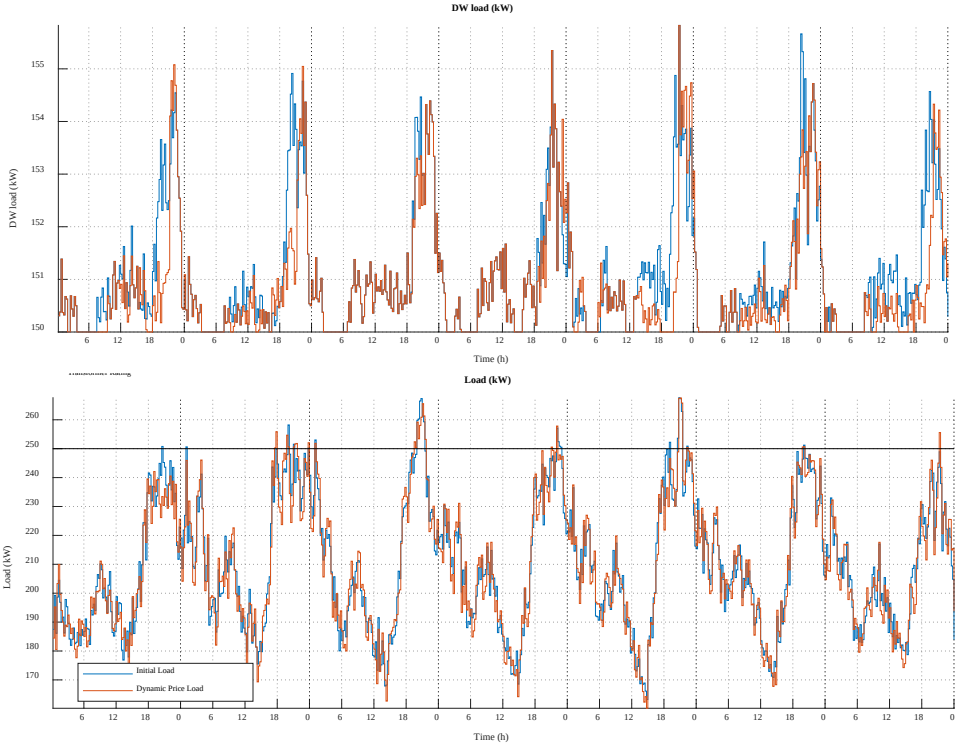

Figure 3-2 Load changes based on dynamic prices.

The simulation is done for a week. The resulting load differences for each flexible appliance, in response to dynamic prices, are shown in Figure 3-2. It can be seen that based on the dynamic prices and constraints, the flexible load will optimize and try to operate during a time where electricity prices are low (orange profiles), with an exception of PV (4th row from top, depicted as negative load). The maximum adjusted load for each corresponding flexible load is shown in the table below.

Table 3-2: Maximum adjusted load for each appliance based on dynamic prices.

Appliances	Maximum Adjusted Load (kW)	Occurrence Time
EV	8.9086	1st Day 21:00
Heat Pump	9.4355	3rd Day 08:45
Washing Machine	2.9505	7th Day 17:15
Freezer	1.2342	3rd Day 23:30
Dishwasher	4.1201	5th Day 20:30

From Table 3-2, it can be seen that the highest modified load pertains to the heat pump and the majority of loads have their maximum changes during the evening. The results are indicative to quantify the amount of flexibility for each appliance, though studies with real data are essential.

The total flexible load combined with the non-controllable load is also shown in the lower subplot of Figure 3-2. The figure shows that, using dynamic prices as control signal can, in some cases, help to reduce the peak load. As in the 1st day, before the load profile is subjected to the optimisation function; the peak load is 1.0031 pu. which is slightly above the transformer rating. The peak load after optimizing based on the dynamic prices is 0.9684 pu. However, this is not always the case in this study, as it can be seen towards

the evenings of days 3 and 5. If the congestion already existed before the optimisation of individual load profiles by dynamic pricing, this could be the result of a lack of availability of flexibility, insufficiently high price signals or limited availability of flex due to the applied constraints. But also based on the optimisation function, there is a potential of occurrence of congestions, during a time when electricity prices are low, as the flexible loads are optimized to be used during low electricity prices, simultaneously. If this happens, the market-based price adjustment is initialised.

3.3.2 Effects of Price Adjustment

Based on Figure 3-2, it is shown that, with exception of day 1, all other day peak loads are higher than the transformer rating. Thus, the market-based price adjustment is initiated, and a new price signal is obtained and used for optimisation. Using the new control signal, each flexible appliance will be optimized again. This mechanism however depends on the availability of flexibility resources. Figure 3-3 presents the market-based price adjustment results on a "successful" day (7th day), i.e. the peak load is successfully lowered and kept below the transformer rating, and an "unsuccessful" day (3rd day), i.e. fails to keep peak load below the transformer rating. In both cases, the adjusted price control signals are higher during dynamic prices peak load time, deterring the flexible appliances to be used during that time. Thus, the device agent that corresponds to each flexible appliance reacts by lowering load consumption at that certain time, with the exception of PV.

In case of unsuccessful peak shaving, neither dynamic prices nor market-based price signals can realise optimal rescheduling of loads to prevent transformer overloading. In the simulated week, this occurs during the 2nd, 4th, 5th and 6th days, where the total network load still exceeds 1 pu. This happens due to the lack of flexible resources to resolve the congestion, the lack of flexibility in that given congestion time period, which may be limited by household constraints.

The aggregator fails, after integrating the optimisation procedure, to lower the peak load, and there will be no load profile changes. From the simulation, it is known that for the days where the market-based price adjustment is failed, the electricity price becomes so high, which is yielded from the iterative optimisation procedure. This happens due to lack of flexibility resources to resolve the congestion. The maximum adjusted load for each corresponding flexible load is shown in the table below.

Table 3-3: Maximum adjusted load for each appliance based on adjusted prices.

Appliances	Maximum Adjusted Load (kW)	Occurrence Time
EV	19.6324	3rd Day 21:15
Heat Pump	9.4286	3rd Day 08:45
Washing Machine	2.8772	1st Day 20:00
Freezer	1.2147	3rd Day 23:30
Dishwasher	4.0761	7th Day 12:00

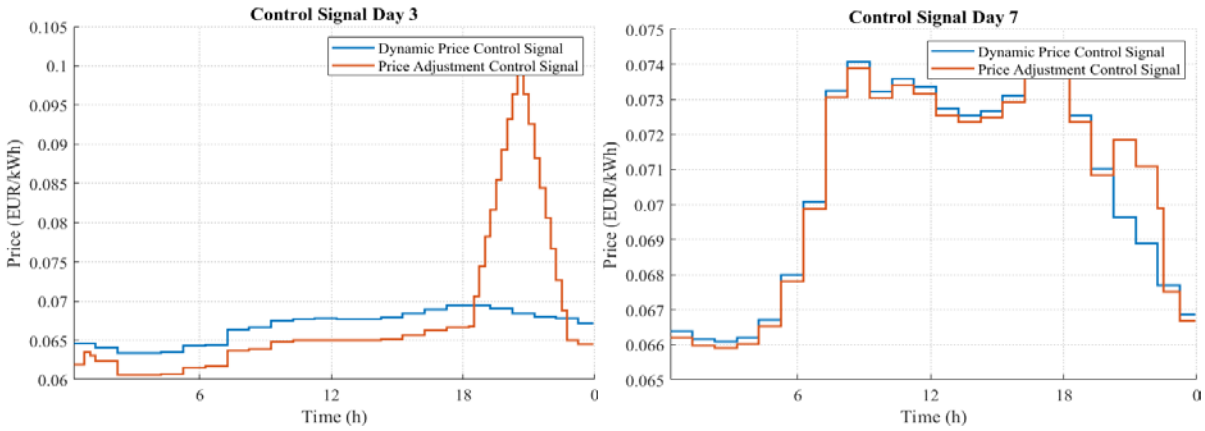

Figure 3-3: Price Control Signal Comparison in Day 3 and Day 7.

The total load changes are the profiles shown at the bottom of Figure 3-4. According to the results, on the 3rd day, the peak load congestion that occurs during 20:45 due to the dynamic price control signal and the peak load, is 1.0623 pu (orange profile). After the market-based price adjustment, the peak load is 0.9874 pu, which is slightly lower than the transformer rating (yellow profile). On the 7th day, a peak load congestion occurs during 21:15 with a peak load at 1.0223 pu. After the price adjustment, the peak load is now 0.9928 pu, which is slightly lower than the transformer rating.

Figure 3-4: Price Control Signal Comparison.

3.4 Summary – deterministic modelling of flexibility

This chapter presents a deterministic modelling approach for flexibility along with a market-based formulation for demand response based on price control signals. Numerical simulations show that a success in peak shaving depends on the availability of demand-side flexibility. To be able to mitigate network congestion, an indirect control method such as price adjustment would require sufficient amount of flexible capacity in the system which might be largely influenced by the certainty and availability of each flexibility resource.

While it may be a possibility to use price control signals to procure flexibility, data driven models might be considered to quantify the amount of flexibility with higher certainty and less computation time.

4 Data-driven models

The previous chapter presented a deterministic approach to quantify flexibility from the residential sector on the distribution network level. Random scenarios of the consumption level for 7 types of household devices at 200 houses were generated. The random load profiles are based on historical data which reflect the consumption patterns in the case of a fixed tariff scheme .

For a dynamic price profile, the load is expected to adjust in order to minimize cost. Each of the household devices adjusts its consumption profile to minimise cost, while satisfying a number of constraints necessary to preserve customer comfort. The difference between the benchmark load profile and the adjusted profile is perceived as flexibility.

The downside of this approach is that a flexibility price has to be proposed and the adjusted load profile is calculated accordingly. The load adjustment requires solving an optimisation problem. During real-time operation, system operators are interested in reciprocating this process. That is, if the system operators require an amount of flexibility, then the operators seek to find the retail price of electricity which would provide the required flexibility. It is therefore necessary to find the optimum price profile heuristically (i.e. trial and error). Solving an optimisation problem for each trial is inefficient, unreliable and impractical when quick decisions are needed in a short period of time.

The aim of this chapter is to develop a data driven model which is capable of replicating the optimisation result, and predict flexibility. A data driven model yields a prediction in far less time than solving an optimisation problem. Consequently, system operators have a fast and reliable tool to search for the optimum price profile that yields the required flexibility. In this chapter, we provide a top-level introduction on machine-learning. Then, we propose two artificial neural networks (ANN) models which are explored in this project, namely: convolutional neural networks, and recurrent neural networks. The working principles of the two models are explained. The performance of each model is analysed and compared.

4.1 Mining flexibility

4.1.1 Brief Introduction to Data Mining:

Data driven models are computer based algorithms which analyse data and learn the latent relationships and patterns within the data. Data driven models can be classified into two types, according to the learning objective [40]:

- **Unsupervised learning**: the algorithms aim to reveal latent trends and patterns in the data, such as identifying clusters in the data. This task becomes challenging when each instance of the data has multiple features (i.e. criteria). In mathematical terms, the data has multiple dimensions, and visual analysis is not possible. One form of unsupervised learning is reducing the dimensionality of the data by identifying the useful features, and eliminating less relevant features.
- **Supervised learning**: find the relation between characteristics of data on one side, and an output of interest on the other side. The ultimate goal of finding such relation is to make useful predictions for new input data. Examples include: Predicting life expectancy of equipment based on usage pattern, text translation, and computer vision.

Supervised learning breaks further down into two types based on the nature of the data [40]:

- **Classification**: There is a finite number of classes (i.e. groups), and the goal is to predict the affiliation of the input data (i.e. predict which group the input belongs to). In mathematical terms, the solution space is finite and discrete. Examples of classification tasks are:
  - Analyse x-ray images and identify a tumor: {*yes, no*}.
  - Predict the occurrence of a weather event such as: {*rain, no rain*}.

  In some advanced applications, the answer can be more than one class only. For example, the model analyses an image and names the objects in the image. Possible answers are limited to a number of objects: {car, horse, cat, dog, bird}. In one picture, a cat and a car are both present. However, the answers are still limited to the 5 objects {car, horse, cat, dog, bird}.

- **Regression**: The output of prediction is a quantity. Examples include: predict the life expectancy of equipment based on usage patterns. Forecast temperature, solar irradiance and wind-speed. Analytical curve fitting models fall under this category. A renowned example of such models is linear regression, which is based on minimising mean-squared-error between predictions and actual output.

Modeling the relationship between an input and output using a mathematical regression model (i.e. curve fitting) is simple, and provides physical meaning of the relationship between inputs and outputs. However, these models are not adequate with highly non-linear and high-dimensional data (i.e. data with numerous characteristics). Other computer algorithms were developed in the past for constructing data driven models. Examples are: decision trees, support vector machines, and Artificial Neural Networks (ANNs).

4.1.2 Machine Learning & Deep Learning

ANNs are mathematical models which imitate the structure of living brains. ANNs consist of neurons connected together. Each neuron carries out a simple mathematical operation and passes its output to other neurons. Consequently, a large network of neurons is capable of reproducing highly non-linear and complex mathematical expressions. Eq. (4-1) represents the general relationship between the input(s) and output of a neurons. While Figure 4-1 shows some of the most common activation functions, Figure 4-2 depicts the previously mentioned process. A simple ANN, consisting of several neurons and layers, is shown in Figure 4-3.

$$\text{Output} = F\left(\sum_i \left(w_i \cdot x_{\text{ij}}\right) + b_j\right) \qquad \textit{Eq. (4-1)}$$

where:

w_i (weight): a coefficient used to scale (weigh) the value of input (x_i).

b: bias term

x_{ij}: input to neuron (i) from previous neuron (j), or from the raw input data.

F(x): activation function of neuron. Common activation functions are:

Hyperbolic Tangent (tanh)	$\frac{e^x - e^{-x}}{e^x + e^{-x}}$	*Eq. (4-2)*
Sigmoid	$\frac{1}{1 + e^{-x}}$	*Eq. (4-3)*
Leaky Rectified Linear Unit (ReLU)	$\begin{cases} \alpha \cdot x & x \leq 0 \\ x & x > 0 \end{cases}$	*Eq. (4-4)*

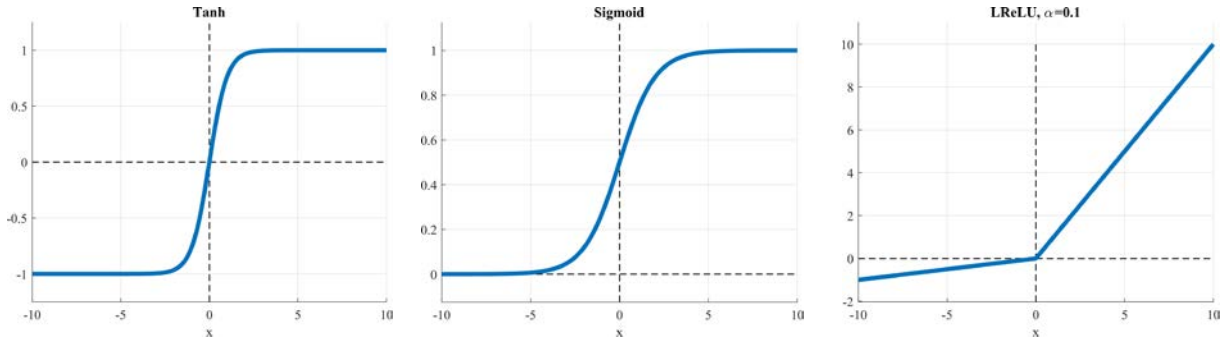

tanh(x) Sigmoid(x) Leaky-ReLU(x), $\alpha = 0.1$

Figure 4-1 Most Commonly Used Activation Functions in Neural Networks

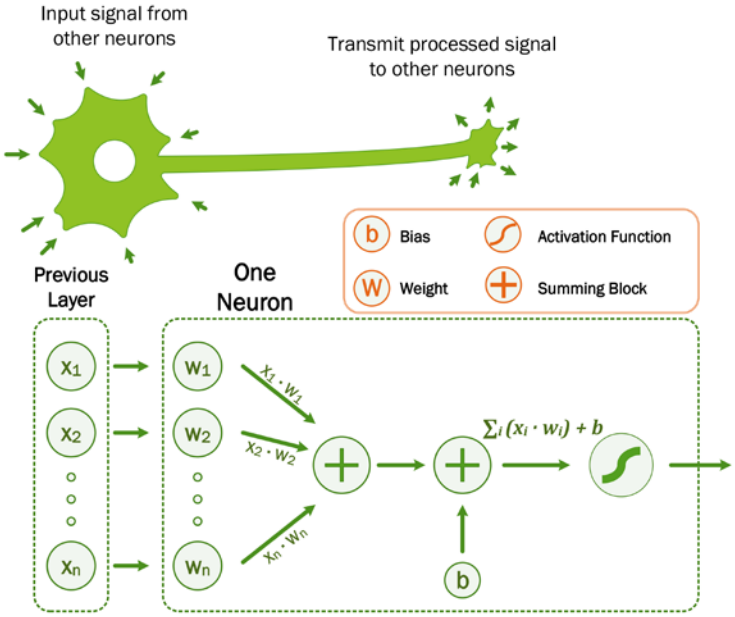

Figure 4-2 Simple Neuron Architecture

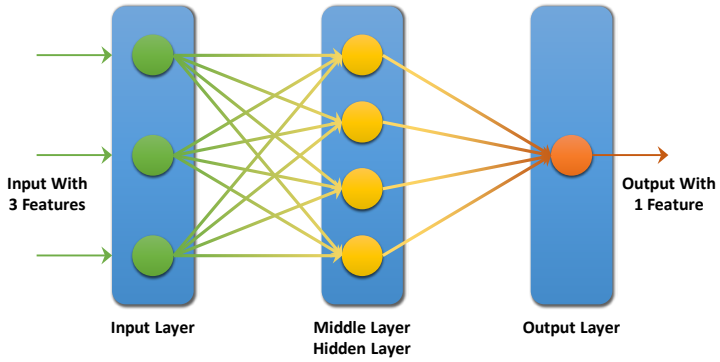

Figure 4-3 Simple ANN with 1 hidden (middle) layer

The task of developing a good ANN lies within optimising (i.e. varying) the values of w_i and b for every neuron, until the ANN, as a whole, makes accurate and useful predictions. This process is referred to as training the neural network.

The earliest attempts to develop computational models which imitate the functionality of the human brain date back to the 1940s [41]. However, the research into such models gained momentum when, in 1975, [42] demonstrated an effective technique to train neural networks. This technique was based on a derivation and optimisation algorithm which was developed not long before. Consequently, ANNs designs and applications developed rapidly over the following decades and ANNs became the most widely implemented tool for building data-driven models.

Advantages of ANNs include:

1) Ability to handle large datasets with multiple dimensions.

2) Ability to learn and reproduce highly complex relationships among data.

3) Versatility: ANNs are utilised in different applications: {classification, regression}, {single output, multiple outputs}

4) And, ANNs are highly customizable.

On the other hand, ANNs have some weaknesses:

1) ANNs are prone to overfitting. Overfitting is the case when a model memorises the data, rather than learns to understand the relationships within the data. The model appears to perform properly and make accurate predictions on data which it has seen before. However, when the model is fed new data, it makes wrong predictions. An example of overfitting is provided in Figure 4-4. Several techniques were developed to suppress overfitting.

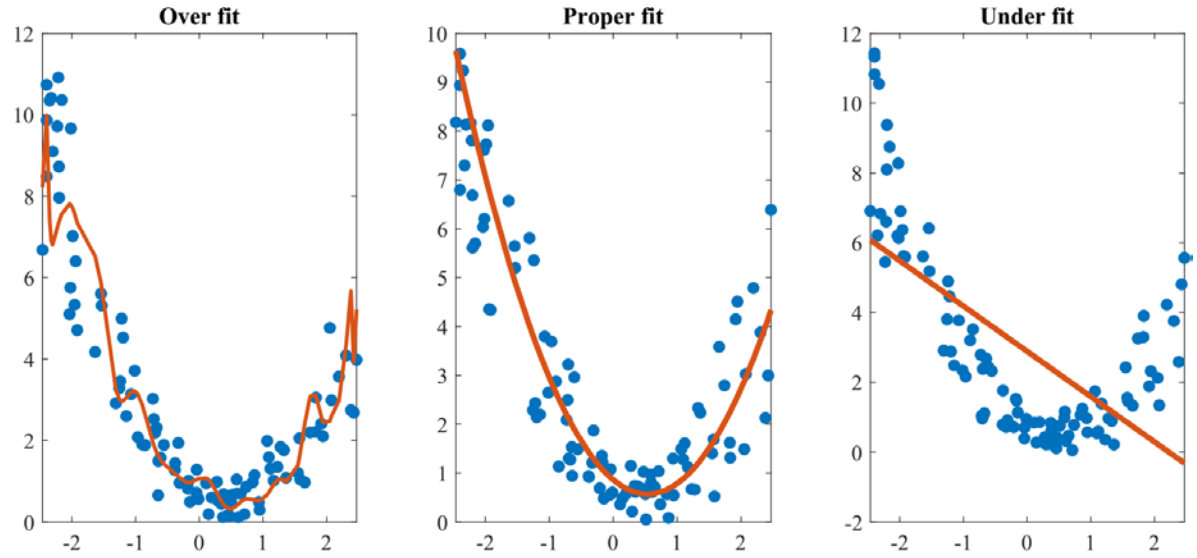

Figure 4-4. Demonstration of overfitting and underfitting Demonstration of overfitting and underfitting

2) In contrast with mathematical regression models (i.e. linear regression), ANNs are unable to provide a physical interpretation of the relationship between the inputs and outputs. For large and modern ANN architectures, it is practically impossible to describe how the ANNs output is calculated from its input, in one mathematical expression.

3) ANNs require big amounts of data to train. A larger and more complex ANN requires more data to train all the parameters.

4) Input and output data must be modelled as quantitative. For example, text must be converted to vectors.

ANNs are used widely in power system studies and analysis. ANN utilisation is not limited to time-series forecasting of weather conditions and load, but also for decision making and optimisation. Azman et. al [43] built a convolutional neural network (CNN) to assess the transient stability of a multi-bus multi-machine power system in real-time. At the same time, a recurrent neural network is utilised to assess the small signal stability of a power system. CNNs are also employed in [44], [45] to classify power quality disturbance events in the power system. Miranda et. al [46] also utilise convolution neural network in predicting the status of remote power protection devices. Wang et. al. [47] utilise an advanced type of recurrent neural networks (RNN) for state-estimation in the power system, based on data feed from phasor measurement units. Yan et. al [48] employ a neural network for load frequency control. Finally, Sun et. al. [40] review the utilisation of neural networks in solving mathematical optimisation problems.

The next section describes the working principles of the special types of ANNs, and how they were employed for mining flexibility in this study.

4.2 Developed data-driven models

4.2.1 Introduction to Convolution Neural Networks

The ANN model depicted in Figure 4-3 consists of a sequence of layers. Different characteristics of the input data are read separately. Visual data, such as images, are represented as matrices. Each pixel in the image is represented by one element in the matrix. The colour of the pixel is represented by the value of the matrix element. Analysing an image using the model in Figure 4-3 requires flattening the image's matrix of size $[m \times n]$ pixels, to a vector of size $[mn \times 1]$ elements. This conversion destroys the shapes in the picture. If two images depict the same object but with a slight shift in position, the flattened images appear completely different to an ANN. This problem inspired the development of a special type of ANN which reads spatial data (i.e. 2D images, 3D maps, 3D topography maps, medical imaging) without flattening. This type of ANN is known as convolution neural networks (CNN). As the name inspires, the ANN uses a small window (also known in the literature as Kernels, or filters) to scan over the image. Adjacent pixels are scanned together, without distorting the shape. The process is depicted in Figure 4-5. In this example, the input to the ANN is the bottom (light blue) image of size [4x4]. The ANN uses a window (dark blue) of size [3x3] to read the image. The weights of the window (kernel) are trainable variables. Training the ANN incurs finding the optimum values of these weights.

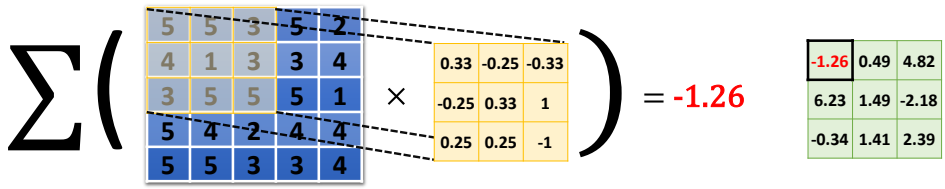

Element-wise multiplication

Numerical Example of Convolution: Input Image size [5x5]. Window size [3x3]. Output size [3x3]

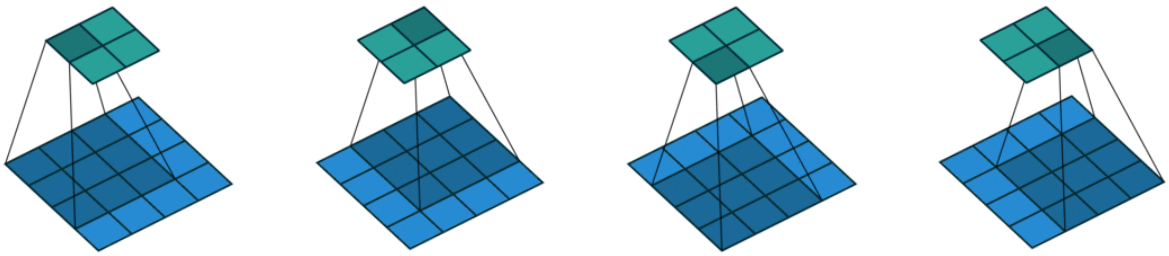

Graphic Depiction of Image Convolution: Input Image size [4x4]. Window size [3x3]. Output size [2x2]

Figure 4-5 Demonstration of Convolution Neural Networks

In order to detect different features in an image, the moving window can be customised to different shapes (height x width), take larger steps, and customise the window's task as well. The window in Figure 4-5 multiplies its weights by the values in the input image, and the sum is taken. A moving window can be programmed to take the maximum value in a region, the average value or the minimum value. For example, taking the maximum value in a region helps detect edges of objects.

In order to detect different features in an image, several windows with different weights are applied on the same image. The 2D output from each window is known as a feature map. The feature maps (also

known as layers, and channels) are stacked in the 3rd dimension as shown in Figure 4-6. The new stack can be fed to another CNN to run deeper analysis. For a 3D matrix (also known as tensor), a 3D moving window reads the same area of all feature maps at the same time, to produce 1 value per step. For example, an image with 9 layers requires a 3D window with 9 layers as well. To generate *N* feature maps from this image, *N* different 3D windows are required. It is customary for later CNN layers to apply a larger number of windows (larger N), and generate more feature maps (i.e. a stack consisting of a large number of feature maps) With each convolutional layer, the data shrinks in height and width, while the depth of the stack (i.e. number of feature maps) grows. These feature maps are independent. Flattening these feature maps does not distort the data, and the data can be fed to a fully-connected layer after a long series of CNN layers.

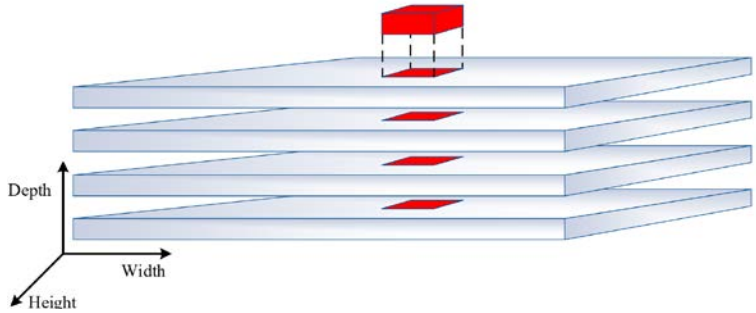

Figure 4-6 Stacking the outputs of several windows operating on the same image

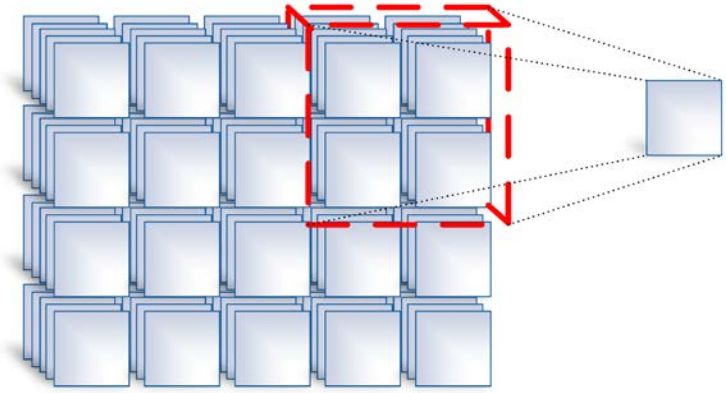

Figure 4-7: 2D Convolution on 3D Tensor:
Input Image (blue) size is [4, 5, 5]. Window (red) size is [2, 2, 5]. Output size is [3, 4, 1]

4.2.2 Auto-encoders

Auto-encoders are composite neural networks (i.e. consisting of several layers) which consist of two subsystems: 1) Encoder, 2) Decoder. The encoder part of an auto-encoder converts the raw input into another format. The data in this intermediate format is converted back to the original readable format by the decoder. The process is as follows:

$$\text{Human readable data (image)} \xrightarrow{\text{Encoder}} \text{encoded data} \xrightarrow{\text{Decoder}} \text{Human readable data (image)}$$

There are many applications for auto-encoders, such as:

- **denoising/repairing distorted images:** Input image is distorted or noisy. Fully connected layers are added in the middle, between the encoder and decoder. The encoded data are processed through these fully-connected layers, and the decoder produces a clean version of the input.
- **encrypting data:** only a person who possesses the right decoder can convert back the encoded data to its sensible format.
- **data compression:** The encoded data in the middle stage has smaller size, which saves storage space.

The encoder consists of CNN layers which reduce the data size. The decoder reverse the convolution process applied by the encoder. The inverse of the convolution process is applied by a type of layer known as transpose-convolution (also commonly known as de-convolution).

4.2.3 Quantification of Flexibility by CNN

Here, we are utilizing the same use case and load profiles as described in chapter 3: Each instance of the data consists of a timestamp for the time of the day, the electricity price profile, and the benchmark consumption profile of an electric device. Each profile has 116 time steps, which represents 29 hours with a resolution of 15-minutes. The 3 profiles together make up a matrix of size [3x116]. Pre-processing the data will be discussed in a later section.

The specific CNN design for the scope of this chapter is depicted in Figure 4-8. This design follows the concept of an auto-encoder. The working principle of the auto-encoder is:

1) The encoder converts the data into another representation in an encoded space.
2) The encoded data are processed by fully-connected layers. The fully-connected layers solve the optimisation problem.
3) The decoder converts back the data from the encoded space to a readable format (i.e. adjusted load profile).

For this auto-encoder to work properly, the model is constructed and trained on two stages:

Stage 1) Create a preliminary model consisting of an encoder and decoder only. The encoder-decoder pair is trained to convert the input data (time, price, benchmark load) to the encoded space, and reconstruct the benchmark load profile as it is. It is important to keep in mind that, at this stage, the decoder should output the benchmark load profile, **not** the adjusted load profile in response to price. After completion of the training, the weights of the encoder and decoder are locked, and the encoder-decoder pair will not be trained in the next stage. This stage can be characterised as follows:

- **Model**: Encoder output is fed directly to decoder output.
- **Trainable layers**: Encoder and decoder
- **Input data**: three time-series: time, dummy flat price of electricity, benchmark load profile
- **Output data**: (to be predicted): Benchmark load profile.

In principle, the encoder and decoder can be based on any type of ANN, and not exclusively CNNs. The role of the encoder-decoder pair in the bigger model is only to convert data from one format to another, and convert it back.

Stage 2) Fully connected layers are inserted between the trained encoder and decoder, which were obtained in Stage 1. The new composite model is trained to produce the adjusted load profile. In this stage, the encoder and decoder are fixed. The scope of training is the fully-connected layers only. The goal of training is for the fully-connected layers to solve the optimisation problem in the encoded space.

- **Model:** Encoder output is fed directly to decoder output.
- **Trainable layers:** Fully connected layer in the middle only.
- **Input data:** three time-series: time, dynamic price of electricity, benchmark load profile
- **Output data** (to be predicted): Adjusted load profile, in response to dynamic electricity price.

The input data are passed by a convolution layer with 8 windows of size [1x1]. The output of this layer has the same height and width of the input data, but a depth of 8 layers. In fact, this step does not involve any convolution in the general meaning. In the output of this layer, each value is a scaled version of the input data. This helps the next layers to detect different features. The remaining of the encoder consists of normal CNN layers. On the other side, the decoder applies a number of transpose-convolution operations to create a vector with 116 time steps.

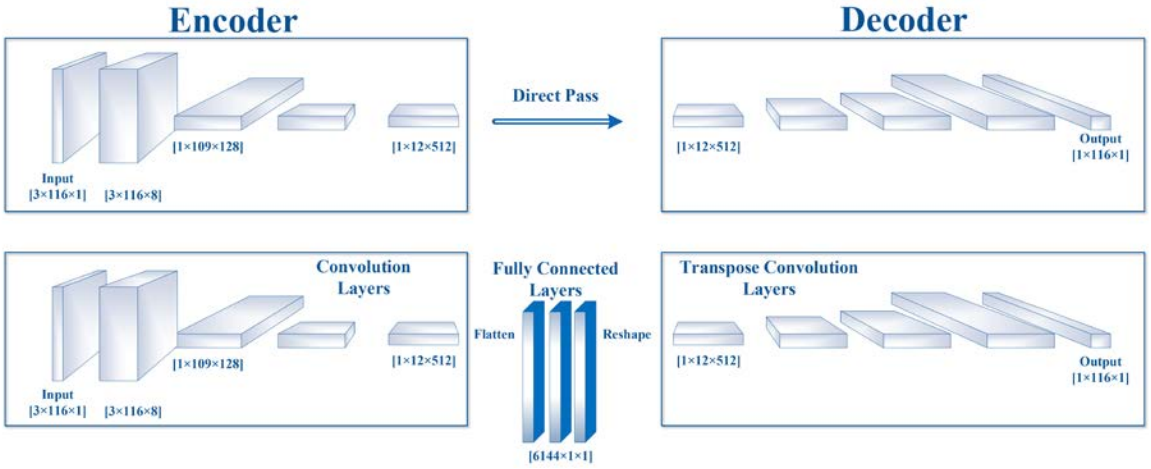

Figure 4-8 Implemented CNN Model for Quantification of Flexibility. a) stage 1: training auto-encoder only. b) stage 2: Training fully connected layer for optimisation.

4.3 Numerical validation

4.3.1 Model Inputs and Outputs

The input and output data of the physical deterministic model illustrated in Chapter 3 are used to train the data-driven model. Unlike the transmission network, line losses in the distribution network are significant. The location of a load on a distribution feeder also plays an important role in the voltage drop over the feeder. Therefore, analysing the aggregate (total) load profile of all houses in the network is not useful for flexibility quantification, and has little meaning or utility to the system operators. It is essential for the load profile of each house in a distribution network to be processed separately. Therefore, a data-driven model must take in the price and historical load data for individual houses, and make predictions accordingly.

Moreover, different electric devices, appliances or other DER have different characteristics, and must be modelled separately. It is important to design a versatile model which can process the input data of any

house, rather than having customised models for each individual house. At the same time, not all houses may have the same 6 responsive devices studied in this report. Therefore, a separate data-driven model is trained for each type of electric device.

It is common practice to process the data before feeding it to the actual model. For example, text data must be converted into a numeric format. For numerical data, such as load profiles, it is necessary to scale the numerical data to a range [-1, 1] or [0, 1].

Different houses have different consumption patterns and characteristics, such as: peak load, cycle length, total connected load, and total daily energy consumption. It is not realistic to design and train separate models for each house. At the same time, if the exact same modulation, with the exact same parameters, is applied to the load profiles of all houses, then small sized houses will have semi-flat near-zero profiles. Alternatively, modulating the load profile of each house separately retains the unique characteristics of the house, while also retaining the unique consumption patterns of the device, from other devices within the same premises. In other words, the profile for each device in each house is normalised separately based on the profile's own characteristics over the full-year. For example, in house #1, the EV consumption profile for the whole year is normalised based on the minimum and peak load over the whole year of this device in this house.

As a result, a single instance of the data fed to the data-driven model has the following characteristics:

- Consists of 3 profiles (3 rows):
    - Time of the day
    - Price
    - Benchmark consumption profile of the electrical device for the same day (historical data)
- The profiles extend for 29 hours, at 15 minutes intervals. Therefore, the profile has 116 time steps
- The input does not contain any information about the house ID.

The goal of training a data-driven model is to reproduce the output of the optimisation. That is, to predict the adjusted consumption profile of the same electric device in response to a dynamic electricity price. The predicted consumption profile can be used by the system operator to assess the available amount of flexibility at each time period

4.3.2 Data Pre-Processing

The load profiles do not follow a Gaussian distribution. Hence, normalizing the data by its standard deviation does not guarantee that the majority of the data will fall within a range. Poor performance is observed with this normalisation technique. Furthermore, by normalising a load profile by its full range, as depicted in Eq. (4-5), rare load spikes inflate the range of the consumption profile, and the average consumption level appears to be close to zero. To mitigate this problem, data outliers or extreme events are removed. That is, instances below the 2.5 percentile, and above the 97.5 percentile are neglected when calculating the range. Consequently, the normalised load profile provides an accurate representation of the original load profile. We emphasize that extreme events above the 97.5 percentile are not removed from the data nor truncated, but merely neglected when calculating the normalisation range. In the normalized profile, these extreme events appear with a very large value (above 1), however, this is tolerable.

$$\tilde{P} = \frac{P - P_{\min}}{P_{\max} - P_{\min}} \qquad \text{Eq. (4-5)}$$

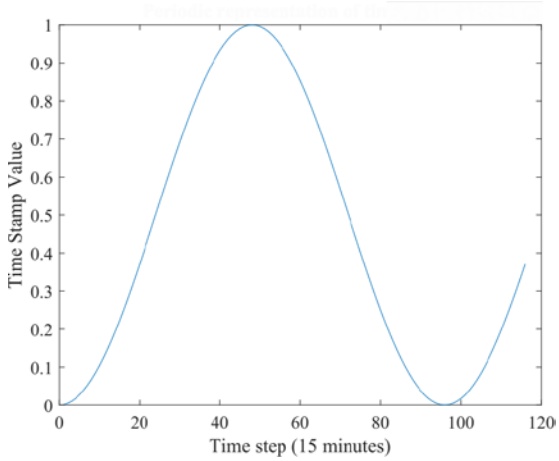

Figure 4-9 Trigonometric representation of time stamp: $q = \frac{1}{2}\left(1 - cos\frac{2\pi t}{T}\right)$

Some household devices are used intermittently or occasionally, such as washing machines and dish washers. In some cases, the device is not switched on at all, and the profile is zero for a full day. No flexibility can be expected or acquired from such device, and it is justified to eliminate such instances from the data.

Finally, it is important to note that representing the time of the day as a number between 1 and 23 provides the ANN with a false impression that there is significant difference between 11PM and 12AM. Therefore, time stamps must be represented by continuous periodic functions.

4.3.3 Training Process

As explained earlier, the model development plan goes through two stages. An auto-encoder is designed and trained first, whose scope is to encode the data into a hidden space, and then decode the data back to a meaningful representation. After that, fully-connected layers are inserted in the middle of the auto-encoder. The fully connected layers solve the optimisation problem in the hidden space. The same network architecture is used with all 6 devices. However, a separate network is trained for each device. The network architecture for stage 1 includes 1,595,417 trainable parameters. Three fully-connected layers are added in stage 2. These layers involve 19,845,044 trainable parameters. The training hyper-parameters are given in Table 4-1.

Table 4-1: Auto-Encoder Training Settings

Parameter	Value
α (Leaky ReLU activation slope)	0.1
Initial Learning Rate	9e-4
Batch Size	32
Learning Rate Reduction Period	Every 100 batches
Learning Rate Exponential Decay Factor	0.8
Training/Validation/Test Split	[70%, 15%, 15%]
Training Algorithm	Adam
Training Objective Function	Mean Squared Error

Since the benchmark tariff of electricity is not known, a dummy flat value is used to represent the price of the input data. The dummy value is taken to be 98% of the lowest price of electricity in the dynamic electricity price profile over the whole year. This choice of this tariff is based on the following notion. With the dynamic price profile, some devices do not adjust their output at all. Therefore, it is expected that for some low value of the dynamic price profile, no device will adjust its consumption. Therefore, we take 98% of the lowest point in the dynamic price profile.

The dataset is split into 3 subsets: training set, validation set, and test set. The actual training process is carried out using the training set data only. The training set is evaluated, and the error in prediction is calculated. The weights of the ANN are updated accordingly. The validation set is evaluated intermittently between steps of training, and the error in prediction is reported. The prediction error while evaluating the validation set is **not** used to update the weights of the ANN. The purpose of keeping a validation set is to monitor the performance of the ANN on extrinsic data, during training, rather than after training.

If the validation error is significantly higher than the training error, then, it is likely that the ANN is overfitting the training data. In rare events, the validation set has a much lower error than the training set. This indicates that the validation set consists of easy cases, or the validation set is too small. In both cases, this means that the validation set is not a good representative of the whole dataset. A programmer can choose to terminate training if validation error plateaus, or even starts increasing (i.e. becomes worse). Finally, the test set is used after training to evaluate the performance of the ANN.

During the training process, the training set is divided into batches of a smaller size. This is necessary when the training set is very large. Each batch is run through the ANN and the error in prediction is calculated. This process is denoted as a training *"step".* The weights of the ANN are updated after each batch (i.e. step). When all batches have been run through the ANN, the ANN has seen the whole dataset. The training continues by feeding the batches again for another round. A full round of batches is denoted an "*epoch*".

4.3.3.1 Stage 1

The training progress and performance of the model for the EV are illustrated in Figure 4-10. The same graphs are illustrated for the WM model in Figure 4-12. The left plot in subfigure (a) depicts the MSE value at each epoch of training. The MSE is used as the objective function for training the ANN. The right plot in in subfigure (a) depicts the mean-absolute error at each epoch of training. This metric is recorded for observation only, and does not affect the training progress.

The final MSE value for the training set is 0.0015. The final MSE value with the validation set is 0.0032. This indicates that the model does not overfit the data. The training is designed to stop after 15 epochs if the percentage improvement in the validation error is below 0.001. It is noticeable that training commences within less than 20 epochs for all cases.

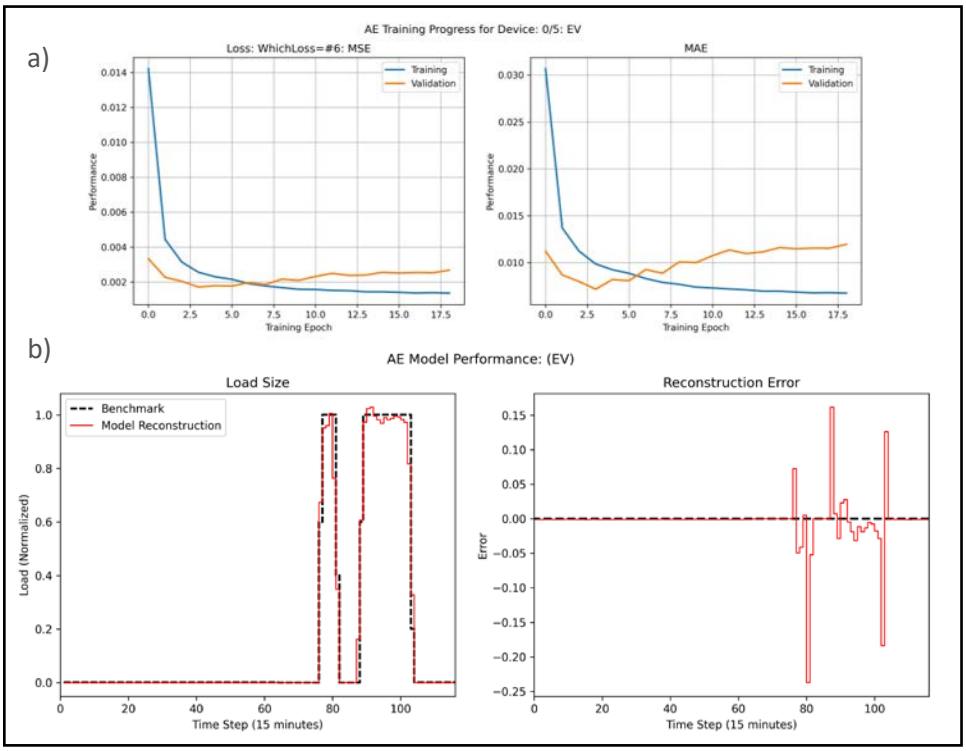

Figure 4-10 EV Load Profile's Auto-encoder training progress (top) and performance (bottom)

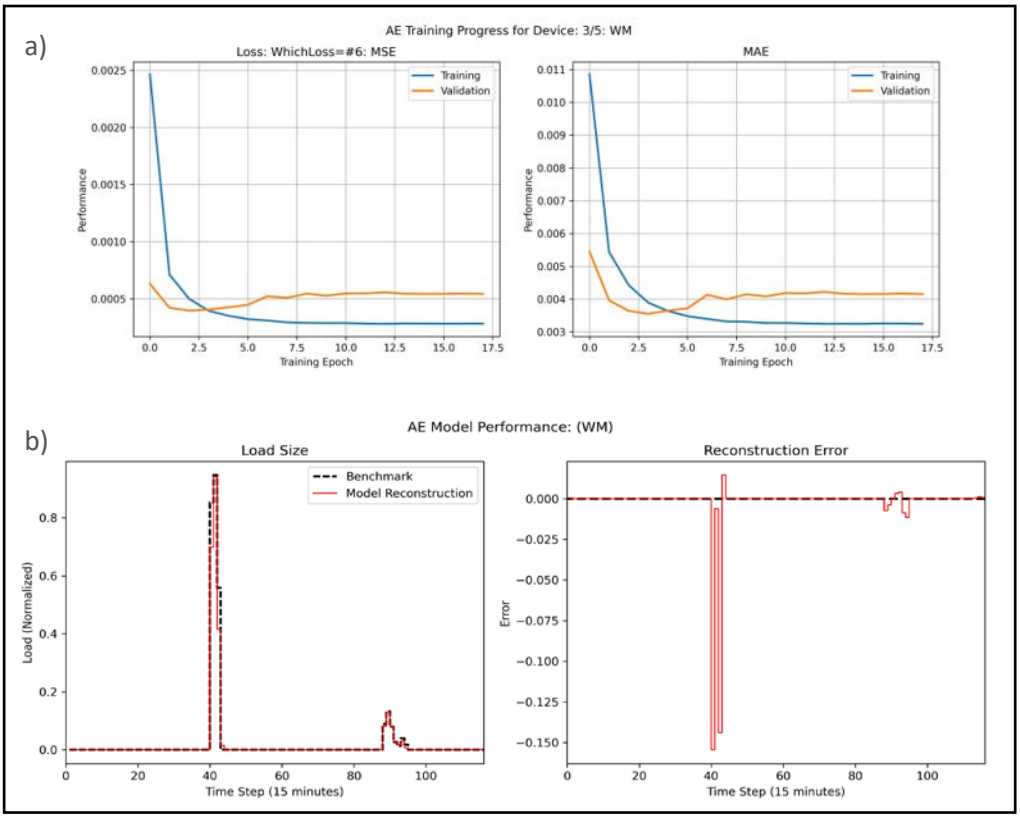

Figure 4-11 WM Load Profile's Auto-encoder training progress (top) and performance (bottom)

The left plot in subfigures (b) depicts the benchmark load, and the reconstructed profile by the auto-encoder. The right plot in subfigures (b) depicts the difference between the benchmark load and the reconstruction (i.e. reconstruction error). In conclusion, the auto-encoder model demonstrates very good performance.

4.3.3.2 Stage 2

Three fully connected layers are inserted between the encoder and decoder. The same hyper-parameters provided in Table 4-1 are used in the second stage, as well. Since a dummy price of electricity was used for the benchmark load (due to lack of data), it becomes necessary to retrain, at least, the CNN layer which applies a convolution window with a height of 3, and consequently, reads the three input profiles together. The augmented model is trained and results for the EV model are shown in Figure 4-12. The results for the WM model are illustrated in Figure 4-13. For the WM model, the final MSE and MAE values are 0.0031 and 0.012, accordingly.

It is observable that the trained network succeeds at predicting the time-shift in the load event most of the time. The network, however, is less accurate at predicting the actual magnitude of the load. This result proves the validity of the design. However, a larger training set can contribute to better models. More importantly, knowing the actual tariff of electricity which the benchmark load is based on, is expected to improve the model's performance.

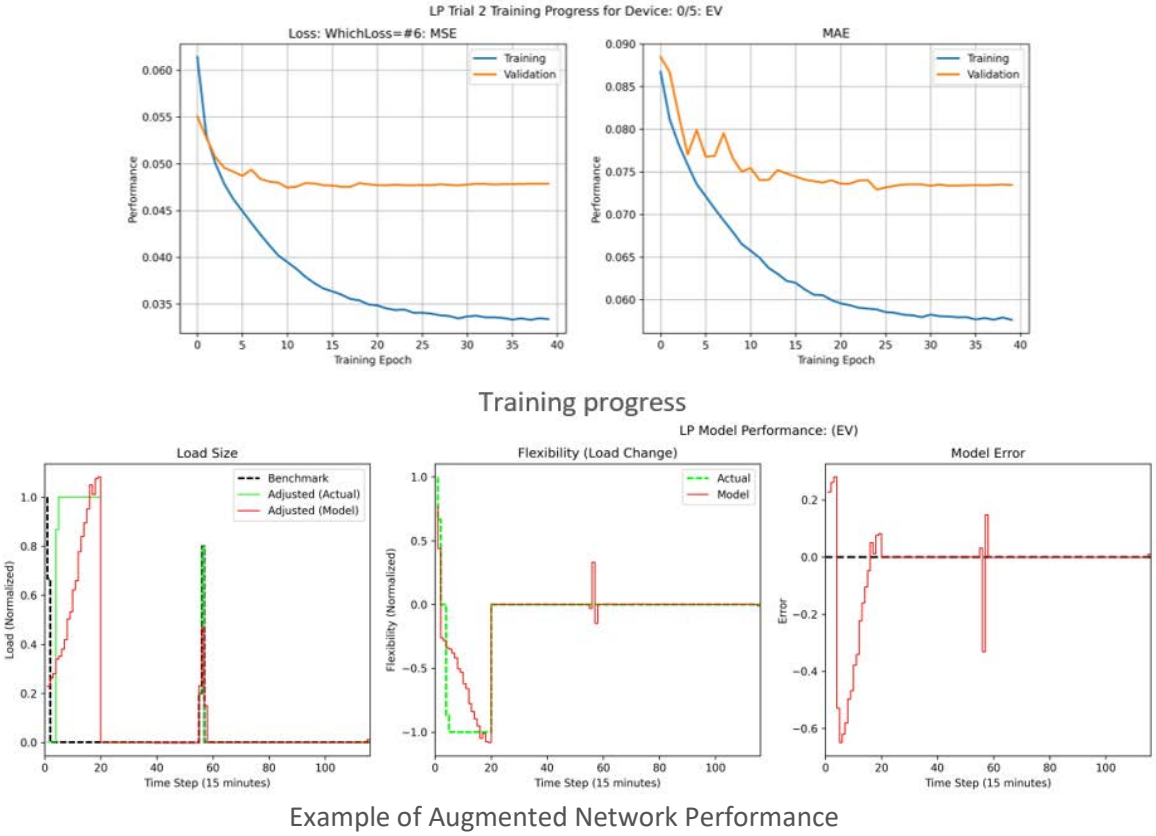

Figure 4-12 EV Load Profile's Auto-encoder

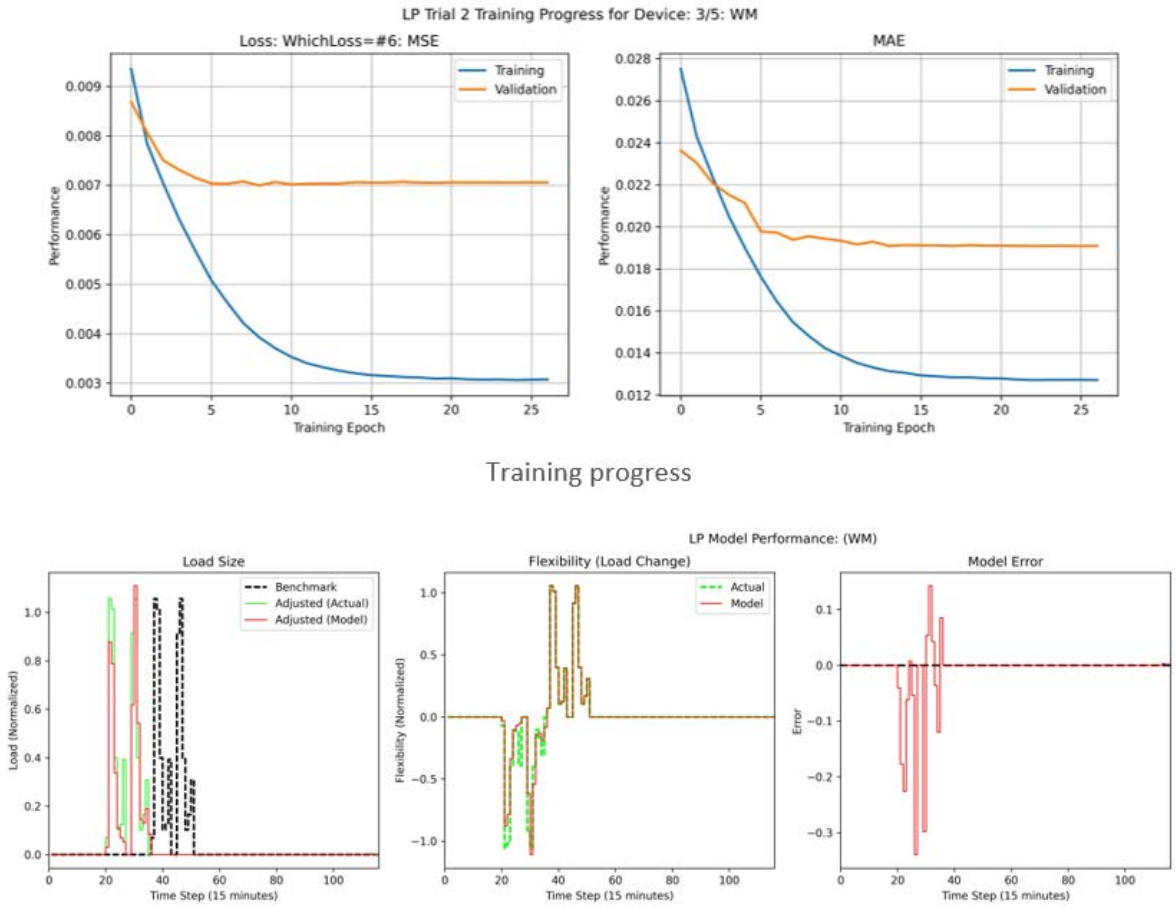

Figure 4-13 WM Load Profile's Auto-encoder

4.3.4 Model Speed

Linear optimisation problems can be solved efficiently (i.e. in polynomial time). However, the flexibility quantification problem tackled in this report involves solving a separate optimisation problem for each of the 6 electric devices in each house. Each optimisation problem involves an iterative search for the optimum (i.e. primal-dual methods, simplex-method, etc.). With data-driven models, the model training process may require substantial amount of time. However, once the model is trained, the model is capable of processing input data to produce results immediately. At the same time, since the distribution network observes the same time stamp and price profile, the data-driven model can process a batch of houses simultaneously.

During the execution of the physics-based deterministic flexibility model, the execution time is recorded for each device and each household. After training the data-driven model, we also take note of the execution time. Table 4-2 compares the execution times for each model. It is important to keep in mind that the deterministic and data-driven model were developed in separate software, which may have a slight effect on execution speed.

Table 4-2 Training & Evaluation Time Comparison

Device	***Python***		***Matlab***
	Convolutional Net		**Linear Program**
	Training (H:M)	Evaluation (milliseconds)	(milliseconds)
EV	00:25 – 00:35	2.7 - 3.5	8.3 - 35.9
WM	00:09 - 00:10	1.17 – 1.89	13 - 32.6
HP	00:37 – 01:18	0.895 – 3.84	0.175 - 6.27
FR	00:10 +		12.7 - 36.2
DW	00:16 – 00:20	0.5 - 2	0.196 - 4.27

4.4 Conclusion – Flexibility assessment by a data-driven model

This chapter developed a data-driven model for assessing flexibility. Data-driven models are computer algorithms which learn the relationship between input and output data, and then, attempt to make predictions on new input data. The data used to train the models in this chapter are the input and output data from Chapter 3. A model based on convolutional neural networks and auto-encoders is built on two stages. In the first stage, a preliminary model learns to convert the time profiles in the input data into another hidden space and reconstructs these encoded data back to meaningful time profiles. When the accuracy of this model is verified, the model is augmented with additional components which are able to solve the optimisation problem in the hidden space. Data driven models require time the first time they are built and trained. However, evaluating an input instance with a trained model proves to be much faster than solving the actual optimisation problem. Data-driven models are also capable of handling batches of instances at once. On the other hand, mathematical optimisation is solved for each instance separately. The preliminary (encoder-decoder) model demonstrates very good performance. The augmented model demonstrates good performance in terms of predicting the time-shift in a load event. The magnitude of the adjusted load is predicted with less accuracy. This can be attributed to the lack of a benchmark electricity tariff for the benchmark load. A larger network design would also perform better, at the expense of more training time, and computing power.

5 Stochastic programming models

The main modelling approaches that represent uncertainty in sequential decision making problems include [49]: 1) stochastic programming, where there are future event scenarios associated with the probability of occurrence of each event, 2) Markov decision processes, where the uncertainty is only modelled for the next-step decision, 3) robust optimisation and chance-constrained optimisation, which uses uncertainty sets to constrain the operating points, and 4) reinforcement learning, which observes (instead of explicitly modelling) uncertainty.

The data-driven models presented in Chapter 4 apply machine learning techniques on historical data to learn the relationship between the data and the available flexibility. In Chapter 5, the uncertainty is tackled via a stochastic programming approach. This approach uses future scenarios of uncertain inputs (e.g., renewable-based generation, electricity demand). These scenarios are generated using the forecasts which are available at the time when the flexibility must be quantified.

The stochastic assessment of flexibility is provided by solving a scenario-based stochastic optimisation problem. The solution yields the minimum cost of operation for the owner of the energy resources, which are clustered together to offer both energy and flexibility services. The considered resources are PV systems and stationary BESSs, which are clustered together with the electricity demand to form a (grid-connected) microgrid (MG) i.e., “a group of interconnected loads and distributed energy resources within clearly defined electrical boundaries that acts as a single controllable entity with respect to the grid” [50]. Grid-connected MGs can be formed by a number of geographically contiguous assets and customers such as, for example, a neighbourhood of buildings. MGs can be represented and operated by local energy communities and they can enable significant amounts of grid flexibility, especially when they own and operate BESSs, which offer short ramp-up and ramp-down time. The MG owner, which is also the microgrid operator, aims to:

1. Minimise the expected energy cost,
2. Minimise the BESS aging cost,
3. Maximise the expected profit from selling energy,
4. Maximise the expected profit from offering flexibility services.

The solution of the stochastic optimisation problem yields both, the microgrid energy scheduling and the dispatch of the BESS-based microgrid flexibility. Thus, the offered flexibility is not only defined by the technical constraints of the resources but also by the economic operational targets of the microgrid owner. The optimisation problem is solved at regular points in time (time steps), where the uncertainty model is dynamically updated before each simulation to consider the most recently obtained forecast profiles for renewable-based generation and electricity load demand. This dynamic update and solution approach is also known as the rolling horizon (RH) approach.

5.1 Mathematical Formulation

This section presents the formulation of the stochastic optimisation model that is used to solve the MG energy management and flexibility dispatch problem. The MG is owned and operated by a third-party MG developer and the costumers of the MG are relieved from risks associated with investment, operation, and maintenance costs. This MG business model is called energy-as-a-service [49]. Thus, the MG can own both small-scale (residential) and utility-scale assets and DERs. The customers only pay for the energy provided by the MG or they might also share with the MG developer the profit of energy and flexibility services that the MG can offer. The MG customers could be, for example, a large commercial building, a number of residential buildings in the same neighbourhood (in which case the MG customers could be represented by a local energy community).

It is assumed that the MG operator has a contract with an electricity retail provider that enables energy trading at wholesale electricity market price. It is also assumed that the MG operator has a long-term contract with a LFM operator to offer flexibility services. The type of flexibility service considered in this study is a capacity limitation flexibility service [50]. With this, the flexibility provider (in this case the MG operator) must ensure that the MG power import from the main grid remains below a threshold set by the LFM operator.

The MG resources include PV system and BESS. The PV system and the BESS of the MG are connected to the upstream AC grid via a converter with bi-directional operation, since the solar energy and the BESS stored energy can be exported to the AC grid and, in addition, the BESS can be charged through both the upstream AC grid and the PV system (see Figure 5-1). Note that the following convention is used in the mathematical formulation of this section: the parameters of the optimisation model are denoted with upper case letters, while the decision variables are denoted with lower case letters.

The positive variables $p_{t,w}^{im}/p_{t,w}^{ex}$ are the imported/exported power from/to the grid at time step t and scenario w, while the positive variables p_t^{ch}/p_t^{dis} refer charging/discharging power that the BESS draws from the grid and the PVs or injects to the grid. The state-of-energy (SoE) of the BESS is denoted by soe_t. The parameters $P_{t,w}^{PV}$, $P_{t,w}^{L}$ and Λ_t respectively refer to PV generation, electric power consumption, and electricity wholesale market price.

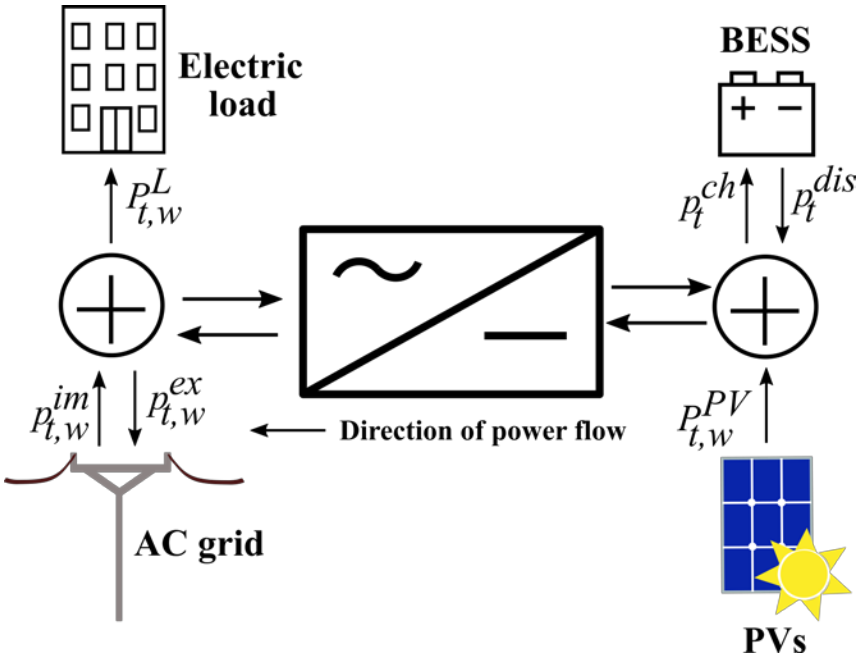

Figure 5-1: Power flow of the MG

The objective of the stochastic optimisation model is to minimize the expected MG cost, during the look-ahead period, while also considering the forecast error of electricity load demand and PV generation. The length of the look-ahead horizon i.e., number of time steps, depends on the time discretization of the scheduling period, which is 24 hours. The length can be reduced if electricity price data are not available for the whole 24-hour look-ahead period at the time of the simulation. The MG cost includes the energy cost (with the income from selling energy being subtracted), the cost due to peak power charge, the battery degradation cost, and the income for offering flexibility service.

The formulated optimisation problem is solved in RH approach (see Figure 5-2) and in order to reduce the size of the optimisation problem (since scalability can be an issue in stochastic optimisation), the BESS control decisions (p_t^{ch}, p_t^{dis}, soe_t) are deterministic i.e., they are not dependent on the scenario. The MG power import and export ($p_{t,w}^{im}$ and $p_{t,w}^{ex}$), which can be controlled to a certain extent by controlling the BESS charging/discharging power (deterministic decision variables), are the only stochastic decision variables of the stochastic optimisation problem. Due to the RH approach, it is only the next step control decisions that are implemented after each simulation and the deterministic control trajectory can be updated considering the latest forecasts available with every new simulation. The rest of the control trajectory of each simulation is a provisional plan which is applied only in the case of loss of communication between the MG and the grid.

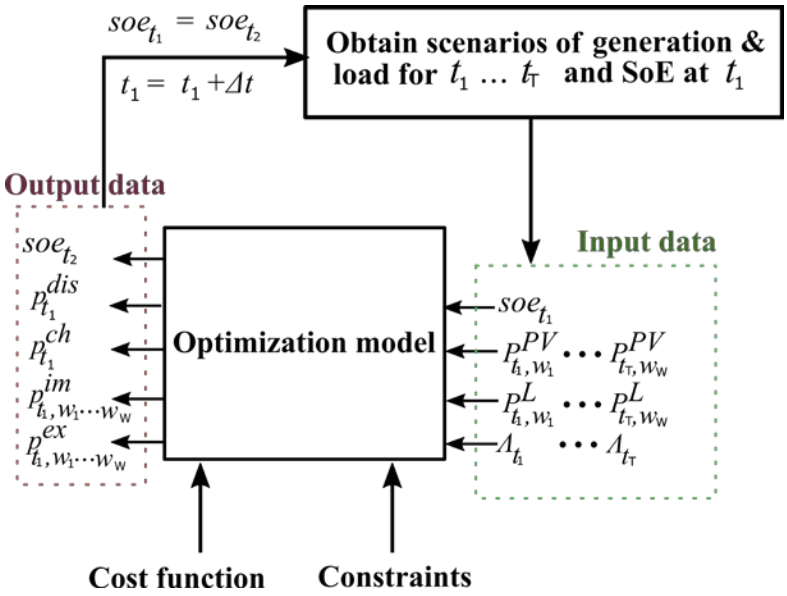

Figure 5-2: Illustrative diagram of the RH approach

The objective function of the model is given by:

$$\min f = f^{im} - f^{ex} + r^{p} + c^{B} - C_{flex}\left(P_{peak}^{L} - p^{flex}\right), \quad (5\text{-}1)$$

where

$$\mathrm{f^{im}} = \sum_{\mathrm{t}\in\mathcal{H}} \sum_{\mathrm{w}\in\mathcal{W}} \Pi_{\mathrm{w}} C_t^{im} \mathrm{p_{t,w}^{im}}\, \Delta\mathrm{t}, \quad (5\text{-}2)$$

$$\mathrm{f^{ex}} = \sum_{\mathrm{t}\in\mathcal{H}} \sum_{\mathrm{w}\in\mathcal{W}} \Pi_{\mathrm{w}}\, C_t^{ex} \mathrm{p_{t,w}^{ex}}\, \Delta\mathrm{t}. \quad (5\text{-}3)$$

The look-ahead time horizon and the time intervals are represented by $\mathcal{H}$ and Δt in Eq. (5-2)-(5-3), respectively, while Π_w is the probability of occurrence of scenario w. In Eq. (5-1) the first term (f^{im}) is the cost of the imported energy and the second term (f^{ex}) is the revenue associated with the energy exported to the grid. The parameters C_t^{im}/C_t^{ex}, which are related with these terms in Eq. (5-2)-(5-3), denote the cost/revenue associated with energy import/export from/to the main grid. The electricity wholesale market price as well as the grid tariff and reimbursement fee related to import and export of MG energy, respectively, are included in these parameters. The term c^B denotes the cost of BESS capacity loss due to cycle aging and r^p is the cost for the peak power drawn from the main grid, which satisfies:

$$\mathrm{r^{p}} \geq \mathrm{C_{pp}} \sum_{w\in\mathcal{W}} \Pi_w\, \mathrm{p_{t,w}^{im}},\ \forall \mathrm{t} \in \mathcal{H}. \quad (5\text{-}4)$$

The power-based grid tariff C_{pp} is linked to the maximum average power of the studied period (measured per Δt). The last term in Eq. (5-1) is the reward for providing flexibility, where the positive variable p^{flex} denotes the flexibility bid and $P_{peak}^{L} - p^{flex}$ is the amount of flexibility in terms of peak power reduction. The parameter P_{peak}^{L} should be based on a value that the LFM operator and the MG operator can easily agree upon, such as for example the capacity at the grid connection point, so that the flexibility service can be quantified in a reliable manner. The value of this parameter is the same for all simulations to avoid the need of additional communication and coordination between the two operators. Constraints (5-5)-(5-6) are added to model the offered flexibility service:

$$\mathrm{p}^{\mathrm{flex}} \geq \sum_{\mathrm{w}\in\mathcal{W}} \Pi_{\mathrm{w}}\, \mathrm{p}_{\mathrm{w}}^{\mathrm{Max,im}},\ \forall \mathrm{t} \in \mathcal{H}_{f}, \tag{5-5}$$

$$\mathrm{p}_{\mathrm{w}}^{\mathrm{Max,im}} \geq \mathrm{p}_{\mathrm{t,w}}^{\mathrm{im}},\ \forall \mathrm{w} \in \mathcal{W}, \forall \mathrm{t} \in \mathcal{H}_{f}, \tag{5-6}$$

where $p_{w}^{Max,im}$ is the expected peak imported power with $\mathcal{H}_{f}$ denoting the time period, when the flexibility should be activated.

The power balance of the MG is given by:

$$\mathrm{P}_{\mathrm{t,w}}^{\mathrm{PV}} + \mathrm{p}_{\mathrm{t}}^{\mathrm{dis}} - \mathrm{p}_{\mathrm{t}}^{\mathrm{ch}} = \mathrm{p}_{\mathrm{t,w}}^{\mathrm{ex}} - \mathrm{p}_{\mathrm{t,w}}^{\mathrm{im}} + \mathrm{P}_{\mathrm{t,w}}^{\mathrm{L}}, \forall \mathrm{t} \in \mathcal{H}, \forall \mathrm{w} \in \mathcal{W}. \tag{5-7}$$

The losses of the grid side converter are ignored. The optimisation model also includes technical constraints that model the BESS operation and degradation. The BESS scheduling and degradation model is described in detail in [51]. This model relates the SoE of the BESS with the charging/discharging power of the BESS (p_t^{ch}/p_t^{dis}).

5.2 Uncertainty Modeling

To represent the uncertainty associated with the input values, the day-ahead forecast error of these values can be assumed to follow a Gaussian distribution [52]-[53] i.e., $\mathcal{E}_t^{\mathcal{PV}} \sim N(0,0.1^2)$ and $\mathcal{E}_t^{\mathcal{L}} \sim N(0,0.05^2)$ for the error of PV generation and power consumption, respectively. Based on this, 2000 scenarios are generated using the Monte Carlo method i.e., random sampling of the input variables, which are the available (most recent) forecasts. The forecast profile has the same horizon length and time resolution (number of time discretization steps) as the considered look-ahead horizon of the simulation and is used as the base scenario. If the forecasts were perfect, then there would be no forecast errors and there would be no need for stochastic optimisation; instead a deterministic problem could be used to decide on energy scheduling and flexibility. Since the forecasts are not perfect, a Gaussian random number generator is used to generate an error that follows the previously mentioned distributions for each time step of the available load profile. The values (of the base scenario) are then adjusted according to the generated errors and the outcome is one future event scenario of electricity load and PV generation. This process is then repeated to generate the desired number of scenarios i.e., 2000. It should be noted that more accurate techniques for the scenario generation can be applied to improve the uncertainty modeling i.e., the stochastic input data ($P_{t,w}^{PV}$ and $P_{t,w}^{L}$) to the optimisation problem.

After the scenario generation, a mix of fast backward/forward methods in the SCENRED tool of GAMS is used to create a reduced number of scenarios i.e., 120 scenarios, which are representative of the real variability of the input values, without substantially compromising the accuracy of the results. These 120 scenarios are not equiprobable. A different probability of occurrence is assigned to each scenario by the scenario reduction technique.

As explained before, the stochastic optimisation problem for optimal energy scheduling and flexibility dispatch is solved in RH. Therefore, after the time horizon is shifted and before the next simulation, the base scenario forecast is updated to consider the most recent forecast (which is again used for generating the scenarios of the next scheduling period). The (shifted) look-ahead horizon of the next simulation also includes the part of the time horizon that was not considered in the previous simulation.

The accuracy of the forecast values is progressively reduced within the horizon (the accuracy deteriorates the further ahead the time step lies in the future), which is why Solanki et al. [54] used non-uniform time resolution. In this report, the time horizon is uniform; however, the error distribution changes within the time horizon. Since the standard deviations ($\sigma_t^{\mathcal{PV}} = 0.1$, $\sigma_t^{\mathcal{L}} = 0.05$), adopted from [52]-[53], referred to the day-ahead forecast error distribution, reduced standard deviations are used during the first parts of the time horizon. Thus, the standard deviation for the forecast error of the next time steps until the next hour ahead, as well as the time steps after the first hour ahead and until six hours ahead are assumed to be $10\%\sigma_t^{\mathcal{PV}}/10\%\sigma_t^{\mathcal{L}}$ and $50\%\sigma_t^{\mathcal{PV}}/50\%\sigma_t^{\mathcal{L}}$, respectively. The change in the intra-day accuracy of the forecasts uses information from [54]; it should be noted, however, that the error distribution over the time horizon should be modeled in greater detail, which could be a part of a future work. Finally, the length of the time horizon in the RH approach might dynamically change before each simulation to avoid the need of forecasting electricity market prices. One example of these future event-scenarios for a scheduling period can be seen in Figure 5-3.

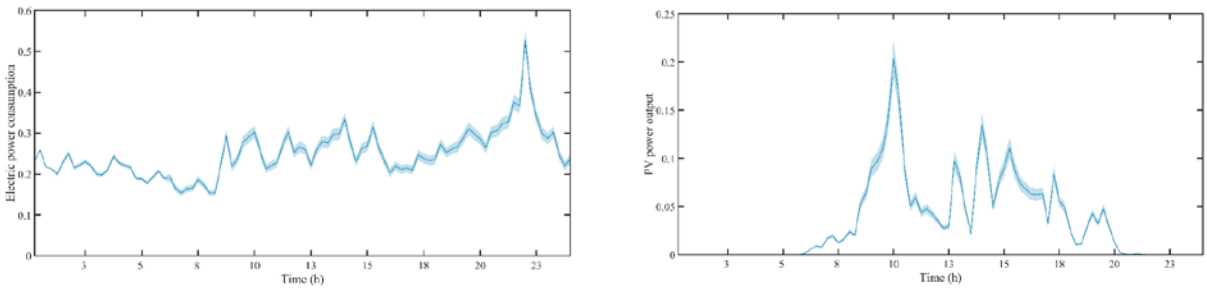

Figure 5-3: Scenarios of the input data (ratio of PV power output and electric power consumption over respective capacities) for the next scheduling period, where lighter shades show the confidence intervals and the dark colour solid line shows the available forecast (base scenario).

5.3 Flexibility Assessment and Dispatch

The process of flexibility evaluation and dispatch, shown in Figure 5-4, corresponds to an intra-day and close to real-time LFM framework. The depicted time discretisation step is $\Delta t = 15$ minutes therefore 96 simulations (solutions of the stochastic optimisation problem) are needed to decide on the optimal energy scheduling of the MG resources for Day 1.

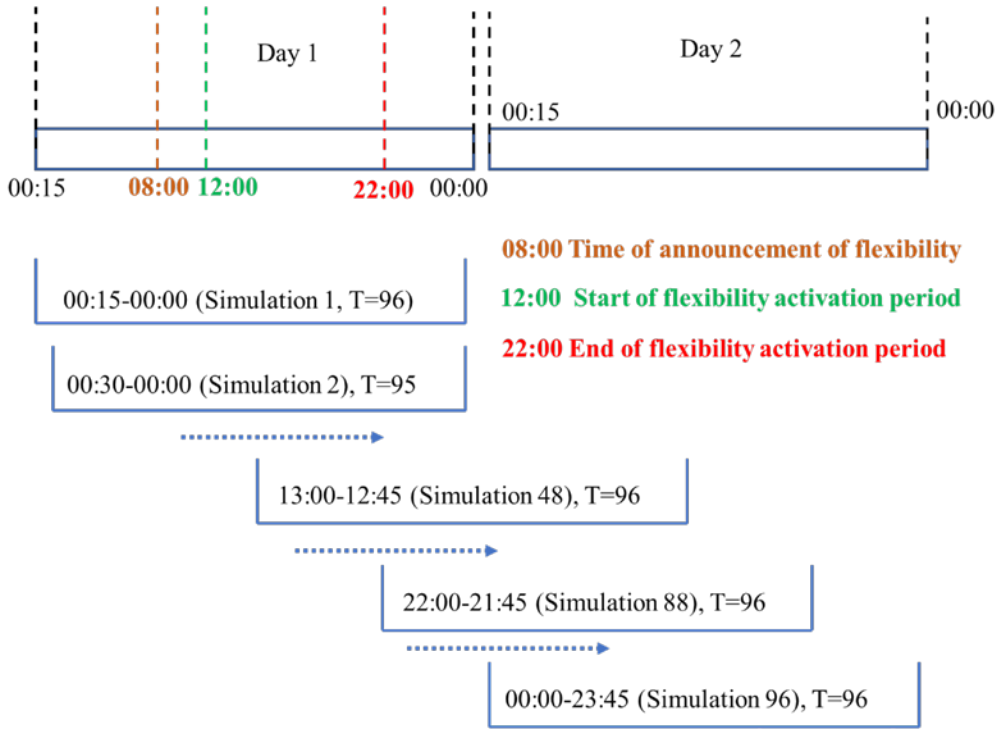

Figure 5-4: Process of flexibility dispatch.

The MG operator does not receive a signal from the LFM operator about upcoming flexibility requirements until a later hour of the day. During this period, the MG operator applies a tentative schedule by solving the stochastic optimisation problem (without the integration of the flexibility service) in RH i.e., one simulation is performed at each time step as shown in Figure 5-4. If the LFM operator requires flexibility on a short notice within a day, then the MG responds with the flexibility amount and a stochastic assessment of the flexibility that can be offered by solving the stochastic optimisation problem as it was formulated in Section 5.1. The response is sent directly after the request e.g., in Figure 5-4 the flexibility request and response process would be initiated at 08:00 (Simulation 48) i.e., the time of announcement of flexibility requirement. After that, the MG proceeds with implementing an energy schedule which allows the dispatch of the flexibility amount. A penalty term can be included in the objective function to penalise deviation from the flexibility bid. The schedule is applied until the simulation horizon moves out of the flexibility activation period (this is between 12:00-22:00 i.e., Simulations 48-88 in Figure 5-4) and then the MG operator can continue solving the energy scheduling stochastic optimisation problem without the integration of the flexibility service for the rest of the simulations.

The simulations in the RH process can be described by the following steps:

- **Step 1**: Choose the length of the time horizon (maximum length is one day). Reduce the length, if electricity price data are not available (the day-ahead spot market prices are updated at about 12:45 at the previous day [55] therefore the time horizon, which is initially 96 steps in Figure 5-4 is continuously reduced by one time step from Simulation 2 to Simulation 47).
- **Step 2**: Obtain the day-ahead available forecast which has the same time resolution as the considered scheduling time horizon. Reduce the length if necessary, update the base scenario and generate new scenarios.

- **Step 3**: Solve the stochastic optimisation problem using the generated scenarios, price data and the SoE of the BESS, which was obtained from the previous simulation. These are the input data illustrated in Figure 5-2.
- **Step 4**: Update the battery charging/discharging power of the next time step according to the solution of the optimisation problem and shift the time horizon by Δt. Go to Step 1.

5.4 Simulation Results

The optimal MG energy scheduling and flexibility dispatch problem was simulated for a day considering the announcement of flexibility requirement and the flexibility activation period as shown in Figure 5-4. The MG resources can be seen in Table 5-1. The residential electricity load data, the PV generation data, and the BESS data were scaled-up measurements obtained from [56]. Nord Pool spot market prices [55] as well as data from the website of the local DSO [57] (energy tariffs, power grid tariffs and reimbursement fee) were used to define the value of the parameters C_t^{im}/C_t^{ex}. The capacity at the connection point was P_{peak}^{L} = 253.2 kW and the time discretisation step is $\Delta t = 15$ minutes. Simulations were performed according to the test cases described in Table 5-2. The stochastic assessment of flexibility, which is presented in Sections 5.4.1 - 5.4.3, is performed right after the time of the flexibility request (denoted as "Time of Announcement" in Table 5-2) with the information known at that moment (SoE of the BESS, electricity prices and most recent forecasts of load/PV power output over the simulation time horizon).

Table 5-1: Electricity load and energy resources of the MG

BESS Capacity (kWh)	625
BESS Maximum Charging/Discharging Power (kW)	521
PV Capacity (kWp)	10.6
Peak demand (kW)	60

Table 5-2: Test Cases

	Time of Announcement	Flexibility Activation Period	Flexibility Assessment and Dispatch	SoE at Time of Announcement
Case A	08:00	12:00-22:00	Flexibility amount over whole activation period	64%
Case B	18:00	20:00-22:00	Flexibility amount over whole activation period	46%
Case C	08:00	12:00-22:00	Flexibility amount per time step of activation period	64%

5.4.1 Case A

The simulation was repeated for three different prices of flexibility i.e., C_{flex} =50$/MW (low price), C_{flex} =100$/MW (medium price), and C_{flex} =200$/MW (high price). Figure 5-5a and Figure 5-5d correspond to the case with the lowest price of flexibility. As mentioned earlier, each stochastic optimisation problem comprises 120 scenarios. For each of the 120 scenarios, the actual amount of flexibility which the MG provided to the grid is recorded, and depicted as a histogram plot in Figure 5-5a. The x-axis represents the actual amount of flexibility achieved. The y-axis reports the probability of

achieving this amount of flexibility (in one or more of the 120 scenarios). Thus, the percentage reported in the y-axis is the weighted sum of the scenarios where a given flexibility amount occurs, divided by the weighted sum of all 120 scenarios (the weights are the probabilities assigned by the scenario reduction technique as explained in Section 5.2). The vertical red dashed line in each figure marks the value of $P^{L}_{peak} - p^{flex}$, where the value of the decision variable p^{flex} (flexibility bid) was obtained from the solution of the stochastic optimisation problem. This implies that the optimum solution of the stochastic optimisation involves few scenarios where more flexibility is provided, or where the system might fall short of meeting its flexibility target due to less offered flexibility.

Similarly, the time at which this flexibility amount was provided to the grid is also recorded for each scenario, and depicted as a histogram plot in Figure 5-5d. Subfigures (b) and (e) report the same data for the case of medium price of flexibility. The data for the case of highest price of flexibility are depicted in subfigures (c) and (f).

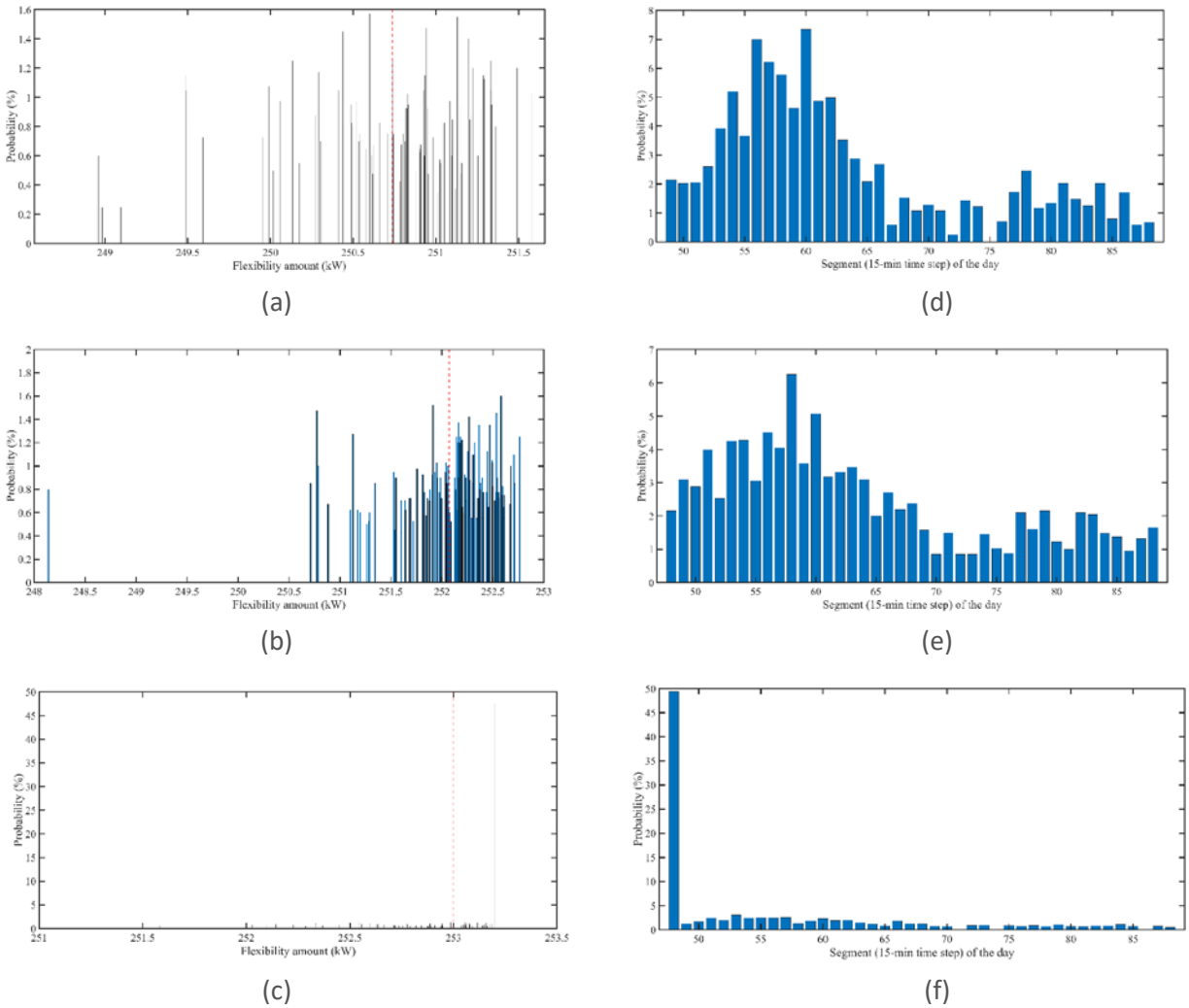

Figure 5-5: The simulation results of Case A, where the probability distribution of dispatched flexibility and the flexibility bid (red dashed line) of the MG operator is shown in (a)-(c), while (d)-(f) show the probability distribution of the time occurrence of the MG peak imported power within the flexibility activation period for the flexibility prices of $50/MW, $100/MW, and $200/MW, respectively for each row.

With the low and medium prices (50$/MW and 100$/MW) of flexibility, there is 61% probability of dispatching the flexibility according to the bid (flexibility is dispatched for about 70 out of the 120 scenarios) When the flexibility price is $200/MW, the probability of dispatching the flexibility increases to 66%. Since deviation from the flexibility bid is penalized during the flexibility activation period, the desired flexibility can be substantially improved by careful tuning of the penalty factor, as long as there are no limitations due the technical constraints of the MG resources. In this case study, for a penalty equal to 180 $/MW (taken from [58]) the flexibility is dispatched for all considered flexibility prices if the base scenario is assumed to be realized.

As demonstrated in Figure 5-5 (d)-(e), it is hard to predict when the peak imported power, which defines the dispatched flexibility amount, will occur. However, there is clearly a higher probability that it will occur before 17:00 (68th segment). This implies that a large part of the BESS capacity is scheduled to reduce imported power during the evening high-peak period for the majority of the scenarios. This is done to increase the certainty of dispatching the desired flexibility; at the same time, however, there is less available capacity for power reduction for the rest of the flexibility activation period. It is also possible that the BESS might have to be charged before the high-peak period to ensure an adequate level of stored energy.

Due to the large size of the battery and the fact that at the time of the announcement of flexibility, the SoE of the battery was 64%, the peak measured during the whole flexibility period is substantially reduced as can be seen in Figure 5-5 (a)-(c), where the peak reduction is above 248 kW (a peak reduction of 253.2 kW would signify no import of power during the flexibility period). In addition, as the flexibility price increases, the probability of dispatching the maximum flexibility also increases. This leads to an almost 50% probability that the maximum flexibility will be dispatched when the maximum flexibility price is applied ($200/MW in this case study).

5.4.2 Case B

In case B, the MG operator receives a flexibility request for a closer period in time. Theoretically, the MG operator has less liberty and fewer options to implement in order to meet the flexibility request. In practice, a shorter notice time did not, significantly, affect the dispatch of the flexibility due to the large BESS size and the adequate SoE level. The tighter flexibility activation period also contributed to improving the certainty of the dispatched flexibility with higher flexibility prices, see Figure 5-6 (a)-(c). The stochastic assessment reports a 59% probability of dispatching the flexibility according to the bid (flexibility is dispatched for about 68 out of the 120 scenarios) when the flexibility price is $50/MW, a result which is as good as that of Case A. At the price of $100/MW the probability was increased to 74% (86 scenarios), while at the price of $200/MW, the probability increases to 88% (102 scenarios). Again, for a penalty of 180 $/MW the flexibility is dispatched for all considered flexibility prices, if the base scenario is assumed to be realized. The time of occurrence of the peak imported power could also be predicted with higher probability in Case B, as seen in Figure 5-6 (d)-(f), where the peak is more likely to appear at the beginning of the flexibility activation period, with a probability above 80% as the flexibility price increases.

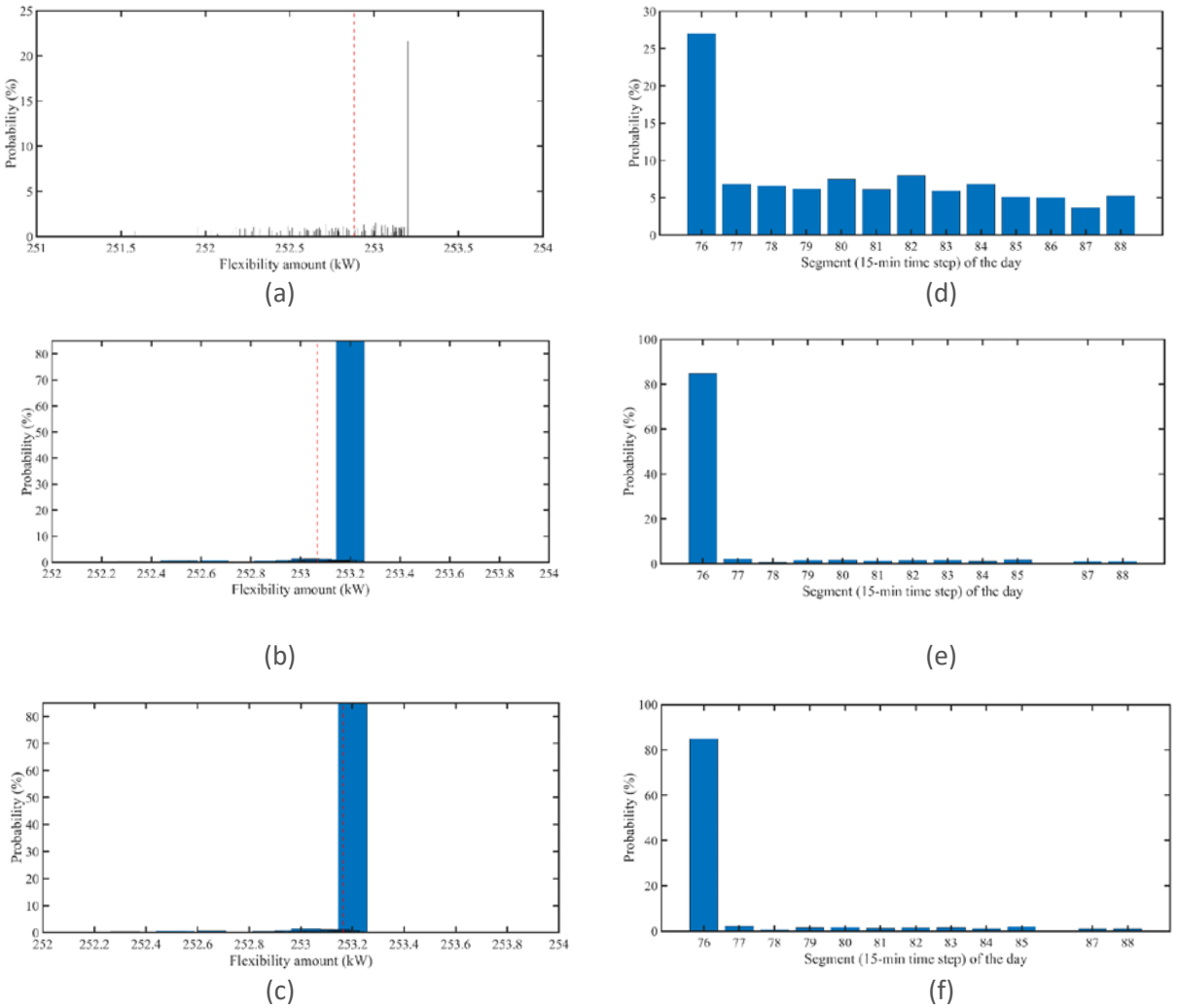

Figure 5-6: The simulation results of Case B, where the probability distribution of dispatched flexibility and the flexibility bid (red dashed line) of the MG operator is shown in (a)-(c), while (d)-(f) show the probability distribution of the time occurrence of the MG peak imported power within the flexibility activation period for the flexibility prices of $50/MW, $100/MW, and $200/MW, respectively for each row.

5.4.3 Case C

In Case A and Case B, the amount of flexibility was calculated for the whole period of flexibility activation and refers to the reduction in the peak imported power during that period. Flexibility could also be dispatched in more frequent time steps during the activation period. In that case, the flexibility bid is indexed by t (p_t^{flex}) and the objective function of the stochastic optimisation problem is modified as follows:

$$\min f = f^{im} - f^{ex} + r^{p} + c^{B} - \sum_{t\in\mathcal{H}_f} C_{flex}\left(P^{L}_{peak} - p^{flex}_{t}\right), \quad (5\text{-}8)$$

while constraint (5-9) is used to model the offered flexibility service:

$$p^{flex}_{t} \geq \sum_{w\in\mathcal{W}} \Pi_{w}\, p^{im}_{t,w},\ \forall t \in \mathcal{H}_f. \quad (5\text{-}9)$$

Figure 5-7 to Figure 5-9 show that the probability of dispatch of a flexibility amount is at least equal to the value shown in the x-axis for each time step of the flexibility activation period at different flexibility prices. The MG is guaranteed to be able to provide its maximum flexibility during periods (48 – 54) and (66 – 86), regardless of the price of flexibility. However, the amount of flexibility and the probability of its occurrence vary in different ways, in response to change in the price of flexibility.

For period t=65, the MG is guaranteed (i.e. probability 100%) to provide 230KW of flexibility with the low price of flexibility. However, it is impossible to provide any bigger amount of flexibility bigger than 230KW. With the medium price, it becomes even less likely to provide the 230KW amount. Increasing the price of flexibility further has the opposite effect. The MG is guaranteed to provide 230KW, and is also 98% likely to be able to provide 240KW. This increase in probability comes at the expense of the amount and probability of flexibility at t=64.

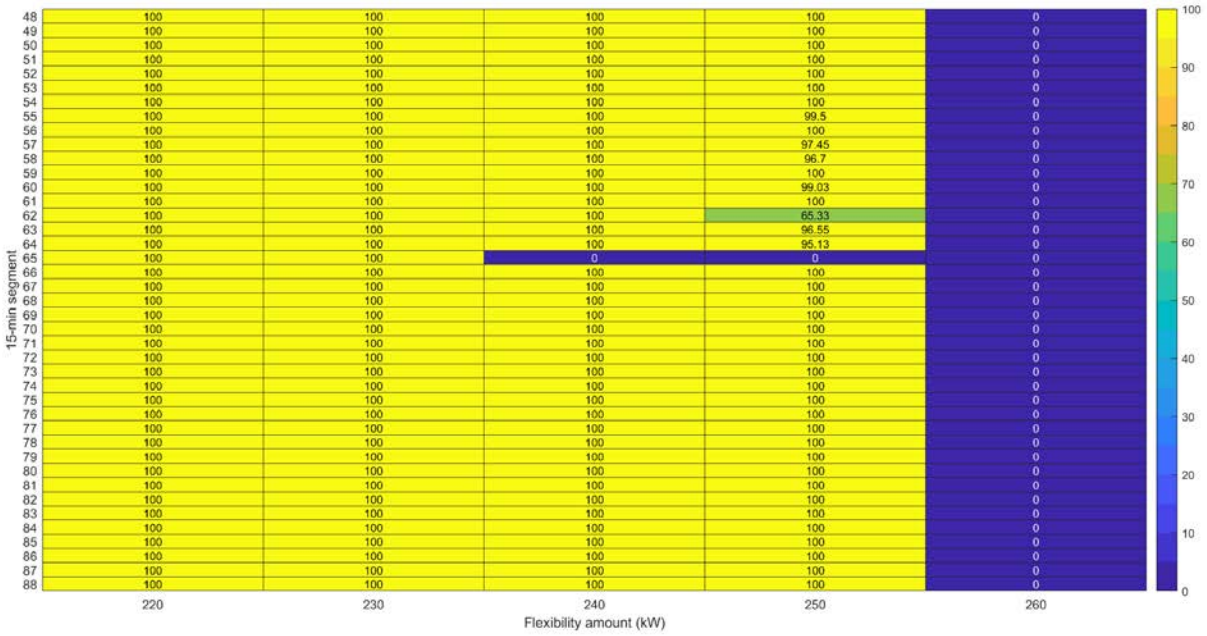

Figure 5-7: The probability distribution of dispatched flexibility at each time step of the flexibility activation period, when the flexibility price is $5/MW.

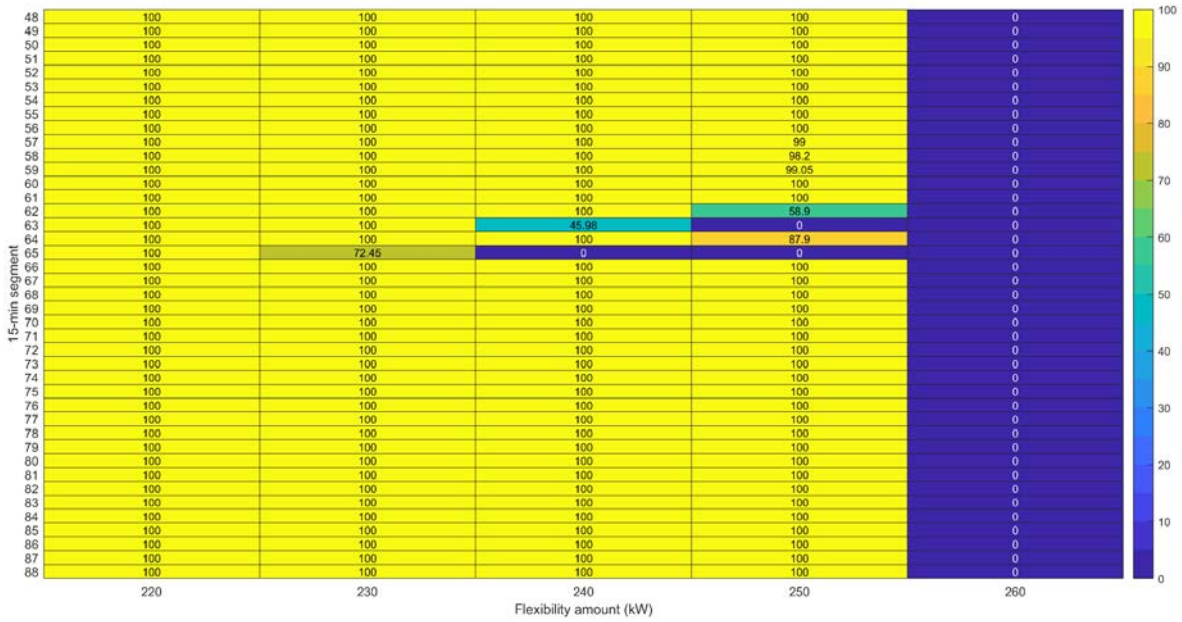

Figure 5-8: The probability distribution of dispatched flexibility at each time step of the flexibility activation period, when the flexibility price is $10/MW.

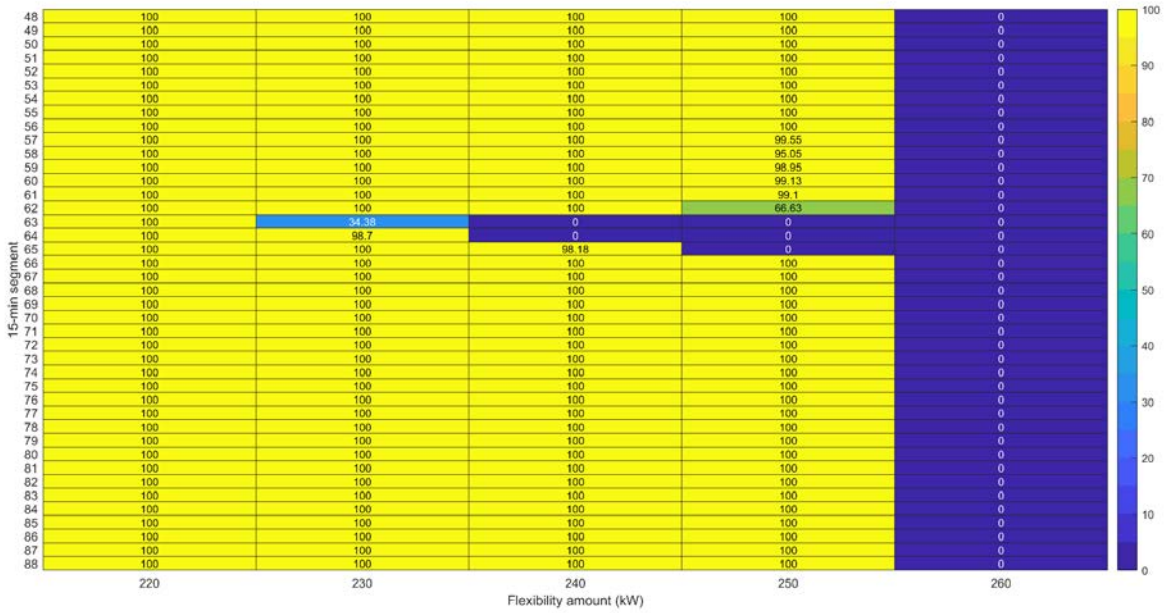

Figure 5-9: The probability distribution of dispatched flexibility at each time step of the flexibility activation period, when the flexibility price is $20/MW.

5.5 Conclusions – Flexibility assessment by a stochastic models

The stochastic programming model, which was developed for assessment and dispatch of MG flexibility, was used to formulate the MG energy scheduling and flexibility dispatch problem as a scenario-based stochastic optimisation problem, which was solved in RH. The stochastic assessment of flexibility showed a 61%-66% (Figure 5-5) probability that the flexibility bid could be dispatched, when the flexibility amount

(peak reduction) was evaluated considering the peak power of the flexibility activation period. A shorter time notice improved the certainty of flexibility dispatch at higher flexibility prices due to the improved accuracy of the forecasts that determine the flexibility bid. It should be noted, however, that BESS capacity limitations or other technical constraints (e.g., a lower initial SoE level) could substantially limit the probability of flexibility dispatch. Thanks to the RH approach, the probability of flexibility dispatch obtained by the stochastic assessment, which is performed at the time of the flexibility request, can be further increased depending on the penalty implemented for the deviation from the flexibility bid and the technical constraints of the DERs of the MG.

6 Conclusion

Within this report, the authors presented the characteristics and constrains of various flexibility resources, such as heat pumps, electric vehicles, decentralized (battery) energy storage or smart appliances. As already demonstrated in pilot-projects and documented in reports and publications, such LV-level flexibility sources can provide flexibility by time-shifting loads, curtailment or buffering of energy.

The Flexi-Grid project consortium develops concepts and procedures for the procurement of local flexibility and the market designs for local flexibility markets, besides other related topics. Stakeholders involved in these concepts require models and approaches to estimate the availability of flexibility for different purposes – be it the aggregators in the operational forecasting or DSOs in planning and operation of LV-grids with the help of flexibility, for instance.

The deterministic modelling approach presented in chapter 3, to estimate the optimal amount of flexibility provision on individual device and household level, uses flexible electricity prices as control signal. This approach was studied using EVs, PV, heat pumps, washing machines, freezers and dishwashers as flexible appliances. Using an agent-based network architecture, the influence of different price control signals has been observed, by means of an optimisation function with the objective to lower energy costs for the households. Using solely cost optimisation on individual household level led to flexibility provision, triggered by the dynamic pricing, but might cause some problems such as congestions in the power grid, if this approach remains unbalanced by corrective measures, aiming at the optimisation of the grid operational state.

An indirect demand-response method, such as market-based price adjustment, is chosen to mitigate this problem. However, by means of simulations, it is found that the price adjustment prevented congestions successfully only on some days, while on others not. It has been found that, on the days where the price adjustment fails to prohibit congestions, there is a lack of flexibility resources in this system which was unknow to the operator. It can be concluded that, when mitigating congestions using indirect control methods such as price adjustment, a higher uncertainty on the amount of flexible resources in the system needs to be considered. Another approach could be to utilize direct control methods for the power system, such as graceful degradation or load shedding.

Identifying the amount of maximum adjusted load based on the control signal, may potentially be used to quantify the amount of power flexibility. Though it means that the amount of flexibility is not certain and will only be a snapshot of the current situation of the devices and households in this distribution grid branch, based on the specific dynamic electricity price profile. While it is certainly a possibility to use deterministic models, such as the one described in chapter 3, using price control signals to procure flexibility, further studies with data driven models might be required to firmly quantify the amount of flexibility and its certainty.

Such a data driven model has been developed in the framework of this project and the approach and its preliminary results are presented in chapter 4. Data-driven models are computer algorithms which learn the relationship between input and output data, and then, attempt to make predictions on new input data. The data used to train the models in chapter 4 are the input and output of above mentioned study, using dynamic pricing to incentives flexibility and the cost optimisation on individual household level. From perspective of a grid operator or aggregator, the cost optimisations (the algorithms, operational

state of the devices etc.) are unknown and running the optimisations for all devices and households during operation might be cumbersome or even too slow (see “model speed“ in chapter 4). Hence, the data driven model learns the behaviour of the optimisation functions based on historic input and output data, in order to be able to reproduce the reaction (available flexibility) based on a future dynamic price profile.

A model based on convolutional neural networks and auto-encoders is built on two stages. A first stage, where a preliminary model learns to convert the time profiles in the input data into another hidden space and reconstructs these encoded data back to meaningful time profiles. And second, when the model is augmented with additional components which are able to solve the optimisation problem in the hidden space. Data driven models require time when they are built and trained. However, evaluating an input instance with a trained model proves to be much faster than solving the actual optimisation problem. Data-driven models are also capable of handling batches of instances at once, while mathematical optimisation is solved for each instance separately. The preliminary (encoder-decoder) model demonstrates very good performance. The augmented model demonstrates good performance in terms of predicting the time-shift in a load event. The magnitude of the adjusted load is predicted with less accuracy. A larger network design would perform better, at the expense of more training time, and computing power.

Another important aspect of estimating the available flexibility, is the handling of uncertainties. Based on a different use case example than the previous mentioned models, the stochastic programming approach presented in chapter 5 incorporates also the uncertainty that is inherent to the load and renewable forecasts used in grid operation. In this use case, the flexibility service provided by the operator of a grid-connected micro grid is a capacity limitation flexibility service, where a financial incentive is set for a certain time period in which the power import from the main grid should stay underneath an agreed threshold. I could be shown that by this approach, it is possible to provide decision support for operators, to assess the certainty with which the agreed max. power import could be met by the micro grid operator, under the uncertainty of renewable and load forecasts. Future studies, can consider combining the data-driven models in Chapter 4 with the scenario-based stochastic optimisation of Chapter 5 and assess the available flexibility by using both historical measurements and the intra-day available forecasts for renewable-based generation and electricity load demand.

7 Reference

[1] R. Fonteijn, P. H. Nguyen, J. Morren, and J. G. Slootweg, "Demonstrating a generic four-step approach for applying flexibility for congestion management in daily operation," *Sustain. Energy, Grids Networks*, vol. 23, p. 100378, 2020.

[2] A. Bloess, W.-P. Schill, and A. Zerrahn, "Power-to-heat for renewable energy integration: A review of technologies, modeling approaches, and flexibility potentials," 2017.

[3] O. Ruhnau, L. Hirth, and A. Praktiknjo, "Time series of heat demand and heat pump efficiency for energy system modeling," *Sci. Data*, vol. 6, no. 1, 2019.

[4] A. Arteconi and F. Polonara, "Assessing the demand side management potential and the energy flexibility of heat pumps in buildings," *Energies*, vol. 11, no. 7, pp. 1–19, 2018.

[5] C. Magni, A. Arteconi, K. Kavvadias, and S. Quoilin, "Modelling the Integration of Residential Heat Demand and Demand Response in Power Systems with High Shares of Renewables," *Energies*, vol. 13, no. 24, p. 6628, Dec. 2020.

[6] "Simplified Model of Flexible Heat Pump Load Profiles." [Online]. Available: https://www.smagrinet.eu/newsflash/blog/simplified-model-of-flexible-heat-pump-load-profiles/.

[7] McKinsey, "The potential impact of electric vehicles on global energy systems." [Online]. Available: https://www.mckinsey.com/industries/automotive-and-assembly/our-insights/the-potential-impact-of-electric-vehicles-on-global-energy-systems.

[8] A. P. Robinson, P. T. Blythe, M. C. Bell, Y. Hübner, and G. A. Hill, "Analysis of electric vehicle driver recharging demand profiles and subsequent impacts on the carbon content of electric vehicle trips," *Energy Policy*, vol. 61, pp. 337–348, 2013.

[9] US Drive and U.S. Drive Grid Integration, "Summary Report on EVs at Scale and the U. S. Electric Power System," no. November 2019, 2019.

[10] IRENA, "Innovation outlook: Smart charging for electric vehicles," 2019.

[11] T. Gnann, A.-L. L. Klingler, and M. Kühnbach, "The load shift potential of plug-in electric vehicles with different amounts of charging infrastructure," *J. Power Sources*, vol. 390, no. March, pp. 20–29, Jun. 2018.

[12] Energy Networks Australia, "Could vehicle-to-grid accelerate the EV revolution?" [Online]. Available: https://www.energynetworks.com.au/news/energy-insider/2020-energy-insider/could-vehicle-to-grid-accelerate-the-ev-revolution/.

[13] IEA, "Vehicle-to-grid potential and variable renewable capacity relative to total capacity generation requirements in the Sustainable Development Scenario, 2030 – Charts – Data & Statistics - IEA." [Online]. Available: https://www.iea.org/data-and-statistics/charts/vehicle-to-grid-potential-and-variable-renewable-capacity-relative-to-total-capacity-generation-requirements-in-the-sustainable-development-scenario-2030. [Accessed: 18-Apr-2021].

[14] International Renewable Energy Agency (IRENA), *Smart Charging System for Electric Vehicles*. Abu Dhabi, 2019.

[15] The International Renewable Energy Agency, "ELECTRIC-VEHICLE SMART CHARGING INNOVATION LANDSCAPE BRIEF," 2019.

[16] Bloomberg, "BNEF, 2021 Energy Storage Market Outlook." .

[17] SolarPower Europe, "European Market Outlook For Residential Battery Storage," 2020.

[18] F. Sterner, M.; Eckert, F; Thema, M.; Bauer, "Der positive Beitrag dezentraler Batteriespeicher für eine stabile Stromversorgung (Kurzstudie im Auftrag von BEE e.V. und Hannover Messe)," Regensburg / Berlin / Hannover, 2015.

[19] "Home battery storage value streams & payback periods — SwitchDin." .

[20] F. A. Qayyum, M. Naeem, A. S. Khwaja, A. Anpalagan, L. Guan, and B. Venkatesh, "Appliance Scheduling Optimization in Smart Home Networks," *IEEE Access*, vol. 3, pp. 2176–2190, 2015.

[21] ADEME and Enertech, "Campagne de mesures des appareils de production de froid, des appareils de lavage et de climatisation," 2016.

[22] J. Taneja, K. Lutz, and D. Culler, "The impact of flexible loads in increasingly renewable grids," *2013 IEEE Int. Conf. Smart Grid Commun. SmartGridComm 2013*, pp. 265–270, 2013.

[23] T. Barbier, R. Girard, F. P. Neirac, N. Kong, and G. Kariniotakis, "A novel approach for electric load curve holistic modelling and simulation," *IET Conf. Publ.*, vol. 2014, no. CP665, 2014.

[24] T. Boßmann, R. Schurk, and J. Schleich, "Unravelling load patterns of residential end-uses from smart meter data," *Eceee 2015*, pp.

1111–1122, 2015.

[25] W. Labeeuw, “Characterisation and modelling of residential electricity demand,” KU Leuven, 2013.

[26] S. Nistor, J. Wu, M. Sooriyabandara, and J. Ekanayake, “Capability of smart appliances to provide reserve services,” *Appl. Energy*, vol. 138, pp. 590–597, Jan. 2015.

[27] D. Materassi, S. Bolognani, M. Roozbehani, and M. A. Dahleh, “Optimal Consumption Policies for Power-Constrained Flexible Loads Under Dynamic Pricing,” *IEEE Trans. Smart Grid*, vol. 6, no. 4, pp. 1884–1892, 2015.

[28] J. Villar, R. Bessa, and M. Matos, “Flexibility products and markets: Literature review,” *Electr. Power Syst. Res.*, vol. 154, pp. 329–340, 2018.

[29] California ISO, “Flexible Ramping Products: Revised Draft Final Proposal,” pp. 1–18, 2015.

[30] North American Electric Reliability Corporation, “Flexibility Requirements and Potential Metrics for Variable Generation: Implications for System Planning Studies,” *Evaluation*, no. August, 2010.

[31] E. Lannoye, A. O. Mahoney, and A. Muireann, “Econometric Analysis of Flexibility Rewards in Electricity Markets,” *Int. Ser. Oper. Res. Manag. Sci.*, vol. 153, pp. 1–26, 2010.

[32] M. Huber, D. Dimkova, and T. Hamacher, “Integration of wind and solar power in Europe: Assessment of flexibility requirements,” *Energy*, vol. 69, pp. 236–246, 2014.

[33] H. Munoz, *Uncovering demand flexibility in buildings : a smart grid inter-operation framework for the optimization of energy and comfort*, no. 2017. 2017.

[34] N. Blaauwbroek, P. H. Nguyen, M. J. Konsman, H. Shi, R. I. G. Kamphuis, and W. L. Kling, “Decentralized Resource Allocation and Load Scheduling for Multicommodity Smart Energy Systems,” *IEEE Trans. Sustain. Energy*, vol. 6, no. 4, 2015.

[35] G. Hoogsteen, *A cyber-physical systems perspective on decentralized energy management*. 2017.

[36] A. N. M. M. Haque, D. S. Shafiullah, P. H. Nguyen, and F. W. Bliek, “Real-Time Congestion Management in Active Distribution Network based on Dynamic Thermal Overloading Cost,” in *2016 Power Systems Computation Conference (PSCC)*, 2016, pp. 1–7.

[37] A. N. M. M. Haque, M. Nijhuis, G. Ye, P. H. Nguyen, F. W. Bliek, and J. G. Slootweg, “Integrating Direct and Indirect Load Control for Congestion Management in LV Networks,” *IEEE Trans. Smart Grid*, vol. 10, no. 1, pp. 741–751, 2019.

[38] F. G. Nievinski, “subtightplot,” *MATLAB Central File Exchange*, 2021. .

[39] “MATLAB Optimization Toolbox.” .

[40] S. Sun, Z. Cao, H. Zhu, and J. Zhao, “A Survey of Optimization Methods from a Machine Learning Perspective,” *IEEE Trans. Cybern.*, vol. 50, no. 8, pp. 3668–3681, 2020.

[41] D. Alexander, *Neural Networks: History and Applications*. Nova Science Publishers, Incorporated, 2020.

[42] P. Werbos, “Beyond Regression : New Tools for Prediction and Analysis in the Behavioral,” *Thesis Diss. Harvard Univ.*, no. January, 1974.

[43] S. K. Azman, Y. J. Isbeih, M. S. El Moursi, and K. Elbassioni, “A Unified Online Deep Learning Prediction Model for Small Signal and Transient Stability,” *IEEE Trans. Power Syst.*, vol. 35, no. 6, pp. 4585–4598, 2020.

[44] O. A. Alimi, K. Ouahada, and A. M. Abu-Mahfouz, “A Review of Machine Learning Approaches to Power System Security and Stability,” *IEEE Access*, vol. 8, pp. 113512–113531, 2020.

[45] S. Khokhar, A. A. Mohd Zin, A. P. Memon, and A. S. Mokhtar, “A new optimal feature selection algorithm for classification of power quality disturbances using discrete wavelet transform and probabilistic neural network,” *Meas. J. Int. Meas. Confed.*, vol. 95, pp. 246–259, Jan. 2017.

[46] V. Miranda, L. Teixeira, and J. Pereira, “Estimating Breaker Status with Electrical State Images and Convolutional Neural Networks,” in *2019 20th International Conference on Intelligent System Application to Power Systems, ISAP 2019*, 2019.

[47] L. Wang, Q. Zhou, and S. Jin, “Physics-guided Deep Learning for Power System State Estimation,” *J. Mod. Power Syst. Clean Energy*, vol. 8, no. 4, pp. 607–615, 2020.

[48] Z. Yan and Y. Xu, “Data-driven load frequency control for stochastic power systems: A deep reinforcement learning method with continuous action search,” *IEEE Trans. Power Syst.*, vol. 34, no. 2, pp. 1653–1656, 2019.

[49] E. Wood, “What Schneider Electric’s Recent Move Reveals about the Microgrid Market.” .

[50] C. Ziras, C. Heinrich, and H. W. Bindner, “Why baselines are not suited for local flexibility markets,” *Renew. Sustain. Energy Rev.*, vol.

135, no. July 2020, p. 110357, 2021.

[51] K. Antoniadou-Plytaria, D. Steen, L. A. Tuan, O. Carlson, and M. A. Fotouhi Ghazvini, “Market-Based Energy Management Model of a Building Microgrid Considering Battery Degradation,” *IEEE Trans. Smart Grid*, vol. 12, no. 2, pp. 1794–1804, 2021.

[52] H. Shuai, J. Fang, X. Ai, J. Wen, and H. He, “Optimal Real-Time Operation Strategy for Microgrid: An ADP-Based Stochastic Nonlinear Optimization Approach,” *IEEE Trans. Sustain. Energy*, vol. 10, no. 2, pp. 931–942, 2019.

[53] M. MansourLakouraj, M. Shahabi, M. Shafie-khah, N. Ghoreishi, and J. P. S. Catalão, “Optimal power management of dependent microgrid considering distribution market and unused power capacity,” *Energy*, vol. 200, 2020.

[54] B. V. Solanki, A. Raghurajan, K. Bhattacharya, and C. A. Canizares, “Including Smart Loads for Optimal Demand Response in Integrated Energy Management Systems for Isolated Microgrids,” *IEEE Trans. Smart Grid*, vol. 8, no. 4, pp. 1739–1748, 2017.

[55] “ttps://www.nordpoolgroup.com/ - Google Search.” .

[56] “HSB Living Lab.” .

[57] “Göteborg Energi.” .

[58] B. V. Mbuwir, D. Geysen, F. Spiessens, and G. Deconinck, “Reinforcement learning for control of flexibility providers in a residential microgrid,” *IET Smart Grid*, vol. 3, no. 1, pp. 98–107, 2020.